Identification of a putative *Litomosoides sigmodontis* phosphate permease, *Ls-ppe-1*, and its role in the interaction between filarial nematodes and their *Wolbachia* endosymbionts

&

Establishment of RNA interference in the rodent filaria *Litomosoides sigmodontis*, a model of human filariasis

Dissertation

by

CLAUDIA ULRIKE KLEMM

from Görlitz

Bonn, 2009

Angefertigt mit Genehmigung der Mathematisch-Naturwissenschaftlichen Fakultät der Rheinischen Friedrich-Wilhelms-Universität Bonn.

In advance publication of the dissertation

Parts of the results of this study have been published in advance by the permission of Prof. Dr. Achim Hörauf, Director of the Institute for Medical Microbiology, Immunology and Parasitology, University Clinic Bonn, Germany.

Publications

Heider, U., Blaxter, M., Hoerauf, A., Pfarr, K.M., (2006) Differential display of genes expressed in the filarial nematode *Litomosoides sigmodontis* reveals a putative phosphate permease up-regulated after depletion of *Wolbachia* endobacteria.
Int J Med Microbiol 296: 287.

Heider, U. and Pfarr, K.M., Hoerauf, A., (2006) RNAi mediated silencing of actin expression in adult *Litomosoides sigmodontis* is specific, persistent and results in a phenotype.
Int J Parasitol 36: 661.

Pfarr, K.M., Heider, U., Schmetz, C., Büttner, D.W., Hoerauf, A., (2008) The mitochondrial heat shock protein 60 (HSP60) is up-regulated in *Onchocerca volvulus* after the depletion of *Wolbachia*.
Parasitology 135: 529.

List of abbreviations

APOC	African Program for Onchocerciasis Control
APS	ammonium persulfate
aRNA	amplified antisense ribonucleic acid
BME	beta-mercaptoethanol
Bm-WSP	*Wolbachia* surface protein of *Brugia malayi*
bp	base pair
BSA	bovine serum albumin
cDNA	complementary desoxyribonucleic acid
CI	cytoplasmatic incompatibility
CoA	coenzyme A
ct	cycle threshold
DD PCR	differential display polymerase chain reaction
DEC	diethylcarbamazin
DEPC	diethyl propyl carbonate
Dicer	dsRNA-specific ribonuclease / RNase III-like enzyme
dNTP	desoxy nucleotide triphosphate
dsRNA	double-stranded ribonucleic acid
EDTA	ethylenediamin-tetraacetic acid
EM	electron microscopy
EtBr	ethidium bromide
FAD	flavin adenin dinucleotide
FCS	fetal calf serum
FITC	fluorescein isothiocyanate
GPELF	Global Program to Eliminate Lymphatic Filariasis
IL	interleukin
i.p.	intraperitoneal
IVM	ivermectin
kb	kilobase
L.s.	*Litomosoides sigmodontis*
LF	lymphatic filariasis

LPS	lipopolysaccharide
Ls-ppe-1	phosphate permease of *L. sigmodontis*
MF	microfilaria (= the first stage larvae L1)
MOPS	3-(N-morpholino) propane sulphonic acid
mRNA	messenger ribonucleic acid
NaAc	sodium acetate
NAD	nicotineamid adenine dinucleotide
OCP	Onchocerciasis Control Program
OD	optical density
OEPA	Onchocerciasis Elimination Program for the Americas
PBS	phosphate buffered saline
p.i.	post infection
PTGS	post transcriptional gene silencing
RdRP	RNA dependent RNA Polymerase
RISC	RNA induced Silencing Complex
RLM-RACE	RNA Ligase Mediated-Rapid Amplification of cDNA Ends
RNAi	RNA interference
RT	Reverse Transcription
RT-qPCR	Reverse Transcription-quantitative PCR
SDS	sodium dodecyl sulfate
siRNA	short interfering ribonucleic acid
SPF	specific pathogen free
SSC	saline-sodium citrate buffer
TEMED	tetramethyl ethylene diamin
*w*Bm	*Wolbachia* of *Brugia malayi*
*w*Mel	*Wolbachia* of *Drosophila melanogaster*
*w*Pip	*Wolbachia* of *Culex pipiens*
w/v	weight per volume

Table of contents

1 Introduction

1.1 Nematodes

The phylum nematoda includes roundworms that are free-living in water and soil, in addition to an impressive number of species that are parasitic to plants and animals. Out of the approximately 20.000 species that have been described thus far, only 138 species have been found to infect humans (Orihel, Ash, 1995). Thus, parasitic nematodes have a substantial impact on the infected individuals and the community through corporal damage and diseases of both humans and domestic animals. These negative effects include the health of the individual, the psychological and social stigmatization of the infected individuals, an immense economic impact due to the loss of productivity, and increased mortality rate (Evans, 1993; Pion, 2002; Little, 2004).

Eight main species of filarial nematodes infect humans. Three of these are responsible for most of the morbidity due to filariasis: *Wuchereria bancrofti* and *Brugia malayi* cause lymphatic filariasis, and *Onchocerca volvulus* causes onchocerciasis (river blindness). The other five species are *Loa loa, Mansonella perstans, M. streptocerca, M. ozzardi* and *Brugia timori,* the last also causes lymphatic filariasis.

1.1.1 Nematode morphology

The filarial nematodes are unsegmented, cylindrical, thread-like worms that are round in transverse sections. They have four main longitudinal chords, a tri-radiate esophagus and an esophageal nerve ring. Nematodes have neither a circulatory nor a respiratory system. The nematodes are sexually dimorphic, and in general the males are much smaller than females. The worms have one or two gonads that open at the vulva in the female and in the rectum of the male. Their exoskeleton is composed of a multilayer collagenous cuticle, which is covered by a lipidic epicuticle, as well as a negatively charged glycocalyx (Page, 1992).

1.1.2 Filarial nematodes

Filarioidea is a superfamily of nematoda. The members of this superfamily parasitize tissues of a great variety of animals, ranging from amphibians to mammals. Insect vectors are required for development of the immature larvae into the infective third stage larvae (L3), and for transmission to the mammalian hosts.

Lymphatic filariasis (LF), also known as elephantiasis, is transmitted by several genera of mosquitoes (*Aedes, Anopheles, Culex,* and *Mansonia*). Onchocerciasis is an eye and skin disease that is transmitted by blackflies of the genus *Simulium*.

The adult nematodes are long, slender and delicate worms that reside in the lymphatic vessels (*Wuchereria bancrofti, Brugia malayi*), subcutaneous nodules (*Onchocerca volvulus, Loa loa*), or connective tissues (*Mansonella ozzardi, M. perstans*) (WHO, 1992; Ottesen, 1994). Because of their habitat selection in tissues, the adults of most species are rarely seen without tissue section analysis. An infection is typically diagnosed by the presence of microfilariae, the first stage larvae (either microscopically, or by finger-prick tests to measure the circulating antigen), which are produced by adult females and are found in the blood or in the epidermis of the host.

1.1.3 Transmission of filarial infections

The insect vectors take up the microfilariae during blood meals on infected individuals. Within the insect, the larvae migrate through the gut wall of the arthropod to the thorax muscles, and develop into infective third stage larvae (L3) in a process that usually takes 7 to 21 days. Then, these L3 larvae migrate to the mouthparts and are deposited with the saliva on the skin of the host during subsequent blood meals. Following, the larvae enter through the lesion made by the insect and develop into adult worms in the definitive host, thus completing the cycle (Figure 1). The development from infective L3 larvae to sexually mature adult worms (separate sexes) requires a few to several months (Orihel, Ash, 1995). The adult nematodes, depending on the species, can survive up to 15 years in the human host.
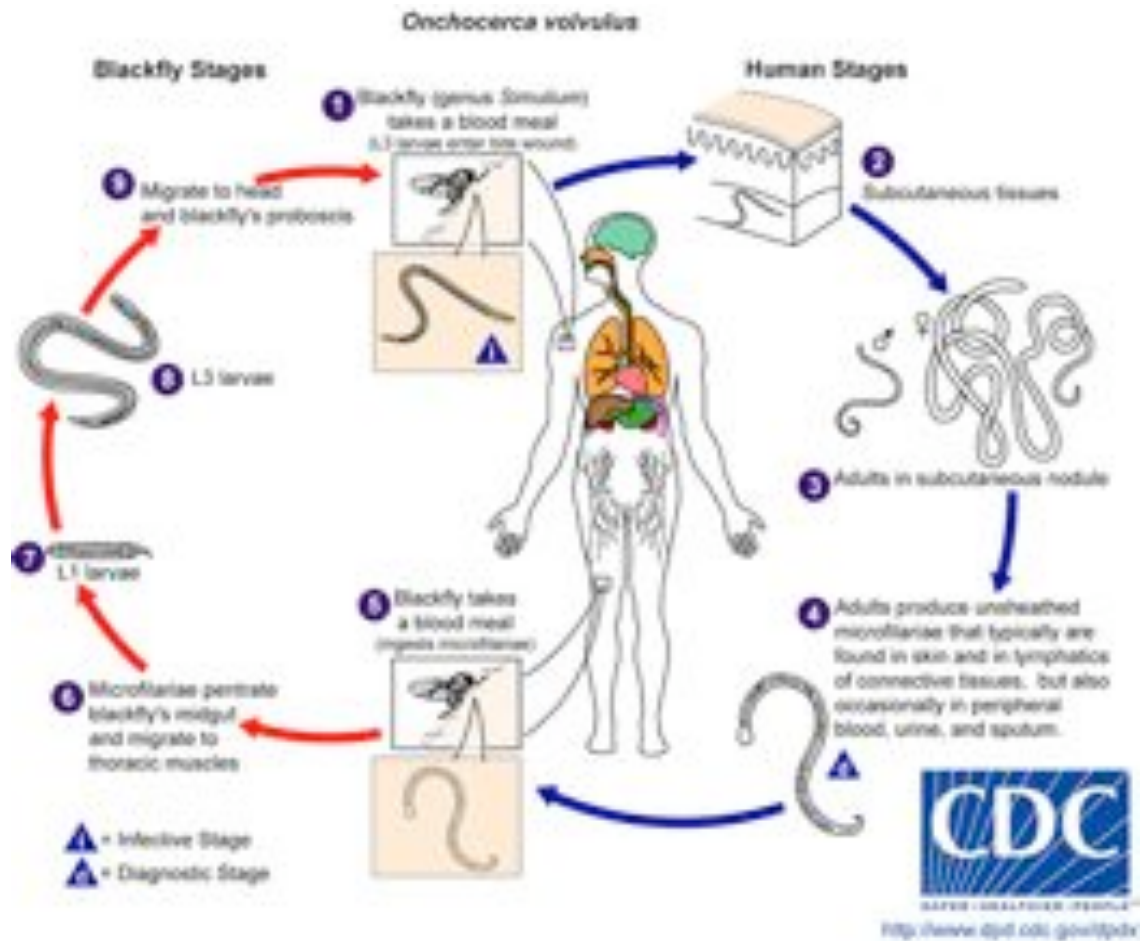
Figure 1. The Life Cycle of *O. volvulus*

During a blood meal, an infected blackfly (genus Simulium) introduces third-stage filarial larvae onto the skin of the human host, where they penetrate into the bite wound (1). In subcutaneous tissues the larvae (2) develop into adult filariae, which commonly reside in nodules in subcutaneous connective tissues (3). Adults can live in the nodules as many as 15 years. Some nodules may contain numerous male and female worms. Females measure 33 to 50 cm in length and 270 to 400 μm in diameter, while males measure 19 to 42 mm by 130 to 210 μm. In the subcutaneous nodules, the female worms are capable of producing microfilariae for approximately 9 years. The microfilariae, measuring 220 to 360 μm by 5 to 9 μm and unsheathed, have a life span that may reach 2 years. They are occasionally found in peripheral blood, urine, and sputum, but are typically found in the skin and in the lymphatics of connective tissues (4). A blackfly ingests the microfilariae during a blood meal (5). After ingestion, the microfilariae migrate from the blackfly's midgut through the hemocoel to the thoracic muscles (6). There the microfilariae develop into first-stage larvae (7) and subsequently into third-stage infective larvae (8). The third-stage infective larvae migrate to the blackfly's proboscis (9) and can infect another human when the fly takes a blood meal (1). (Centers of Disease Control and Prevention, http://www.dpd.cdc.gov/dpdx)

1.1.4 Geographic distribution

The geographic distribution of human filariasis is closely linked to the availability of the specific insect vectors (Figure 2). Filarial infections are endemic in more than 80 countries of the tropics. In these countries 200 million individuals are already infected and more than 1.33 billion people are at risk of infection (WHO, 2000b, 2008). The major forms of the human filarial infections are lymphatic filariasis, caused by *W. bancrofti* (90%) and *Brugia* spp. (10%), and onchocerciasis (river blindness), caused by *O. volvulus*.

Lymphatic filariasis is a major health problem in the tropics and sub-tropics of Asia, Africa, the Western Pacific and part of the Americas. Although the disease is global in its distribution, around one third of infected people live in India. Another third resides in the countries of Africa, and most of the remaining in the countries of South-East Asia and the Pacific Islands. Onchocerciasis is the major cause of blindness in 28 countries in tropical Africa, but is also prevalent in isolated foci in Latin America (six countries) and Yemen. It is estimated that there are about half a million blind people due to river blindness. *L. loa,* the African eye worm, is distributed in the rain forests of West and Central Africa (Nutman, 1986). Additionally, *Mansonella* species can be found in the tropical regions of Africa and the Amazon region of South America (WHO, 1995; Fischer, 1997).

Figure 2. Global distribution of lymphatic filariasis.

The areas indicated in red show the countries and territories endemic for lymphatic filariasis.

1.1.5   Pathology of lymphatic filariasis

In lymphatic filariasis, the adult nematodes reside in the in the afferent lymphatic vessels. Some patients develop a severe dysfunction of the lymphatic system caused, in part, by high plasma levels of lymphangiogenic factors (i.e. vascular endothelial growth factor-C [VEGF-C] and soluble vascular endothelial growth factor receptor-3 [(s)VEGFR-3]) (Debrah, 2006), that finally results in lymph vessel dilation, lymphoedema and elephantiasis (a painful disfiguring swelling of the limbs) (Figure 3). Damage and swelling of the scrotum in males, hydroceles, or enlarged breasts in females often occur. Filariae are responsible for a variety of clinical manifestations. The majority of infected people are asymptomatic but all of them have hidden damage to the lymphatic vessels and as many as 40% have damaged kidneys (proteinuria, haematuria). In the acute and chronic stages of the disease, recurrent debilitating fever attacks occur by secondary bacterial infections, as well as lymphangitis and elephantiasis (WHO, 2000a).

Figure 3. A typical example of chronic lymphatic filariasis.

Lymphatic filariasis can progress to elephantiasis, a painful, disfiguring disease that has a devastating effect on the victims and their families and carries a huge social stigma.

1.1.6 Pathology of onchocerciasis

In contrast to lymphatic filariasis, host inflammatory reactions to dead *O. volvulus* larvae (microfilariae) in the skin can cause dermatitis with intensely itching rashes, wrinkling and depigmentation of the skin (also known as Sowda form, or leopard/lizard skin), and onchocercomata (subcutaneous nodules) (Figure 4A and B). Nevertheless, the most serious manifestation consists of ocular lesions that can progress from visual impairment to blindness (river blindness) (Figure 4C). Onchocerciasis can also lead to lymphadenitis, resulting in elephantiasis of the genitals and to general debilitation (WHO, 1995).

Figure 4. The clinical symptoms of onchocerciasis.

The skin is the principle site of infection. A) Intense irritation and itching of the skin occurs in response to *O. volvulus* antigens and can lead to cutaneous lesions (Sowda form). B) Subcutaneous nodules are a significant indicator of infection with *O. volvulus* and appear in 30% of all cases. Nodules vary in size and number. C) Ocular lesions appear during chronic onchocerciasis because of the migration and death of microfilariae in the eye. Conjuctivitis is the first reaction to the microfilariae. Dead microfilariae also cause corneal infections that can result in sclerosing keratitis and vascularization. Sclerosing keratitis is the main cause of irreversible blindness due to onchocerciasis.

1.1.7 The WHO control programs

Endemic countries have established control programs with the aid of the World Health Organization (WHO) to fight against filarial infections. The Onchocerciasis Control Program (OCP) has successfully targeted transmission of the blackfly vector, eventually included ivermectin treatment at the end, but this program ended in 2002.

Currently, there are two programs to control onchocerciasis, the African Program for Onchocerciasis Control (APOC; http://www.who.int/ocp/apoc), administered in areas of participating countries hyperendemic for onchocerciasis, and the Onchocerciasis Elimination Program for the Americas (OEPA; http://www.cartercenter.org) (Richards, 2001; Benton, 2002). Efforts to control lymphatic filariasis are managed by the Global Program for the Elimination of Lymphatic Filariasis (GPELF) (Molyneux, Zagaria, 2002; Ottesen, 2002; Molyneux, 2003). The ambitious goal of all programs is to reduce the infection rate, prevent new infections, and eliminate the disease as a major public health problem. Thus, these control programs use microfilaricidal drugs once or twice a year in mass administered chemotherapy to interrupt transmission. Administering a single dose of two drugs concurrently, optimally albendazol (ALB) with either diethyl-carbamazin (DEC) or ivermectin (IVM) is effective only for one year after treatment. There are indications that IVM and DEC treatment alone are not sufficient to completely interrupt transmission since it does not sustainably suppress micro-filaraemia. The remaining microfilaria level is still high enough to re-establish the infection within a few years (Borsboom, 2003).

APOC and OEPA administer IVM in regions where onchocerciasis alone is endemic. The GPELF administers DEC and ALB where lymphatic filariasis is mono-endemic, and IVM and ALB in areas where lymphatic filariasis is co-endemic with oncho-cerciasis (most of Africa). There, DEC cannot be used because severe side reactions can occur when other infections, such as onchocerciasis are also present. The appearance of severe side effects upon IVM treatment, when given to patients that are co-infected with *L. loa* (fast killing of microfilariae leads to encephalitis), inhibits the current mass drug administration in places where *L. loa* is co-endemic with onchocerciasis.

The current drugs administered are not sufficient to eliminate filariasis but other anthelminthic drugs tested are either less effective or they are too toxic (Awadzi, 2004c; Hoerauf, 2006; Pfarr, Hoerauf, 2006). Drug resistance, especially for DEC (Esterre,

2001) and ivermectin (Awadzi, 2004a; Awadzi, 2004b), is also becoming more of a concern to the control programs. Research, which has lead to a new antifilarial therapy, focuses on the intracellular, endosymbiotic *Wolbachia* bacteria in filarial nematodes (see also section 1.2.5).

APOC's strategy to eliminate the disease is the community-directed treatment with IVM, which relies on active community participation to distribute IVM treatment to the individuals who need it. These circumstances lead to an inadequate coverage, and therefore this program might not succeed. In contrast, the OEPA is rather successful. Already in 2003, all endemic countries have reached the necessary treatment coverage of at least 85%. Since then, these countries maintained at least 85% treatment coverage, which must be sustained to halt the transmission by the end of the decade. Additionally, there has been no new case of blindness from river blindness, and six of the 13 endemic areas have likely interrupted transmission.

Mathematical simulation models can help to understand the complex transmission dynamics of parasitic diseases and are useful tools for studying the prospects of lymphatic filariasis elimination (Stolk, 2006). The predictions conclude that it is possible to eliminate lymphatic filariasis by yearly mass treatment, but that the number of treatment rounds depends on coverage, pre-control MF prevalence and the macrofilaricidal effects of drugs.

1.2   *Wolbachia* endosymbionts

Intracellular bacteria were first detected 1924 by Hertig and Wolbach in the reproductive organs of the mosquito *Culex pipiens*; a similarity to Rickettsiae was already noted. In the following years, up until the 1990s, intracellular bacteria with a similar morphology were detected in most of the insects and many other arthropods like mites, crustaceans, and spiders. Almost 30 years ago, McLaren and Kozek (McLaren, 1975; Kozek, Marroquin, 1977) first described *Rickettsia*-like structures in filarial nematodes using electron microscopy. In the last decade, interest in the endosymbiotic bacteria in filarial nematodes has rekindled, and the bacteria were positively assigned to the alpha proteobacteria of the genus *Wolbachia* (Genchi, 1998; Hoerauf, 1999). *Wolbachia* are obligate intracellular bacteria that belong to the order Rickettsiales (Anderson, Karr, 2001). Further, *Wolbachia* are present in nearly all species of filarial

nematodes, including the human infective nematodes *W. bancrofti, O. volvulus*, and *B. malayi*. A few exceptions for nematodes that lack *Wolbachia* (sporadic losses during evolution) are the human pathogenic species *L. loa* and *M. perstans*, the rodent filariae *Acanthocheilonemea viteae*, and the red deer filariae *O. flexuosa* (Hoerauf, 1999; Taylor, Hoerauf, 1999).

1.2.1 Phylogeny of *Wolbachia*

Wolbachia are classified by their place in molecular phylogenies and can be divided into eight supergroups (denoted clades A–H). These supergroups were defined by analyses of the *16S* rRNA, *wsp* (*Wolbachia* surface protein) and *ftsZ* genes (O'Neill, 1992; Lo, 2002; Casiraghi, 2004; Baldo, Werren, 2007). An overview is shown in Figure 5.

The majority of arthropod *Wolbachia* belongs to clades A and B, and a restricted set of crustaceans, chelicerates, hexapods and filarial nematodes belong to clades E and F. The analysis of intracellular bacteria of filarial nematodes revealed two additional clades (C and D). In detail, clade C contains *Wolbachia* from the nematodes *O. volvulus* and *Dirofilaria immitis*, and clade D contains *Wolbachia* from *B. malayi, W. bancrofti* and *L. sigmodontis* (Bandi, 2001b; Lo, 2002; Lo, 2007). *Wolbachia* of Australian spiders belong in clade G (Rowley, 2004), while *Wolbachia* from termites belong in clade H (Bordenstein, Rosengaus, 2005).

Very recently, Ros *et al*. discovered a new *Wolbachia* supergroup (K) in the spider mite *Bryobia* species V and have shown that other *Bryobia* species (*B. praetiosa, B. sarothamni, Bryobia* species I, and *Tetranychus urticae*) harbor B-group *Wolbachia* (Ros, 2009). The occurrence of two supergroups (B and K) within a single host genus is very unusual and has previously noted only for arthropod species where they are known to recombine.

Complete sequences have been determined for three *Wolbachia* genomes: *w*Mel of *Drosophila melanogaster* in clade A (Wu, 2004), *w*Bm of *Brugia malayi* in clade D (Foster, 2005), and *w*Pip from *Culex pipiens* in clade B (Klasson, 2008).

Work is underway to sequence eight additional genomes of other *Wolbachia* strains of clades A, B, and D, where only partial sequence information is available.
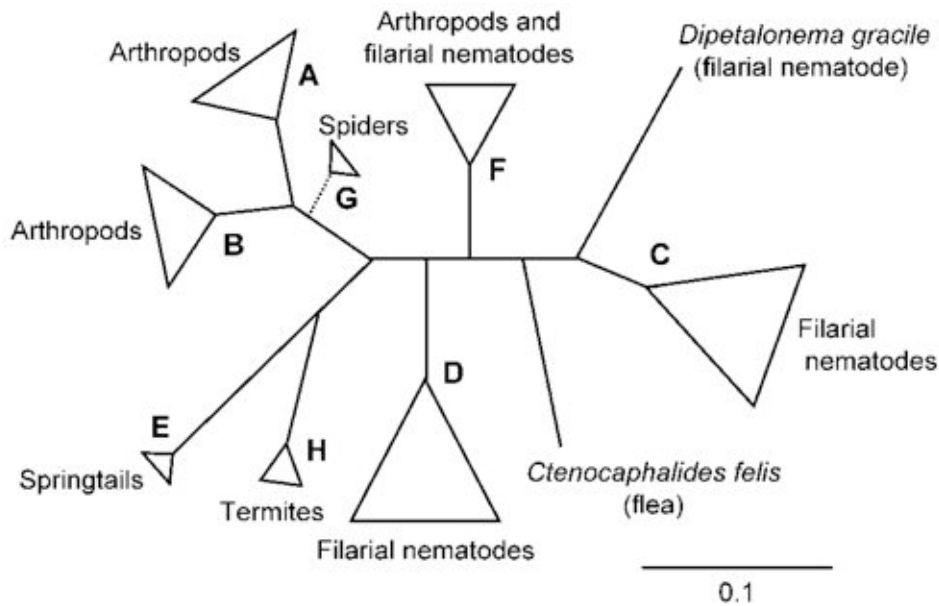
Figure 5. Phylogenetic diagram of *Wolbachia* based on various studies of the genes *ftsZ, groEL, gltA* and *dnaA*.

Letters represent supergroups that have been confirmed on the basis of *ftsZ, groEL, gltA* and *dnaA*. The position of supergroup G is tentative since it was estimated using the *wsp* and 16S rRNA genes. Host species are indicated next to each clade or lineage. (Lo, 2007)

1.2.2 Localization of *Wolbachia*

Wolbachia are found throughout all stages of the life cycle of the filarial nematodes, and occur clustered within host-derived (presumed) vacuoles. In adult nematodes of both sexes, *Wolbachia* are predominantly found in the hypodermal cells of the lateral chords. In females, *Wolbachia* are also present in the ovaries, oocytes, and all embryonic and larval stages within the uteri (Hoerauf, 2003a), whereas they have not been demonstrated in the muscles, the epithelia of the digestive and genital tracts, nor in the male reproductive system (Taylor, Hoerauf, 1999; Sacchi, 2002; Büttner, 2003; Kozek, 2005).

1.2.3 The lifestyle of *Wolbachia* in filarial nematodes

In filarial nematodes, the *Wolbachia* endobacteria are transmitted strictly vertically (transovarially) to the next generation. No evolutionary recent horizontal transmission to distantly related species, as is seen with insect *Wolbachia*, has been described. The treatment of infected nematodes with antibacterial agents not only harms the *Wolbachia*, but also adversely affects the biology of the nematode host. These facts suggest a mutualistic symbiotic co-evolution between *Wolbachia* and their filarial hosts (Bandi, 2001a; Taylor, Hoerauf, 2001; Fenn, Blaxter, 2004). Consistent with this, the phylogenies of the *Wolbachia* strains from various nematodes closely parallel that of the worm host (see also Figure 6) (Bandi, 1998; Lo, 2002; Taylor, 2005a). There are also no indications for multiple infection of a single host, or for the presence of different types of *Wolbachia* in a given species.

The *Wolbachia* of filarial nematodes appear not to be under any genetic selection pressure, probably due to their mutualistic lifestyle, nor has there been any evidence of recombination found. These facts are contrary to the positive genetic selection and recombination documented in arthropod *Wolbachia* (Jiggins, 2002a; Jiggins, 2002b). As nematode *Wolbachia* lack both of these factors the rapid development of resistance to any drug found to have anti-wolbachial activity would be hindered.
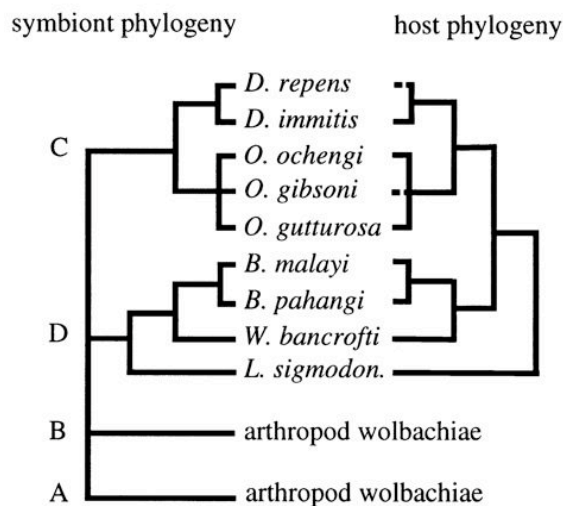
Figure 6. Comparison of *Wolbachia* and filarial nematode trees.

Symbiont tree (left) is based on results of *ftsZ* and 16S rDNA phylogenetic analyses. Host tree (right) was derived from the phylogeny inferred by Xie *et al*. (1994), after assuming the monophylogeny of the genera *Dirofilaria* and *Onchocerca* and introducing *D. repens* and *O. gibsoni* (not included in Xie *et al*.'s study). A –D indicate the four main lineages of *Wolbachia* (Bandi, 1998).

1.2.4 The role of *Wolbachia* phenotypes

1.2.4.1 In arthropods

The interactions between *Wolbachia* and their hosts are very complex and range from parasitism to mutualism. The *Wolbachia* bacteria are mainly vertically transmitted from infected females to progeny through the egg cytoplasm (Werren, 1997). Insect *Wolbachia* live mostly parasitic and alter host reproduction in a number of ways to enhance their own transmission. These alterations include induction of parthenogenesis (Stouthamer, 1993), feminization of genetic males (Bouchon, 1998), cytoplasmic incompatibility (CI) (Hurst, 1999), and even killing of male embryos, leading to sex ratio distortion (Stouthamer, 1999). All these effects are advantageous to *Wolbachia* and allow them to persist in the host populations.

Horizontal transmission from one species to another is generally assumed to be rare. In nature, horizontal transfer can occur when a donor and a recipient host are in close contact because *Wolbachia* is assumed to be incapable of surviving outside the host's tissues. High rates of natural horizontal transfers were first shown in the parasitoid wasp, *Trichogramma kayakai* (Huigens, 2000; Huigens, 2004). Further, insect *Wolbachia* are rarely found to be beneficial to their hosts. Although *Wolbachia* engage in a wide range of interactions with their hosts, they have never been demonstrated to be obligate symbionts, but rather facultative (secondary symbionts) to their hosts, because cured (aposymbiotic) individuals are unaltered physiologically. Then, Dedeine *et al*. (Dedeine, 2001) showed that the removal of *Wolbachia* by antibiotic treatment had a totally unexpected effect on the parasitic wasp *Asobara tabida,* aposymbiotic female wasps were completely incapable of producing mature oocytes and therefore could not reproduce. In contrast, oogenesis was not affected in the closely related species *Asobara citri* that is devoid of *Wolbachia*. Male reproduction or other physiological functions in females were unaffected, indicating that the effect on oogenesis is highly specific. These findings demonstrated the first obligate association between *Wolbachia* and their arthropod hosts.

1.2.4.2 In filariae

In filarial infections of animals and humans it has been demonstrated that *Wolbachia* are essential for embryogenesis, larval development and worm survival. Depletion of *Wolbachia* by the use of tetracycline antibiotics or its derivates lead to larval moulting and growth defects, sterility of females, a block in embryogenesis (Genchi, 1998; Langworthy, 2000; Hoerauf, 2001; Gilbert, 2005; Hoerauf, 2006), and to death of adult worms (Hoerauf, 2003c; Taylor, 2005a; Hoerauf, 2008). The block of the embryogenesis after antibacterial treatment is a direct effect to the loss of the *Wolbachia* as there are no alterations on embryogenesis or worm vitality seen in treatment of the *Wolbachia*-free nematode *A. viteae* (Hoerauf, 1999).

Several reports have demonstrated that the release of *Wolbachia* after killing the microfilariae correlate with pro-inflammatory responses of the infected individuals with a high microfilaria load by increased serum levels of interleukin (IL)-6, IL-10 and tumor necrosis factor. These patients show severe reactions directly after treatment with antifilarial drugs, including periodic fever attacks, headache, and enlargement of the lymph nodes. Following death of microfilariae, increased levels of *Wolbachia* antigen, detectable in the blood, are responsible for these adverse reactions (Allen, 2008; Masud, 2009). Therefore, to lower the potential of these undesired side effects, doxycycline antibiotics effective against *Wolbachia*, were applied prior to DEC or IVM treatment. After doxycycline treatment, the patients had milder reactions to the antifilarial drug, and their level of inflammatory cytokines was significantly decreased, which in turn could also be associated to lower microfilaria- and *Wolbachia* loads (Keiser, 2002; Masud, 2009).

Turner *et al*. (Turner, 2006) reported the results of a placebo-controlled trial of doxycycline for the treatment of *W. bancrofti* infection. Patients were treated for 3 weeks with doxycycline and were then administered ivermectin plus albendazole 4 months later. The results showed that doxycycline treatment for 3 weeks is sufficient to significantly reduce the microfilaremia level. Further, the patients of the doxycycline group experienced moderate adverse events after receipt of treatment with ivermectin and albendazole, compared to the placebo group.

A similar setup was used to treat patients infected with *B. malayi* (Supali, 2008). In a placebo-controlled trial, doxycycline was administered for 6 weeks, and then 4 months later, the participants received DEC plus albendazole. The prevalence of microfilaremia

was significantly reduced after doxycycline treatment alone and in combination with DEC–albendazole. This effect sustained for at least 12 months. The adverse reactions were lowest in the group receiving doxycycline plus DEC–albendazole and highest in the placebo group plus DEC–albendazole. These results lead to the conclusion that the "slow death" of nematodes should be considered to avoid the pathologic symptoms.

1.2.5   Anti-*Wolbachia* treatment in humans

Doxycycline, used in initial trials against *O. volvulus*, is an antibiotic that targets the intracellular, endosymbiotic *Wolbachia* bacteria, which are found in many filarial nematodes. The loss of *Wolbachia* leads to a complete block of the embryogenesis that remains for at least 24 months after the start of the therapy, and is possibly irreversible (Hoerauf, 2003b; Hoerauf, 2003c; Hoerauf, 2008). Macrofilaricidal effects were seen in *W. bancrofti* when doxycycline was administered for either eight weeks (200 mg/day) (Taylor, 2005b) or even as few as four weeks (Debrah, 2007). Similarly, a 70% macrofilaricidal rate was observed when patients infected with *O. volvulus* were treated for 6 weeks (100 mg/day). Killing of adult nematodes was detected 27 months post doxycycline treatment in *B. malayi* and *O. volvulus* (Hoerauf, 2008).

Nonetheless, doxycycline regimens are not suitable for mass drug treatment. The therapy duration of 4 weeks is still too long, and pregnant and/or breast-feeding women as well as children under eight years of age are excluded from the therapy concept because of the high risk of sustainable damage caused by the antibiotic.

1.2.6   Host adaptation in the endosymbiont genome

The ubiquity of *Wolbachia* and their capacity to drastically alter host biology, including disruption of host reproduction, lead to research strategies that aimed at controlling vector-borne diseases. *Wolbachia* were suggested as potential chemotherapeutic targets. Despite extensive interest in *Wolbachia* for many years, relatively little is known about the molecular mechanisms that mediate its varied interactions with different hosts. A project has been initiated to complete sequencing and annotation of *Wolbachia* genomes from different species.

The first *Wolbachia* genome from *Drosophila melanogaster* (*w*Mel) was published in late 2004 (Wu, 2004). Some incomplete but informative sequences of two more *Drosophila* strains, as well as the first complete *Wolbachia* genome of a filarial nematode, *B. malayi* (*w*Bm), revealed a lot of new information in understanding the host–symbiont interactions (Foster, 2005; Brownlie, 2007). Very recently, the third complete genome sequence of another *Wolbachia* strain from the *Culex pipiens* group of mosquitoes (*w*Pip) has been published (Klasson, 2008). Comparative analyses of *w*Bm, *w*Mel and *w*Pip (Foster, 2005; Fenn, Blaxter, 2006; Brownlie, 2007; Klasson, 2008) with other related endosymbionts such as *Rickettsia spp.*, *Anaplasma marginale,* and *Ehrlichia ruminantium* offer new means for empirical study of the symbiosis, thus finding potential metabolites that might be supplied from *Wolbachia* to their hosts (Dale, Moran, 2006).

A characteristic of intracellular endosymbionts is the loss of genetic information following adaptation to the host. This is verified by the reduced genome size of *w*Bm (1.1 Mb), which is smaller than *w*Mel (1.3 Mb) and *w*Pip (1.5 Mb), that are strictly parasitic, and *Rickettsia prowazekii*, but larger than *Mycobacterium*, thus reflecting a long-term endosymbiotic relationship (Sun, 2001).

Wolbachia encode only a limited number of metabolic pathways, and they are able to make only one amino acid *de novo*. *Wolbachia* have lost genes needed to infect new cells and genes needed to invade the host system. The *w*Bm lack some genes necessary for DNA repair and genes required for RNA modifications. *Wolbachia* are not able to synthesize lipopolysaccharide (LPS), a component of the cell membrane of most gram-negative bacteria. They also lack genes necessary to cross-link and degrade the carbohydrate backbone of peptidoglycan that is needed to form a cell wall. Incomplete pathways for the biosynthesis of vitamins and co-factors like CoA, NAD, biotin, folate and pyridoxal phosphate makes *w*Bm dependent upon supply of these precursors from the host.

However, for a better understanding of the symbiosis it is not only important what *Wolbachia* has lost, but also what has been kept in the *w*Bm genome. In contrast to other endobacteria, *Wolbachia* are able to synthesize the full range of purine and pyrimidine nucleotide triphosphates. Further, *Wolbachia* has retained all genes for cofactors riboflavine, FAD, and heme. To date, there is no evidence of genes for riboflavine and heme synthesis in the genome of *B. malayi* (Ghedin, 2004; Ghedin, 2007). Thus, heme might play an important role in filarial reproduction and

development, as there is evidence that moulting and microfilarial release in *D. immitis* and *B. pahangi* are affected by ecdysteroid-like hormons (Warbrick, 1993), whose synthesis requires heme. In contrast to most endosymbionts, *w*Bm has preserved the genes to make all nucleotides. Therefore, *Wolbachia* could be an essential source of nucleotides for the host during embryogenesis, when more DNA is required (i.e. embryogenesis). Additionally, *Wolbachia* has the genes for a type IV secretion system (*vir* genes) that is normally used by intracellular bacteria to secrete various molecules to the host cells (Masui, 2000; Christie, 2005; Rances, 2008), suggesting that the above described metabolites could be provided from *Wolbachia* to the nematode. The postulated dependencies indicate an exchange of metabolites between *w*Bm and *B. malayi,* but the traffic across the host derived vacuolar and the bacterial cell membranes remains unknown. These transport mechanisms should be further investigated because they might be excellent drug targets.

1.3   An animal model for helminth infections

The *Litomosoides sigmodontis* mouse model (Chandler, 1932) is the only fully permissive mouse model for filariasis. To overcome the non-permissivity of inbred mice to filarial parasites and the inaccessibility of fully permissive rodents to analyses of all developmental stages, the *L. sigmodontis* mouse model, originally established by Petit (Petit, 1992), was used in these studies. This model accommodates the full cycle from the infective third stage larvae (L3) to the release of microfilariae (MF) in BALB/c mice, and therefore allows the study and the modulation of distinct states of infection.

L. sigmodontis belongs to the family Onchocercideae. Phylogenetic analyses of the 5*S* ribosomal DNA spacers carried out by Xie *et al*. (Xie, 1994) show high similarity (97%) to the other members of this family. While in BALB/c mice the full parasite development was observed, in C57BL/6 mice the worm development cannot proceed beyond the L4 stage (Le Goff, 2002). Immunological modulation, such as depletion of CD4^{+} T cells, results in a higher *L. sigmodontis* worm burden and an increased and prolonged microfilaraemia (Al-Qaoud, 1997). IL-5 appears to control adult worm development and microfilaremia in primary infections (Al-Qaoud, 2000; Martin, 2000; Volkmann, 2003a). In contrast to wild type mice, IL-5 deficient mice have an up to 200-fold higher parasite load and prolonged patency (Volkmann, 2001; Volkmann, 2003a),

which permits prolonged therapeutic regimens (>2 weeks), which is impossible in wild type BALB/c mice. Another benefit in using IL-5 deficient BALB/c mice rather than wild type mice is the reduction in inflammatory nodule formation around the adult nematodes (i.e. less accumulation of neutrophils and eosinophils in the pleural cavity), facilitating parasite recovery for further analyses.

1.3.1   The parasite life cycle of *Litomosoides sigmodontis*

This rodent parasite lives naturally in the cotton rat (*Sigmodon hispidus*), which can survive very high blood microfilariae levels (up to 10.000 MF/μl blood). During the blood meal from an infected rat, the arthropod intermediate host (*Ornithonyssus bacoti* mite) ingests the microfilariae, which then migrate through the gut wall into the thoracic muscles where they molt twice to develop into infective L3 larvae within 10-12 days (see also Figure 7). The L3 larvae migrate to the head and are frequently localized in the blood-sucking mouthparts. L3 larvae are then transmitted at the next blood meal with the saliva, and make their way through the skin via the lymphatic vessels to the heart, the blood circulation and finally to the lungs, from which they penetrate into the thoracic cavity (Marechal, 1996). Ten days post infection, up to 90% of L4 larvae are detected in the thoracic and peritoneal cavities, and about 99% reach the thoracic cavity 28 days post infection (Marechal, 1996). The female and male adult worms mature within 25-33 days when they become sexually mature. The viviparous females release microfilariae into the thoracic cavity. These microfilariae penetrate the heart and eventually reach the blood circulation. Microfilariae are detectable in the blood between days 50-130 post infection. The infection of BALB/c mice ends with the encapsulation of adult worms by host inflammatory cells and the eventual absorption of dead parasites by the host.

Mice deficient for IL-5 were used in the following studies. The parasite life cycle is maintained in cotton rats, due to longer worm survival in the natural host.
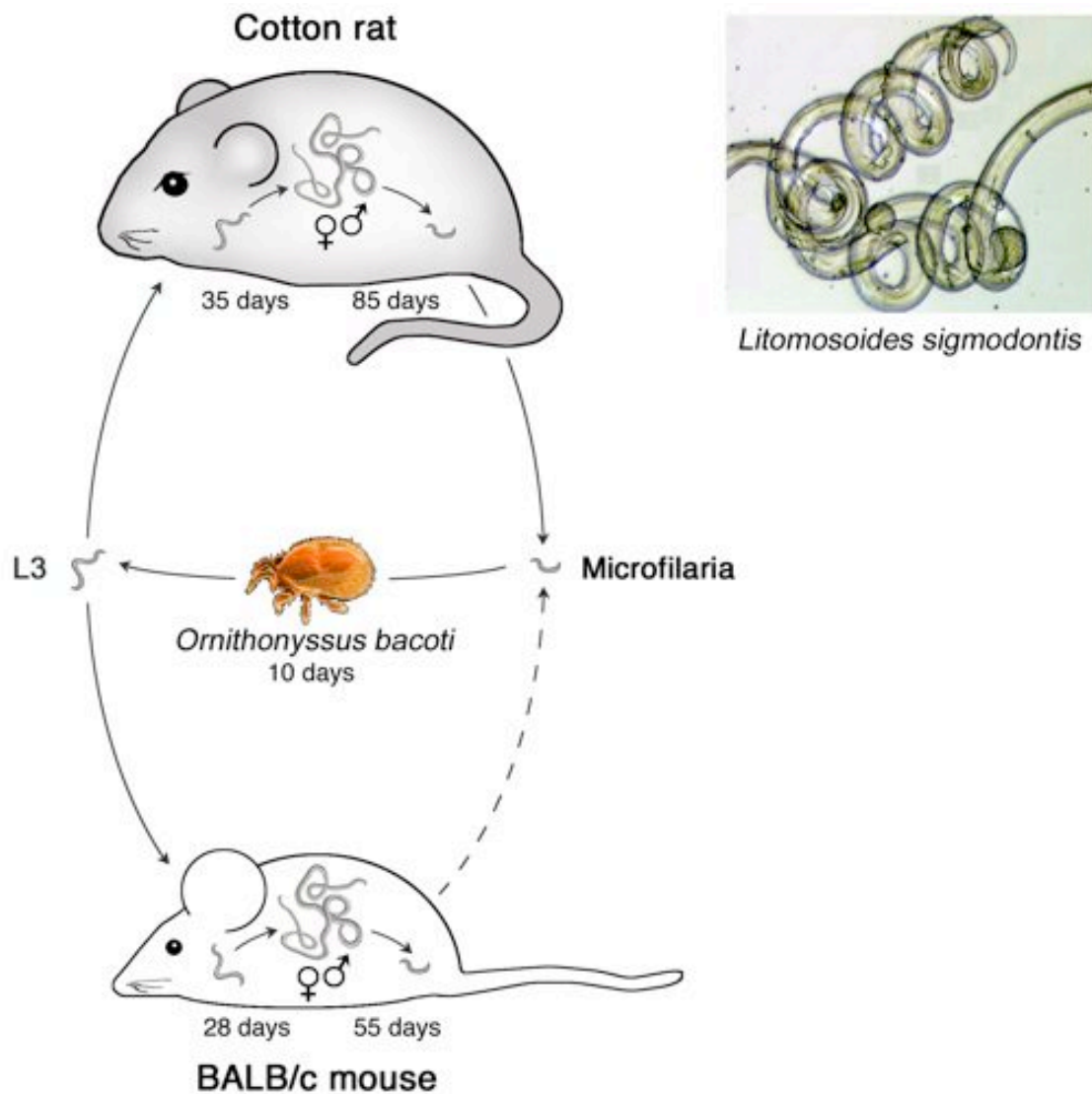
Figure 7. The life cycle of *Litomosoides sigmodontis* in its natural host, the cotton rat (*Sigmodon hispidus*), and the experimental IL-5 deficient BALB/c mouse.

During a blood meal on *L. sigmodontis* infected rats, the mites (*O. bacoti*) ingest the microfilariae (MF). The microfilariae then molt twice into infective third stage larvae (L3). These L3 are transmitted in a subsequent blood meal to either infect new rats (to close the life cycle) or to Balb/c mice deficient for IL-5, which were used in subsequent experiments.

1.4 RNA interference: a robust reverse genetics tool for the future

1.4.1 The biological function of RNAi

During the last decade, RNA interference (RNAi), the sequence specific degradation of mRNA mediated by homologous double-stranded RNA (dsRNA), has become a valuable tool for determining the biological role of genes, especially in organisms for which knockouts cannot be made (i.e. parasitic nematodes). A fundamental difference between the traditional antisense approaches of the past (the ribozyme technologies) and the siRNA-based technologies for gene silencing is the use of a very ancient and natural mechanism found in most cells.

The natural function of RNAi is thought to be a defense mechanism against repetitive and mobile genetic elements, such as transposons and viruses that are found in all eukaryotic genomes, from yeast to humans (Scherer, Rossi, 2003; Meister, Tuschl, 2004). Some of these elements replicate through DNA intermediates while others (i.e. retroelements) replicate through RNA intermediates, but all have the potential to harm if the host could not fight back by silencing expression. RNAi denotes the ability of double-stranded RNA (dsRNA) to inhibit homologous gene expression at the RNA or DNA level. RNAi is an evolutionarily conserved gene-regulatory mechanism with many species-specific variations, for example in the origin of the dsRNAs and in the number of homologous RNA silencing proteins expressed.

1.4.2 The RNAi pathway

RNAi refers to a group of related gene-silencing mechanisms, which is triggered by dsRNAs that vary in length and origin. One mechanism uses relatively long dsRNA (Figure 8). On entry into the cell cytoplasm, these dsRNAs are recognized by a protein complex containing a dsRNA binding protein (Rde-4), the dsRNA-specific ribonuclease (dicer), which rapidly cleaves the dsRNA into short interfering RNA duplexes (siRNA), a DexH box helicase (drh-1) and a Rde-1 protein which is thought to transport the siRNAs to the RNA induced silencing complex (RISC) (Geldhof, 2007). The siRNAs are typically 21-28 base pairs in length and have 5' phosphates and 2-nucleotide 3' overhangs. Assisted by an RNA helicase (drh-1), the siRNA-duplexes are unwound prior to assembly into RISC to help interactions with the target mRNA (Martinez,

2002). The functional RISC contains only single-stranded siRNA, i.e. the strand complementary to the targeted mRNA (antisense) is incorporated into RISC. Then the single-stranded siRNAs in RISC guide the complex to the appropriate sequences in cellular RNA or DNA. RISC contains an endonuclease that cleaves the targeted mRNA within the hybridized region. As mentioned, siRNAs are also able to target DNA (Dernburg, 2000). Complementary sequences in DNA are most likely targeted by pairing of RISC with nascent RNA transcripts, leading to a histon methylation, which in turn recruits histone deacetylase to silence the chromatin. Alternatively, siRNAs can also serve as a primer for a RNA-dependent RNA polymerase, creating many more siRNAs, thus amplifying or maintaining the RNAi signal. This could explain the catalytic mechanism of RNAi, because only a few dsRNA molecules are required to degrade a much larger mRNA population (Fire, 1998).
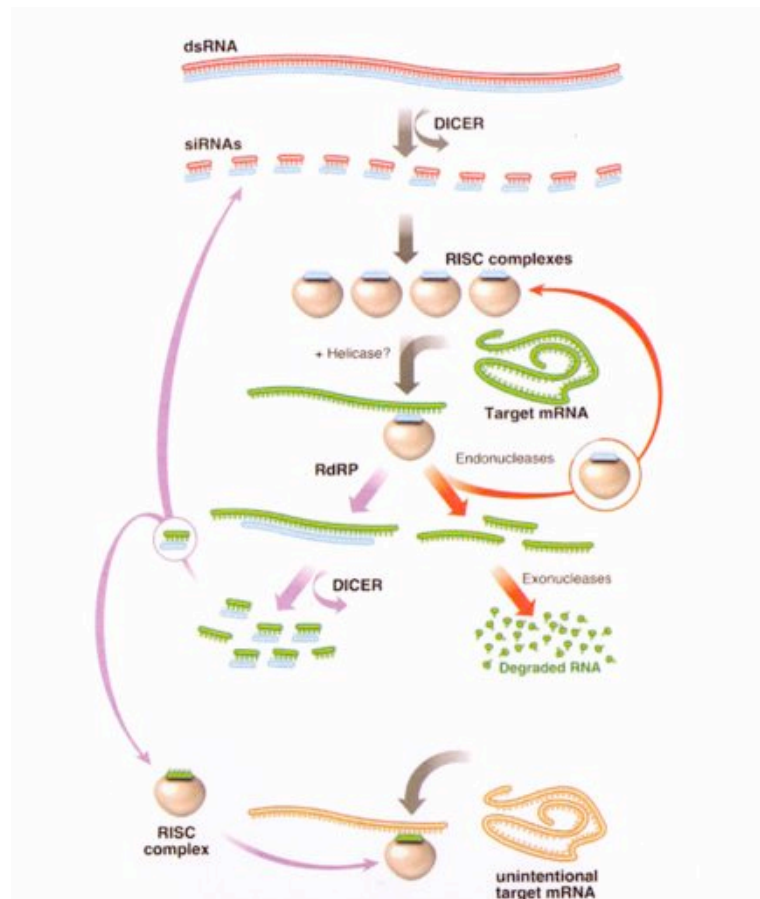
Figure 8. Schematic overview of RISC formation and dsRNA-mediated mRNA degradation.

On entry into cells, dsRNA is cleaved by Dicer into 21- to 23-nucleotide siRNAs. These siRNAs bind several proteins to form a large multiprotein complex, RISC, which is thought to unwind the siRNA to help target the appropriate mRNA. The siRNA/mRNA hybrid is cleaved, releasing the siRNA, and the mRNA is degraded by endo- and exonucleases. In worms and plants, the siRNA can also serve as a primer for an RNA-dependent RNA Polymerase, creating more siRNAs (Dillin, 2003).

1.4.3   The characteristics of RNAi

Sequence-specific gene silencing can be found in almost every organism (Maine, 2000), but was first described in *Caenorhabditis elegans* (Fire, 1998), and later demonstrated in a wide range of other organisms, including parasitic nematodes (Hussein, 2002; Urwin, 2002; Aboobaker, Blaxter, 2003; Lustigman, 2004; Ford, 2005; Issa, 2005).

Fire *et al*. (1998) showed in *C. elegans* that the RNAi effect spreads systemically by the activity of the SID and RSD proteins throughout the whole organism. Systemic RNAi, the RNAi signal travels from cell to cell over long distances, is apparently restricted to worms and plants, where it is called posttranscriptional gene silencing or PTGS (Weiner, 2003). Feinberg and Hunter (Feinberg, Hunter, 2003) discovered a single transmembrane protein (SID-1) in *C. elegans* that allowed passive uptake of dsRNA in *Drosophila* cells that naturally lack systemic RNAi. SID-1 preferentially transports large dsRNA with the result that 500 bp dsRNA silenced up to 1000-fold better than 100 bp dsRNA, and 100 bp dsRNA silenced about 10^5-fold better than 21 bp siRNAs. Other research groups have shown that the RNAi effect is heritable to several consecutive generations without alteration of the genome by microinjection of dsRNA (Montgomery, Fire, 1998; Chuang, Meyerowitz, 2000; Grishok, 2000; Shi, 2000; Mello, Conte, 2004). Methods developed for RNAi in *C. elegans* have also been used in parasitic helminths of animals and plants with variable success (Lendner, 2008). It is unclear why some of the genes tested are more susceptible to RNAi than others. Differences in location, stability and/or levels of target transcript in the parasite could be important.

However, several research groups were unable to identify genes, which are thought to be essential for a functional systemic RNAi pathway, including *rde-4* (RNA binding in dicer complex), *rde-2* (siRNA accumulation), *sid-2* and *rsd-2* (both: systemic RNAi) in *H. contortus* and *B. malayi* and the corresponding available species EST data sets (Zawadzki, 2006; Knox, 2007). In recent studies, there was also no functionally conserved SID-1 orthologue in filarial worms identifiable (Ghedin, 2007; Hong, 2008; Kang, Hong, 2008; Viney, Thompson, 2008).

The possible absence of the mentioned genes in some parasitic nematodes could infer the lack of an effective uptake and spreading pathway. It is also possible that there are fundamental differences between the RNAi pathways of these nematodes such that alternative pathways might exist.

1.4.4 Delivery methods of dsRNA

Several delivery methods including soaking, hairpin transgenes, microinjection and feeding of bacteria expressing the dsRNA are known to effectively knockdown transcript levels of targeted genes in *C. elegans* (Mello, 1991; Tabara, 1998; Timmons, Fire, 1998; Tavernarakis, 2000; Timmons, 2001; Britton, Murray, 2002; Johnson, 2005). All these methods have been successfully used in large-scale screens of gene function in *C. elegans* (Maeda, 2001; Simmer, 2003; Sonnichsen, 2005).

In parasitic nematodes, Issa *et al.* (Issa, 2005) showed effective RNAi in the sheep gastro-intestinal parasite *Trichostrongylus colubriformis* by electroporation using dsRNA and small synthetic siRNA molecules. Another group introduced dsRNA via electroporation in *Schistosoma mansoni* and obtained specific and long-lasting suppression for >30 days (Correnti, 2005).

1.4.5 RNAi in filarial nematodes

RNAi in filarial nematodes was first described in *B. malayi* (Aboobaker, Blaxter, 2003). This group experimentally demonstrated the uptake of dsRNA by adult *B. malayi* by soaking the worms in FITC-labeled dsRNA. Soaking of these nematodes with dsRNA to β-tubulin, microfilarial sheath protein and RNA polymerase II large subunit led to a reduction in gene expression and a visible phenotype when using microfilarial sheath protein dsRNA. Another group established RNAi in *Onchocerca volvulus* L3 larvae and observed a significant molting defect phenotype when targeting two cysteine proteases, *Ov-cpz* and *Ov-cpl* (Lustigman, 2004), and the serine protease inhibitors *Ov-sp-*1 and *Ov-sp-2* (Ford, 2005). The success of this technique in adult *B. malayi* and then later in *O. volvulus* larvae was exciting to the field of filariasis as previously there were no genetic tools for filarial nematodes. However, the technique as described for *B. malayi* had its limitation. The dsRNA concentration used was extremely high, circa 15 μM. The financial cost to perform experiments with such high concentrations of dsRNA would hinder effective RNAi studies in filariae. Additionally, the authors themselves conceded that there was apparent off-target gene inhibition in *B. malayi*. Off-target effects in other systems have been shown to be the result of toxicity due to high dsRNA concentration (Yang, 2000; Huppi, 2005).

1.5 Objectives

Wolbachia, the obligate intracellular endosymbionts of most filarial nematodes, are essential for embryogenesis and larval development into adult worms, and thus represent a new target for antifilarial drug development. Despite many years of interest, very little is known about the molecular basis of the interaction in the symbiosis between *Wolbachia* and its filarial host. Thus, the aim of this study was to address questions concerning the biological function of *Wolbachia* in the mutualistic symbiosis with its nematode host.

- Why do filarial nematodes carry *Wolbachia*?
- Why are *Wolbachia* so important to their filarial hosts?
- What kind of metabolites and/or pathways may be provided from *Wolbachia* to the nematode?

Differential display PCR, a molecular technique to enrich differentially expressed genes, was used to screen for alterations in gene expression, as the microarray technique was not yet available for filariae at the beginning of this work. The goal of this study was to find nematode genes that were up-regulated after depletion of *Wolbachia* endobacteria upon tetracycline treatment, and to define the potential function of these genes in the mutualistic relationship. Further analyses and characterization of these genes would contribute to a better understanding of the symbiosis.

The second part of this thesis describes the establishment of RNA interference in our model organism, the rodent filaria *L. sigmodontis*. Therefore, specific silencing of the *Ls-actin* gene was performed. The former success of RNAi in filarial nematodes (adult *B. malayi* and *O. volvulus* L3) was exciting to the field of filariasis since, in the past for filarial nematodes, no other genetic tools were existent. Thus, the following questions arose:

- Is RNAi in *L. sigmodontis* a viable method to assess the biological function of filarial genes?
- If yes, is it advantageous to use *L. sigmodontis* for RNAi studies to identify and validate potential new drug targets?

2 Material and Methods

The specific instruments used in these studies will be mentioned in the corresponding section of the materials and methods. All of the chemicals whose supplier is not specified in this section are either from Sigma-Aldrich (Taufkirchen, Germany), Fluka (Neu-Ulm, Germany) or Merck (Darmstadt, Germany); the culture medium and its additives are from PAA Lab. (Coelbe, Germany).

2.1 Animals

2.1.1 Animal maintenance

IL-5 deficient mice on BALB/c background (Kopf, 1996), kindly provided by Dr. Klaus Matthaei (Division of Biochemistry and Molecular Biology, John Curtin School of Medical research, Australian National University Canberra, Australia), were housed under specific-pathogen-free (SPF) conditions in micro-isolator cages. The mice, jirds (*Meriones unguiculatus*) and cotton rats (*Sigmodon hispidus*) were bred at the animal facilities of the Bernhard Nocht Institute of Tropical Medicine, Hamburg, and after the year 2004 at the animal facilities of the Institute for Medical Immunology, Microbiology and Parasitology, University Clinic Bonn.

Clearance for animal studies had been given to the laboratory by the appropriate authorities (Behörde für Arbeit, Gesundheit und Soziales der Hansestadt Hamburg, Genehmigungsnummer 34/99, and Bezirksregierung Köln Nummer50.203.2-BN15, 40/04 respectively).

2.1.2 Infection cycle

The parasite *L. sigmodontis* was maintained by passage through cotton rats (*S. hispidu*s) and an arthropod intermediate host, the *Ornithonyssus bacoti* mite, as previously described (Zahner, Wegerhof, 1986).

The natural infection of mice with *L. sigmodontis* was carried out as follows. Ten days prior to infection of mice, the mites, which had been kept in glass containers filled with 10 cm of bedding material and a removable cover, were allowed to have a blood meal

on an infected rat (>1000 MF/μl blood). Therefore, the infected rat was kept in a small wire cage and then placed for 4-6 hours onto the hungry mites in a mouse cage. Afterwards, the rat cage was hung overnight on the inside of the cover to allow the remaining mites to fall back into the bedding material after the blood meal. Upwards crawling mites were trapped by cotton pieces placed on the upper side of the removable cover and were returned back to the glass container. To avoid contamination of the rooms with mites, the rat cage was placed in a large tray containing water with a detergent for another 12 hours to guarantee the death of any mites that fell off during the night. After 10 days, during a subsequent blood meal, the mites transmitted the L3 larvae to the cotton rats to close the cycle, or in case of mice infection, the L3 larvae containing mites were allowed to take blood from naïve mice and thereby transmit the L3 larvae. Prior to the blood meal, the mice received 50 μl Rompun/Ketanest intramuscular as long-term anesthetic. All mentioned processes were at 80-90% air humidity and a room temperature of 26-28°C.

In the rodent host the L3 larvae migrate to the thoracic cavity and reach sexual maturity within 25-33 days. After copulation, the viviparous female worms start producing microfilariae (MF), which are detectable in the blood after 50 days.

2.1.2.1 Anesthetic

Rompun (20 mg/ml, Bayer, Leverkusen, Germany)
Ketanest (10 mg/ml, Parke-Davis, Berlin, Germany)

Rompun is diluted 1:5 (v/v) in Ketanest, (1:1 (v/v) in PBS)

Mix: 200 μl Rompun
      400 μl Ketanest
      400 μl PBS

50 μl – 100 μl of the solution were injected intramuscular depending on the size (body weight) of the mice.

2.1.3 Animal model

The fully permissive IL-5 deficient BALB/c mice (usually 6 to 8 weeks old with an average weight of 20 g) were chosen to infect with *L. sigmodontis*. IL-5 deficient mice have a parasite load up to 200-fold higher than wild type mice and a prolonged patency (Volkmann, 2001; Volkmann, 2003a). This allows a prolonged therapeutic regime of more than 2 weeks that would be difficult to perform in wild type BALB/c mice. In wild type mice, most of adult nematodes are already eliminated by their immune system on day 80 post infection. The recruitment of neutrophils and eosinophils into the pleural cavity promote encapsulation and killing of adult worms.

Another benefit in using IL-5 deficient BALB/c mice rather than wild type mice is the reduction in inflammatory nodule formation around the adult nematodes, facilitating parasite recovery for further analyses.

2.1.4 Antibiotic treatment and worm recovery

The treatment of IL-5 deficient mice infected with *L. sigmodontis* was started at day 58 post infection (the time of patency, when released MF are detected in the blood) with intraperitoneal injections of 50 mg tetracycline per kg body weight per day (Hoerauf, 1999). A single cycle of infection and treatment takes three to four months. Therefore, multiple infections and treatments were accomplished.

In separate infections, gentamicin, an antibiotic known to be ineffective in eliminating Rickettsiales, was applied at 15 mg per kg body weight per day (Hoerauf, 1999). The animals were treated daily for 36 days. Nematode worms were collected on days 3, 6, 15, 30 and 36 of the treatment trial by flushing the thoracic cavity with PBS. The nematodes were separated by sex, snap frozen in liquid nitrogen and stored at -80°C for RNA isolation. In additional experiments, the nematode worms were also collected on days 50 and 70 to analyze the expression pattern of *Ls-ppe-1*, two weeks and one month after the treatment has been stopped.

Ornithodoros moubata ticks infected with *A. viteae* (a filaria devoid of *Wolbachia*) were a kind gift from Prof. Dr. Richard Lucius (Humboldt University, Berlin, Germany). The L3 larvae were isolated and naïve *Meriones unguiculatus* were infected with 80 L3 larvae as described (Lucius, Textor, 1995). Infected animals carrying adult nematodes

were treated orally for 6 weeks with tetracycline in drinking water at a concentration of 0.5% (w/v). The water was changed daily. Treated animals were sacrificed at days 3, 6, 15, and 36 post infection and the nematode worms isolated. Nematodes were then snap frozen in liquid nitrogen and stored at –80ºC for later RNA isolation.

Tetracycline:

50 μg tetracycline dissolved in 10 ml PBS

treatment: intraperitoneal injection of 0.2 ml/mouse daily (for 36 days)

   or

   jirds: 0.5% (w/v) in drinking water (36 days)

Gentamicin:

original stock solution = 50 mg/ml

dilute to 3 mg/ml (900 μl in 15 ml PBS)

treatment: intraperitoneal injection of 0.1 ml/mouse daily (for 36 days)

PBS (phosphate-buffered saline solution)

10×PBS: 80 g NaCl

    11.6 g Na_2HPO_4

    2 g KH_2PO_4

    2 g KCl

    ad 1000 ml nanopure water

    adjust to pH 7.4 when preparing 1×PBS

2.1.5 Exposure of *L. sigmodontis* to heat and oxidative stress

Oxidative stress was applied to adult *L. sigmodontis* nematodes (recovered from the pleural cavity of jirds) with three reagents: 2 mM xanthine-xanthine oxidase; 100 μM plumbagin; and 200 mM paraquat.

Following a previously described protocol (Liebau, 2000), three replicates of five female nematodes were used for a single experiment. Nematodes were incubated for 2 hours at 37°C under different oxidative stress conditions. Each experiment was conducted twice. In parallel, *L. sigmodontis* were incubated for 2 hours at 42°C to heat

stress the nematodes (Thompson, 2001). RNA from these worms was extracted and the transcription levels of *Ls-ppe-1* quantified by RT-qPCR (see section 2.5.3). Additionally, steady state mRNA levels of the *L. sigmodontis* heat shock protein 60 gene (*Ls-hsp-60*) was measured to compare *Ls-ppe-1* expression to a known stress response gene. For further details see also Table 2 and Table 3 in section 2.5.3.

Xanthine (Sigma-Aldrich)

Stock solution: 10 mM dissolved in 0.1 N NaOH

Working solution: 0.5 mM, 1 mM, 2 mM in RPMI

Xanthine oxidase (Sigma-Aldrich)

Stock solution: 5 U/200 μl

Working solutions: 0.5 mU, 1 mU, 2 mU in RPMI

Plumbagin (Sigma-Aldrich)

Stock solution: 1 mM dissolved in 50% EtOH

Working solutions: 25 μM, 50 μM, 100 μM in RPMI

Paraquat (Sigma-Aldrich)

Stock solution: 1 M dissolved in nanopure water

Working solutions: 50 μM, 100 μM, 200 μM in RPMI

For the medium control approaches, the same amount of the appropriate solvent was added to the RPMI culture medium to exclude an effect on the gene expression coming from culturing conditions.

2.2 RNA extraction

2.2.1 Worms from human patients

Onchocercomata from 16 untreated controls and 23 doxycycline treated patients in Ghana were extirpated prior to ivermectin treatment, 5 months after the commencement of doxycycline treatment. Total RNA was isolated from these nodules using the RNeasy

Maxi kit (Qiagen, Hilden, Germany). The collagenase protocol for heart and muscle tissue was followed. DNase treatment of the RNA was performed on the column.

2.2.2 Worms from animals

Ten adult female nematodes in 350 μl RLT buffer (containing 10mM BME) were finely minced with scissors. To homogenize the solution, the lysate was applied onto a QIAshredder column (Qiagen) and centrifuged for 3 min at maximum speed in a tabletop centrifuge (Eppendorf). Total RNA was then isolated using the RNeasy kit (Qiagen) according to the manufacturer's protocol. The RNA was eluted in 50 μl water. To eliminate genomic DNA contamination, a DNA digest with RNase free DNase I (Ambion, Austin, TX, USA) was performed for 30 minutes at 37°C. Next, the RNA was extracted with phenol chloroform and then precipitated with lithium chloride at a final concentration of 2.5 M (Ambion) and 10 μg/ml linear acrylamide (Ambion) as co-precipitant.

For better isolation of small quantities of RNA and to reduce genomic DNA contamination, a modified Trizol extraction recommended for small volumes was used. In detail, ten female nematodes in 800 μl Trizol reagent (Invitrogen GmbH, Karlsruhe, Germany) were finely minced with scissors and then homogenized with a glass-glass homogenizer at 1200 rpm (Sartorius BBI Systems, Melsungen, Germany). Instead of chloroform, 80 μl 1-bromo-3-chloro-propane (BCP*) (Sigma-Aldrich, Steinheim, Germany) was added to separate the homogenate into RNA-containing aqueous and DNA- and protein-containing organic phases. DNase treatment was performed as described above and then removed following the RNeasy clean up protocol (Qiagen).

For the RNAi experiments, DNase removal and RNA concentration was achieved using the RNeasy MiniElute Kit (Qiagen), for which the elution volume could be reduced to 10 μl per sample.

Note: BCP is less toxic than chloroform and its use reduces the possibility of contaminating RNA with DNA (Chomczynski, Mackey, 1995).

2.2.3 Determination of the RNA concentration

RNA concentration was determined at 260 nm using an Eppendorf BioPhotometer (Eppendorf Inc., Wesseling, Germany). The quality of extracted RNA was assured by spectrophotometric determination of the $OD_{260/280}$ ratio. A ratio of $1.7-2.0$ was considered to be free of contaminations such as phenol and proteins.

2.2.4 Reverse Transcription

In general, 1 μg of total RNA was reverse transcribed with the Omniscript RT Kit (Qiagen) according to the manufacturer's instructions with oligo-dT primer (Roche), which bind to the poly-A tail of the mRNAs and thus lead to a selective transcription. Briefly, the reagents listed in Table 1 were combined and vigorously mixed. Template RNA was added and the solution mixed again, followed incubation at 37°C for one hour to reverse transcribe the template RNA into cDNA. The cDNA was then stored at –20°C for further analysis.

Table 1. Reaction mixture for Reverse Transcription

Components	Volume	Final concentration
10× buffer RT	2.0 μl	1×
dNTP mix	2.0 μl	0.5 mM (of each dNTP)
oligo-dT primer (10 μM)	2.0 μl	1 μM
RNase inhibitor (10 units/μl)	1.0 μl	10 U
Omniscript Reverse Transcriptase	1.0 μl	4 U
RNase-free water	variable	
RNA template	variable	1 μg
Final volume	20 μl	

2.3   Differential Display

Differential display PCR, first reported in 1992 (Liang, Pardee, 1992; Liang, 1994), is the method of choice, which allows the identification of differentially expressed genes in a less labor-intensive way than subtractive library screening and differential hybridization. Compared to the other techniques mentioned, DD-PCR has some important advantages: (i) no need to construct and screen libraries, (ii) only small quantities of RNA are required, (iii) recognition of subtle changes, (iv) study of more than two variables simultaneously. The procedure consists of two major steps: (i) reverse transcription of RNA isolated from different cell populations with anchored oligo-dT primers to generate cDNA pools, and (ii) PCR amplification of random sequences from the cDNA pools with the original anchored dT primer and an upstream arbitrary primer (Figure 9).
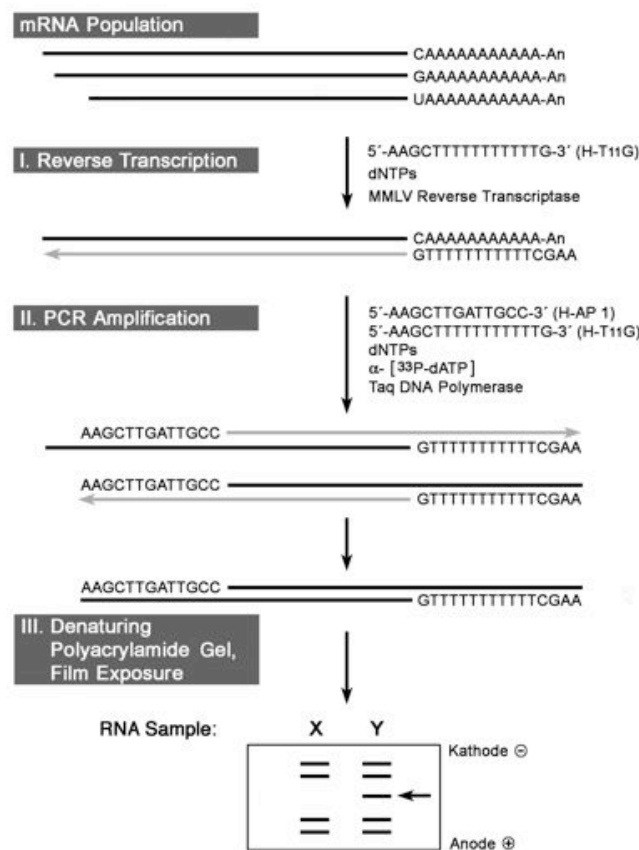
Figure 9. The principle of Differential Display.

RNA is reverse transcribed with one-base anchored oligo-dT primer (HT$_{11}$A, HT$_{11}$C, and HT$_{11}$G, GenHunter); 3 cDNA pools result. DD PCR is performed using a series of arbitrary primers (H-AP-1 to H-AP-14, GenHunter) and the original anchored oligo-dT primer. PCR products run on a sequencing gel, and following exposed to X-ray film to identify differentially expressed genes. Subsequently, the selected fragments are re-amplified and cloned for further confirmation analyses.

2.3.1 cDNA synthesis for Differential Display

To facilitate the resolution of specific differential display PCR (DD PCR) products in denaturing polyacrylamide gels, three sub-populations of cDNA were generated for the DD PCR (Figure 9). For this, 200 ng total RNA were reverse transcribed in separate reactions with three one-base anchored oligo-dT primer: $HT_{11}\underline{A}$, $HT_{11}\underline{C}$, and $HT_{11}\underline{G}$ (GenHunter, Nashville, TN, USA) using the Omniscript Reverse Transcriptase kit (Qiagen) (see Table 1). Finally, 2 μl of the generated cDNAs were used as template in the DD PCR.

2.3.2 Differential Display PCR

In the DD PCR amplification, 2 μl (= 20 ng) of the resulting cDNA subpopulation were used in a 20 μl reaction mixture consisting of 1× PCR Buffer (Qiagen), 20 μM dNTPs (without dATP), 0.2 μM arbitrary primer (H-AP-1 to H-AP-14, GenHunter), 5 μCi ^{33}P-dATP (Amersham Biosciences, Freiburg, Germany), 1.25 U Taq DNA polymerase (Qiagen) and 0.2 μM of the one-base anchored oligo-dT primer originally used for the cDNA synthesis. The reaction mixture was then covered with oil to avoid evaporation. After an initial denaturation at 95°C for 5 min, amplification was performed for 25 cycles of 94°C - 30 s; 40°C - 2 min; 72°C - 30 s, and a final extension step at 72°C - 10 min, followed by a 4°C hold.

During the optimization process, the dNTP concentration was lowered from 200 μM to 20 μM, the annealing temperature was finally changed from 45°C to 40°C, and the PCR cycle numbers were also reduced from 40 to 25 cycles to avoid the amplified products reaching the plateau phase, where changes in the expression pattern could not be analyzed.

2.3.3 Preparation of denaturing polyacrylamide gels

Prior to pouring the gel, the two siliconized glass plates were cleaned in three steps: first with 0.1 M NaOH, then rinsed with 10% SDS, followed again by rinsing with 0.1 M NaOH, and subsequently rinsed off with hot water followed by a rinse with deionized water. Finally, 80% ethanol was used to clean the glass plates and to make them fat-free. This procedure is not necessary every time. For regular use, the glass plates were cleaned in soap water, rinsed with deionized water, and finally rinsed with 80% ethanol to dry the plates.

The polyacrylamide solution was then carefully poured between the two glass plates (without air bubbles) while the upper glass plate was slowly moved forwards. After including the comb, the gel was allowed to completely polymerize overnight (wrapped in wet paper towels to avoid drying out).

Denaturing gel (6% polyacrylamide/ 8M urea)

for 100 ml: 42 g   urea

10 ml   10x TBE

20 ml   40% acrylamide (19:1)

340 μl 10% APS

140 μl TEMED

Loading dye for denaturing gels

for 1 ml: 98%   formamide (980 μl)

10 mM   EDTA (20 μl)

0.025%   xylene cyanol

0.025%   bromophenol blue

store at –20ºC.

2.3.4   Differential Display gel electrophoresis

It is recommended to pre-electrophorese the gel prior to loading the samples on the gel. This step helps to remove reactive charged compounds (persulfate anions) and low molecular weight impurities from the gel that may cause artifacts. Additionally, it heats the gel (no temperature gradient) to facilitate the separation of the PCR products. Therefore, the empty gel was started for at least 30 min at 1500 V in TBE buffer. Meanwhile, 3 μl loading dye and 3 μl of the radioactive DD PCR product were mixed, heated for 2 min at 95ºC, and then the tubes placed directly on ice. The samples were loaded onto the gel (controls and tetracycline treated samples of each time point side-by-side for a better comparison) and run for ~3 hours at 1500 V. For a better separation of the bands on top of the gel, 100 ml 3 M sodium acetate (NaAc) were added to the lower buffer chamber and the run continued for another 30 to 60 min until the lower dye front (bromophenol blue) reached the bottom of the gel.

2.3.5   Visualization of DD PCR amplicons

After carefully removing the gel from the glass plates, it was placed onto Whatman paper, covered with Saran Wrap and dried for 2 hours at 80ºC in a gel-dryer under vacuum. After an overnight exposure to a Kodak Biomax MR, the film was developed and the visualized bands were examined for differential gene expression by comparing control and tetracycline treated samples. The bands of interest were then excised from dried gels.

2.3.6   DNA gel elution and re-amplification

To isolate the gene fragments, the dried gel was carefully realigned with the autoradiograph, and a sterile scapel was used to excise the cDNA fragments. A second exposure to X-ray film was then performed to confirm that the correct fragments had been excised. To elute the DNA fragments from polyacrylamide gel, the bands were placed in 100 μl H_2O_{DEPC}, incubated for 5 min at room temperature and then heated for

15 min at 95ºC. After ethanol precipitation with 3 M NaAc the DNA was dissolved in 10 μl H_2O_{DEPC}.

4 μl of the gel-eluted fragments were used to re-amplify the differentially expressed bands by PCR using the matching set of primers and the same conditions as in the initial DD PCR reaction, omitting radioactivity. The PCR products were then cloned with the TOPO-TA cloning kit (Invitrogen, Karlsruhe, Germany) following the manufacturer's protocol.

Ethanol precipitation of DNA

1/10 Vol.	3 M NaAc
3 Vol.	absolute Ethanol

The mixture was precipitated for at least 1 hour at -20ºC, then centrifuged at 4ºC, at 14.000 rpm (Hettich Universal 32R, Tuttlingen, Germany) for 20 to 30 min. The supernatant was then removed, and the pellet dissolved in 10 μl H_2O_{DEPC}.

2.4   Antisense RNA (aRNA) amplification

To produce hundreds to thousands of antisense RNA copies of each mRNA in a sample, the MessageAmp aRNA kit (Ambion) was used following the manufacturer's protocol (Baugh, 2001). Briefly, for first strand cDNA synthesis 2 μg total RNA from tetracycline-treated or untreated control nematodes have been reverse transcribed with an oligo-dT primer bearing a T7 promoter. Second strand synthesis was achieved using the Second Strand Synthesis Buffer, dNTP mixture, RNase H, and DNA polymerase I of the kit (Ambion). T7 RNA polymerase was then used in the *in vitro* transcription to generate antisense RNA, whose primary application is the preparation of labeled cDNA probes for hybridization (Figure 10).
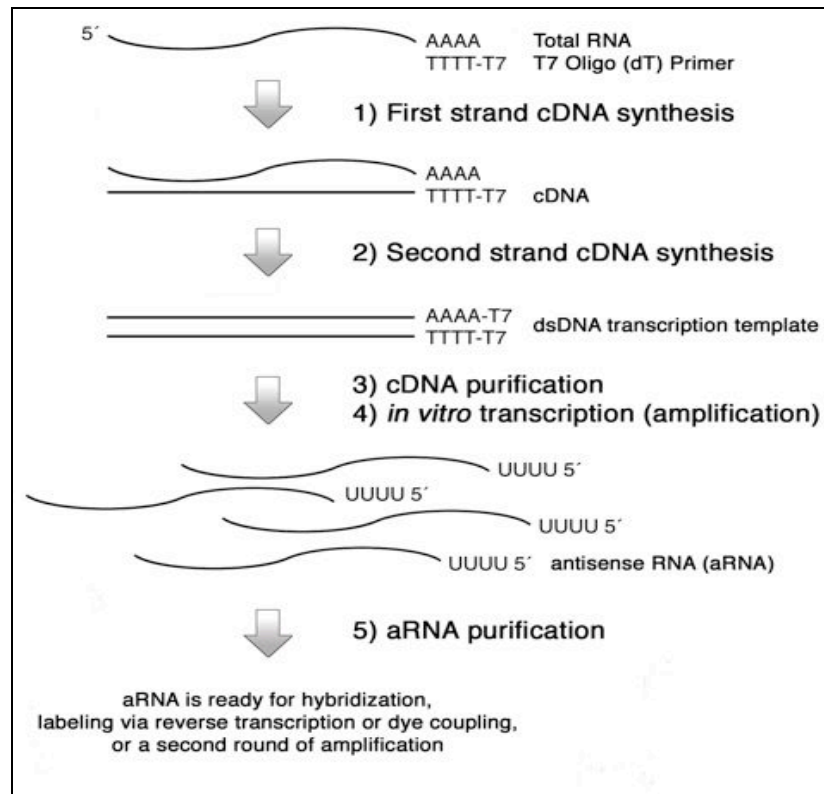
Figure 10. Schematic MessageAmp aRNA procedure.

2.4.1 Synthesis of fluorescein labeled cDNA probes

In general, 2 μg of aRNA were reverse transcribed with the Omniscript RT Kit (Qiagen) according to the manufacturer's instructions with 10μM oligo-dA primer (Roche). Briefly, the reagents listed in Table 1 were combined and vigorously mixed. The aRNA was added and the solution mixed again, followed by one hour incubation at 37°C to reverse transcribe the aRNA into single-stranded cDNA. The cDNA was then stored at –20°C for future use. The generated cDNAs were labeled with Amersham ECL Direct™ Nucleic Acid Labeling and Detection System (Amersham Biosciences). Therefore, 1 μl of the cDNA (= 100 ng) were mixed with 19 μl H_2O and boiled for 5 minutes. Afterwards, the following kit components were added:

> 10 μl dNTP mix
>
> 5 μl primer
>
> 14 μl H_2O
>
> 1 μl Klenow enzyme
>
> 50 μl final volume

The mixture was incubated for 1 hour at 37ºC, and the reaction stopped with 2 μl 0.5 M EDTA. The labeled probes were then kept in the dark at -20ºC.

25 μl (= 50 ng) of the ECL-labeled probes were denatured for 5 min at 99ºC, and subsequently used for dot blot hybridization (see section 2.5.1).

Note: The ECL kit is based on the direct labeling of DNA or RNA probes with horseradish peroxidase (HRP) in a simple chemical reaction. The resulting probe can be used without purification. Detection is achieved by generation of light via the HRP-catalyzed breakdown of luminol.

2.4.2   Synthesis of ^{32}P labeled cDNA probes

Radioactive labeled cDNA probes were made from aRNA using the SuperScript II RNaseH-RT Kit (Invitrogen), following the method from Poirier and Erlander (1998). 2 μg aRNA and 750 ng random hexamers were mixed together and incubated for 10 min at 70°C, the tubes were placed on ice and the following components added:

5 μl	5× first strand buffer
2.5 μl	25 mM MgCl$_2$
2.5 μl	0.1 M DTT
1 μl	20 mM d(GAT)TPs
1 μl	120 μM dCTP
5 μl	conc. ^{32}P-dCTP (3000 Ci/mmol = 100 μCi)
24 μl	final volume

Following an initial incubation at 42°C for 5 min, 1 μl SuperScript RNaseH-Reverse Transcriptase was added and incubated at 42°C for 1 hour. Then, RNA was hydrolyzed with 3 μl 3M NaOH (68°C, 30 min) and the reaction subsequently neutralized with:

10 μl	1 M Tris-HCl (pH 7.4)
3 μl	2 M HCl
9 μl	water
50 μl	final volume

Unincorporated nucleotides were removed using a Nucleotide Removal Kit (Qiagen) following the manufacturers protocol. The probe concentrations were normalized by comparing the incorporation of ^{32}P-dCTP as assessed by liquid scintillation counting (LKB Wallac 1205 Betaplate, Perkin Elmer, Waltham, MA, USA) before and after the clean up step.

2.5   Validation of Differential Display results

After DD PCR and cloning of the differentially expressed fragments, three independent methods: Reverse Northern (Reverse dot blot), Northern blot analysis (to semi-quantify) and RT-qPCR (to quantify) were used to confirm the genes obtained by differential display and exclude false-positive candidates from further investigations.

2.5.1   Reverse Northern

For the reverse dot blot method, plasmids containing each candidate gene were isolated with the Qiaprep Spin Miniprep kit (Qiagen). Plasmids (6 μg each) were spotted onto Hybond N+ nylon membranes (Amersham Biosciences, Buckinghamshire, UK) using a 96-well dot blotter (BioRad, Hercules, CA, USA) and then UV cross-linked. Separate blots were hybridized overnight at 45°C in Perfect Hyb solution (Sigma-Aldrich) with either ECL-labeled or α-^{32}P dCTP-labeled cDNAs from control or the different tetracycline treatment time points.

The radioactive cDNA probes were generated according to the procedure previously described by Poirier and Erlander (1998) using 2 μg aRNA and 100 μCi (3000Ci/mmol) α-^{32}P dCTP. In another approach, radioactive PCR products (see 2.3.2) generated by a second DD PCR (for which gel-eluted fragments of the initial DD PCR served as DNA template) were also hybridized to the dot blot membranes. Both kinds of radiolabeled probes, the DD PCR products from different primer combinations and the cDNA probes generated from aRNA, were cleaned with a Nucleotide Removal Kit (Qiagen), normalized by comparing the incorporation of α-^{32}P dCTP by liquid scintillation counting, and then mixed (the same counts) to probe a single blot for either controls or tetracycline. As expected from the literature (Poirier, Erlander, 1998), an average

incorporation of 20 to 30% could be obtained. Hybridization of the dot blots was performed in the presence of 4.5×10^6 to 2×10^7 cpm/cDNA probe.

The hybridized blots were washed three times in $1 \times$ SSC, 0.1% SDS for 30 min at 45°C and then exposed to X-ray film or Phosphor Imager SI screen (Amersham Biosciences). The program Image Quant for Macintosh version 1.2 (Molecular Dynamics, Sunnyvale, CA, USA) was used to analyze the data. Only genes that were up-regulated by at least a factor of 1.5 (arbitrary decision) were analyzed further using Northern blot and qPCR.

$20\times$ SSC (pH 7.0)

      0.3 M Na_3 citrate

      3   M NaCl

2.5.2 Northern blot analysis

2.5.2.1 RNA gel preparation and running conditions

For a 1.2% formaldehyde gel, 0.9 g agarose were dissolved in 50 ml H_2O_{DEPC} (RNase-free water) by heating in a microwave and allowed to cool to ~60°C. In a fume hood, 7.5 ml of $10\times$ Running buffer, 13.4 ml formaldehyde (18% fin. conc.) and H_2O_{DEPC} were added to a final volume of 75 ml. The gel was then poured into a gel tray. After 30 min the gel is completely solid and the samples can be loaded.

The RNA samples were mixed with 5 μl RNA-loading dye (Invitrogen), heated for 5 min at 65°C, and then chilled on ice. The samples were loaded onto a horizontal gel and the RNA electrophoresed at 100 V for 2 hours (until the bromophenol blue dye had migrated two-thirds the length of the gel).

Note: Adding ethidium bromide at a final concentration of 1 mg/ml to each sample made staining and destaining of the gels unnecessary.

$10\times$ Running Buffer

0.2 M	MOPS buffer, pH 7.0 [3-(N-morpholino) propanesulphonic acid]
50 mM	NaAc
10 mM	EDTA, pH 8.0

H₂O$_{DEPC}$

Working solution (0.1%):

   1mL DEPC [diethylpyrocarbonate] in 1L destilled water

   solution stirred overnight under a fume hood and autoclaved next day

   (DEPC in water dissociates in volatile CO_2 and ethanol)

Note: DEPC-water is typically used to treat water and other solutions to remove RNases.

2.5.2.2   Northern blot technique

For Northern blots, RNA (2-4 μg/lane) was separated on a 1.2% agarose gel containing 18% formaldehyde (see section 2.5.2.1) and transferred overnight to Hybond N+ nylon membrane in 10× SSC. Radioactive probes for *Ls-ppe-1* (using the initial differential display clone) and *O. volvulus 5S* ribosomal RNA were made from 25 ng of excised insert fragments labeled with α-^{32}P dCTP using the Random Primers DNA Labeling System (Gibco BRL, Eggenstein, Germany). The blot was probed overnight at 45°C in 7 ml Perfect Hyb solution (Sigma-Aldrich) and 1 ml formamide. Blots were washed three times in 1× SSC, 0.1% SDS for 30 min at 45°C and exposed to X-ray film. The software ImageQuant for Macintosh version 1.2 (Molecular Dynamics) was used to quantify the data.

2.5.3   Real time-quantitative PCR

In general, RT-qPCR was carried out on a RotorGene 3000 (Corbett Research, Sidney, Australia) using Sybr Green I (Roche). The LightCycler (Roche) was only used to measure the *Ov-hsp60* transcript levels, at a time when the RotorGene was not yet available in the laboratory. Both cycling machines use hot air to achieve rapid, controlled heating and cooling of the samples. The RT-qPCR delivers reproducible quantification of the amplification products. As tested, the results were comparable between these two machines. Gene specific primers (listed in Table 2) were designed using the online program Primer 3 located at the URL http://frodo.wi.mit.edu/cgi-bin/primer3/primer3_www.cgi.

40

Primer requirements

- primer length: 18-23 bp
- primer melting temperature: min. 58°C, max. 62°C
- product size: 100-200 bp
- GC content: 30-70%

Table 2. Primer sequences used in RT-qPCR

gene target	primer name	sequence 5'→ 3'
Ls-ppe-1	DD9_F1	AGGCCAAGTTTACTGGCTGTT
Ls-ppe-1	DD9_R1	CTGGATGTTCGACAACGAAGT
Ls-hsp60	LsHspLC_F2	TACGTGAGCCAATCATGACA
Ls-hsp60	LsHspLC_R2	ATCATATCCAAACGCCAACTC
Ls-gst2	UnivGst2_F1	GTGCAGTCCGGTGCTATTCT
Ls-gst2	UnivGst2_R1	ATCACGGATGCCTTCACAG
Ls-18S	Ls18S_F1	GTACAAAGGGCAGGGACGTA
Ls-18S	Ls18S_R1	CATTGCCGAAAGGTACTGGT
Ls-act / Ov-act	OvActin_F1	GTGCTACGTTGCTTTGGACT
Ls-act / Ov-act	OvActin_R1	GTAATCACTTGGCCATCAGG
Ov-hsp60	OvHsp60LC Fw	CCGGTATGGGAGGAATGTACT
Ov-hsp60	OvHsp60LC Rv	TAAGACTCCCTGTTCGCTCAA
Ov-ftsz	Ov wFtsZ F	AGGAATGGGTGGTGGTACTG
Ov-ftsz	Ov wFtsZ R	CTTTAACCGCAGCTCTTGCT

2.5.3.1 Cycling conditions

RT-qPCR was performed in duplicate (LightCycler) or in triplicate (RotorGene) using the following conditions: 1× PCR buffer (Qiagen), 0.2 μM dNTPs, 0.1 μl Sybr Green (1:1000 dilution of stock in DMSO; Roche), 0.25 U Hotstar Taq polymerase (Qiagen) and 2 μl cDNA in a reaction volume of 10 μl. For the LightCycler: the reaction volumes were scaled up to 20 μl final volume). The optimized reaction conditions including final $MgCl_2$- and primer concentrations for each gene and the corresponding cycling

41

conditions used in RT-qPCR are listed in Table 3. Fluorescence was acquired at the end of each cycle at 72°C using the Sybr Green channel. After amplification, the melting curve from 62°C to 99°C was measured to check specific product amplification. The number of RNA molecules (copies/μl) was determined using a gene specific standard curve of plasmids linearized with *Hind*III in every run. The transcript levels were normalized to *Ls-act*, or in the case of the RNAi experiments to *Ls-18S*, to compensate for differences in expression due to under- or over-estimation of the RNA template in the reverse transcription reactions.

Table 3. Optimized reaction and cycling conditions used in RT-qPCR

gene target	[MgCl$_2$]	[primer]	initial denaturation	cycle number	cycling conditions
Ls-ppe-1	4.0 mM	300 nM	94°C 15 min	35	94°C 10 s 58°C 15 s 72°C 15 s
Ls-act	3.0 mM	900 nM	94°C 15 min	35	94°C 10 s 52°C 15 s 72°C 15 s
Ls-hsp60	4.5 mM	300 nM	94°C 15 min	40	94°C 15 s 58°C 20 s 72°C 20 s
Ls-gst2	2.5 mM	200 nM	94°C 15 min	40	94°C 10 s 58°C 20 s 72°C 20 s
Ls-18S	2.0 mM	300 nM	94°C 15 min	35	95°C 10 s 54°C 10 s 72°C 15 s
Ov-hsp60 *	4.5 mM	F 900 nM R 300 nM	94°C 15 min	40	94°C 20 s 58°C 20 s 72°C 20 s
Ov-ftsz	1.5 mM	F 300 nM R 300 nM	94°C 15 min	30	94°C 15 s 58°C 30 s 75°C 30 s

* BSA at a final concentration of 2 μg/μl was included in the reaction mix using the LightCycler (Roche).

2.6   Optimization of the RT-qPCR

Besides optimizing the assay conditions (temperature profile), the optimal primer and $MgCl_2$ concentrations have to be determined separately for each target gene. This is especially important for SYBR Green detection assays, as relatively low primer concentrations are preferable to avoid primer-dimer formation, because SYBR Green is a generic fluorophore that detects any double-stranded DNA (dsDNA) by intercalating into the minor groove of the DNA double helix.

For most applications, primer concentrations between 50 nM and 300 nM were tested against $MgCl_2$ concentrations ranging from 1.5 mM to 5 mM. Once the run is completed, the cycle threshold (Ct) for each combination was examined. The combination that resulted in the lowest Ct value and the highest fluorescence was selected. It is also crucial to analyze the melting curve for each combination tested to ensure that only a single homogenous product has been generated. All amplified products can be visualized in the melting curve following the amplification reaction. If several primer combinations give very similar results, the one with the lowest overall concentration should be used.

2.6.1   Cloning of PCR products

PCR products were cloned into the TOPO-TA cloning vector (Invitrogen, Karlsruhe, Germany) according to the manufacturer's instructions. Therefore, 4 μl of the PCR product, 1 μl salt solution (kit reagent) and 1 μl TOPO-TA cloning vector were combined and gently mixed. After 15 min incubation at room temperature, 4 μl of the reaction mixture was added to chemically competent *Escherichia coli* DH5α bacteria (supplied with the kit), and incubated for 5 min on ice. Then, 10 μl and 40 μl of the transformed bacteria solution were spread on pre-warmed agar plates containing ampicillin (100 μg/ml), IPTG (0.5 mM), X-gal (40 μg/ml). Plates were incubated overnight at 37°C. The plasmid-containing positive colonies (white) as determined by blue/white screening were picked, confirmed by colony PCR with either vector primers or gene-specific primers, and subsequently cultured overnight in 5 ml Circlegrow medium containing 50 μg/ml ampicillin for plasmid isolation.

2.6.2 Indicator plates for blue/white selection

35 g LB (Luria-Bertani, Sigma) agar were dissolved in 1000 ml nanopure water and autoclaved for 20 min at 15 psi. The solution was allowed to cool to 55ºC, and was then supplemented with 100 μg/ml ampicillin, 0.5 mM IPTG and 40 mg/ml X-gal. The solution was poured into culture dishes, allowed to solidify and then stored at 4ºC until further usage.

2.6.3 Liquid medium for overnight cultures

40 g Circlegrow powder (Q-Biogene, Heidelberg, Germany) were dissolved in 1000 ml nanopure water and autoclaved for 20 min at 15 psi and stored at 4ºC until further use. Circlegrow is used as liquid medium for overnight cultures and contained 50 μg/ml ampicillin.

Ampicillin (Sigma-Aldrich)

Stock solution: 100 mg/ml ampicillin dissolved in sterile nanopure water

X-gal

(5-bromo-4-chloro-3-indolyl-beta-D-galactoside; Labscientific, Livingston, NJ, USA)

Stock solution: 20 mg/ml X-gal dissolved in dimethylformamide

                              stored at 4ºC in the dark

IPTG

(isopropylthio-beta-D-galactoside; Labscientific, Livingston, NJ, USA)

Stock solution: 1 M dissolved in nanopure water with subsequent sterile filtration

2.6.4 Long-term bacterial storage

To prepare a frozen permanent stock solution, 850 μl of the overnight culture were mixed with 150 μl sterile glycerol, shock frozen in liquid nitrogen and then stored at –80°C until further use.

2.6.5 Plasmid preparation and sequencing

Alkaline lysis was performed to isolate the plasmids from 5 ml overnight culture using the Qiaprep Spin Miniprep kit (Qiagen) according to the manufacturer's instructions. About 2 μg of the yielded plasmid were sent for sequencing to verify the insertion of the cDNA into the vector (MWG Biotech AG, Ebersberg, Germany).

2.6.6 Standard gel electrophoresis

In electrical fields, DNA molecules of different sizes can be determined by separation in standard agarose gels. Agarose was dissolved in TBE buffer by heating in a microwave, after cooling down to ca. 50°C, 0.2 μg/ml ethidiumbromide (EtBr) was added. The solution was poured into a horizontal gel tray (BioRad, Munich, Germany). 5 μl of the PCR product were mixed with 1 μl 6× loading dye (MBI-Fermentas, St. Leon-Rot, Germany) and applied into the slots of the gel. Electrophoresis was performed at 100 Volt for 30 to 40 min in TBE buffer. DNA was then visualized by the activation of the DNA intercalating substance ethidiumbromide by UV light and photographed (Mitsubishi, Japan). The molecular weight was standardized with a DNA molecular weight marker (100 bp Marker; MBI-Fermentas, St. Leon-Rot, Germany) run on the same gel.

TBE (Tris-borate-EDTA)

10× Stock solution: 108 g Tris
                                     55 g boric acid
                                    9.3 g $Na_2EDTA \cdot 2H_2O$
                                    ad 1000 ml nanopure H_2O

Working solution: 0.5× stock solution

2.6.7 Generation of plasmid standards for RT-qPCR

The circular plasmid DNA purified from overnight cultures of transformed *E. coli* bacteria was linearized with *Hind*III in the appropriate buffer system (both from New England Biolabs GmbH (NEB), Frankfurt, Germany) to avoid the formation of secondary structures and allow a reproducible performance of the polymerase enzyme activity in each PCR run. Serial dilutions of the gene specific standard curve, in general 1:10 dilutions ranging from 10^6 to 10^1 copies/μl, were used in every run to quantify the steady state mRNA level (copies/μl) in each sample.

2.6.7.1 Estimation of copy numbers for a plasmid standard

Calculation of copy numbers by means of the *Ov-hsp60* plasmid standard

(using OvHsp60LC primers):

insert	151 bp
vector	+3957 bp
total	4108 bp

$$4108 \text{ bp} \times 660 \text{ Da/bp} = \underline{2.71 \times 10^6 \text{ g/mol}}$$

$$\text{OD}_{260} \text{ (plasmid stock)} = \underline{0.551 \; \mu g/\mu l}$$

$$\frac{(0.551 \times 10^{-6} \text{ g/}\mu l) \times (6 \times 10^{23} \text{ copies/mol})}{(2.71 \times 10^6 \text{ g/mol})} = \underline{1.22 \times 10^{11} \text{ copies/}\mu l}$$

2.6.7.2 Standard curves for absolute quantification

The most direct and precise approach to measure the exact level of template in a sample is to use a standard curve (absolute quantification) that is prepared from a dilution series of control template of known concentration. The data generated from a serial dilution of a standard curve also determines the overall performance of the RT-qPCR assay in terms of efficiency, precision, and sensitivity. To accomplish this, the reactions were performed in triplicate, for high and low concentrations of starting template. The standard curve plot of the log of starting template vs. PCR cycles generates a linear fit with a slope between approximately –3.1 and –3.6, a typically acceptable range required

for accurate quantification (90-100% reaction efficiency). An example is illustrated in Figure 11. A standard curve of defined concentration was always included in the same RT-qPCR run as the unknown samples. The software compared the threshold cycle (Ct) values of the unknown samples to the standard curve to determine the starting concentration of each unknown. The Ct value is inversely proportional to the initial copy number.
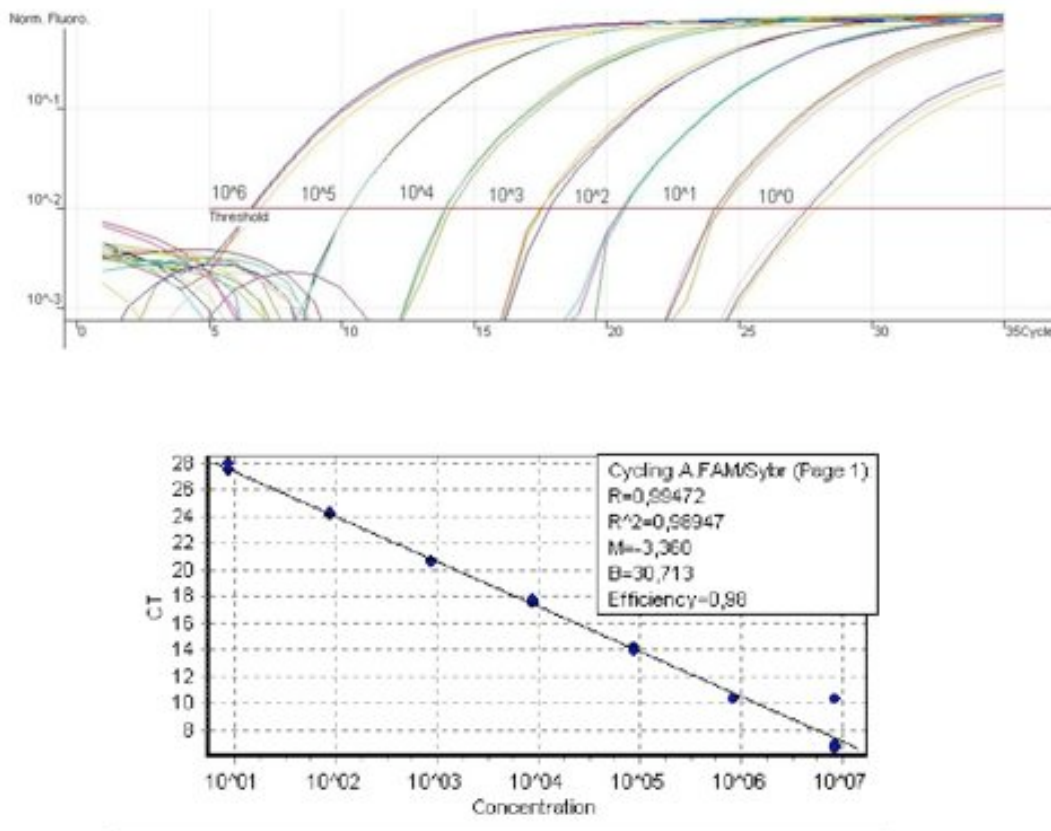
Figure 11. **An example for a gene specific standard curve.**

The amplification blot (upper panel) and the resulting standard curve (lower panel) are shown. In this example, the data of a dilution series ranging from 10^6 to 10^0 copies/μl generate a linear standard curve with a slope of –3.36, which is well in the acceptable range, and an amplification efficiency value of 0.98 (98%) was considered acceptable.

2.7   RLM-RACE PCR

The FirstChoice® RLM-RACE Kit (Ambion) was used to obtain full-length cDNA clones of *Ls-ppe-1* mRNA. The RNA Ligase Mediated Rapid Amplification of cDNA Ends (RLM-RACE) permits ligation of a synthetic RNA adapter only to the 5' end of decapped RNA, thus selecting for full-length messenger RNA.

Total RNA was used to ligate the adapter sequences to the 5'end and the 3'end following the manufacturer's protocol. Using the adaptor primers and gene specific nested primers, a nested PCR was performed. The PCR amplification for both rounds of PCR was carried out in 50 μl reaction volumes containing 1× PCR buffer, 4 mM $MgCl_2$, dNTPs to a final concentration of 0.2 μM, 0.3 μM of the adapter primer and the gene-specific primer, 1.25 U Super Taq Plus extended range DNA polymerase (Ambion) and 1 μl cDNA. After denaturing at 95°C for 5 min, there were 35 cycles of: denaturation at 94°C for 30 s, annealing at 58°C for 30 s, and extension at 68°C for 2 min. The gene specific nested *Ls-ppe-1* primers used are listed in Table 4.

The resulting PCR products were cloned into the TOPO-TA cloning vector (Invitrogen), the plasmids isolated with Qiaprep Spin Miniprep Kit (Qiagen) and sequenced by MWG Biotech AG (Ebersberg, Germany). Individual clones were sequenced on both strands using vector primers. The Swiss EmbNet ClustalW server, BioEdit version 7.0.0 and GeneDoc version 2.6.002 (Nicholas, Nicholas, 1997) were used to align and edit the *L. sigmodontis* sequences.

The translated protein, *Ls*-PPE-1, was scanned for prediction of signal peptides and sub-cellular localization with Signal*P* 3.0 (Bendtsen, 2004b), Target*P* 1.1 (non-plant network) (Emanuelsson, 2000) and Secretome*P* 2.0 (Bendtsen, 2004a). For each organism class in Signal*P*, Eukaryote, Gram-negative and Gram-positive, two different neural networks were used, one for predicting the actual signal peptide and one for predicting the position of the signal peptidase I cleavage site. The hidden Markov model (HMM) calculated the probability of whether the sequence contained a signal peptide or not. The eukaryotic HMM model also reported the probability of a signal anchor. Furthermore, a possible cleavage site was assigned. The Target*P* server predicted the localization (i.e. chloroplast transit peptide, mitochondrial targeting peptide or signal peptide for secretory pathway). The Secretome server was trained to predict the possibility of non-classical secreted proteins.

Table 4. **Primers for *Ls-ppe-1* used in RLM-RACE**

gene target	primer name	sequence 5'→ 3'
Ls-ppe-1	DD9-pcDNA-R	GAGGATTAACGTCAAACCCAT
Ls-ppe-1	DD9-Ls-R3	TACAGTAACACATAGATCGG
Ls-ppe-1	DD9-5Race1R	AAGTTACCGCTGCACCGAAT
Ls-ppe-1	DD9-5Race2R	ATACCACGCTTCCCACCAAT
Ls-ppe-1	DD9-gwR1	CAATATCCAACGAATGAACTTCAT
Ls-ppe-1	DD9-gwR2	CGGTAAAAGCTTGTATCGAACT
Ls-ppe-1	DD9-gwR3	CAATCCTTGATAGCTAGCGG
Ls-ppe-1	DD9-gwR4	ACGCGCAAGTGTAGCAATTAAT
Ls-ppe-1	DD9-gwR5	GTATTCCAGCAACACCTCGT
Ls-ppe-1	DD9-gwR7	CAAGCACAAAAGCCAAAATTACAC
Ls-ppe-1	DD9-gwR8	GACATCTTCCTTTATTTCTCAGTTA
Ls-ppe-1	DD9-gwF	GAAACGAAAAAGGGTGAAGAAAA
Ls-ppe-1	DD9-gwF2	ATTAATTGCTACACTTGCGCGT
Ls-ppe-1	DD9-gwF3	GGCAATGGGTTTGACGTTAATC
Ls-ppe-1	DD9-gwF4	CATCAGTTCACTCATTCTCATC
Ls-ppe-1	DD9-pcDNA-F	CCGATCTATGTGTTACTGTA

2.8   Establishment of RNAi in *L. sigmodontis*

2.8.1   Plasmid preparation for RNAi

A 99 bp fragment of *L. sigmodontis* actin (*Ls-act*) was cloned into the TOPO-TA cloning vector (Invitrogen) according to the manufacturer's instructions. The clone was confirmed by sequencing both strands (MWG Biotech AG).

For RNA transcription, the actin sequence was sub-cloned into the Litmus28i vector (NEB). The *C. elegans* yolk receptor (*Ce-rme-2*) in the pL4440 vector was the kind gift of Dr. Collette Britton, Glasgow University, Veterinary School, UK (Britton, Murray, 2004). The plasmids were purified with the Qiaprep Spin Miniprep Kit (Qiagen). Both vectors have two T7 polymerase sites flanking the cloned insert. Thus, it was necessary to linearize the plasmids downstream of the insert prior to *in vitro* transcription reactions so that only one of the two T7 promoters could make RNA. For each plasmid, in two separate reactions of 300 μl, 10 μg of plasmid were linearized as follows. The *Ls-act* plasmid was linearized with *Bam*HI or *Xho*I (see Figure 12). *Ce-rme-2* was

linearized with *Xho*I or *Xba*I. All digestions were performed overnight at 37°C using enzymes and appropriate buffers from NEB. After the complete digestion was checked on a standard agarose gel, the linearized plasmids were purified following the MEGAscript T7 Kit (Ambion) protocol.
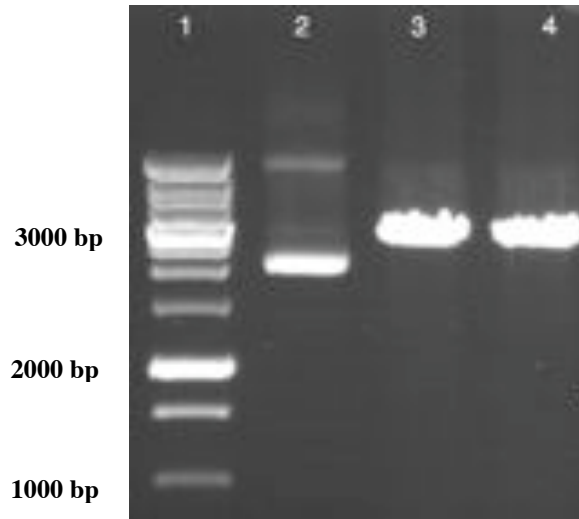
Figure 12. Linearization of *Ls-act* sequence cloned in Litmus28i vector.

Digestion of the *Ls-act* plasmid was complete after 24 hours incubation at 37°C, confirmed on a 0.8% standard agarose gel. Lane 1: molecular weight marker (1 kb DNA ladder; Fermentas); lane 2: *Ls-act* plasmid uncut for comparison; lane 3: linearized with *Bam*HI; lane 4: linearized with *Xho*I.

Plasmid purification

300 μl of the digest were incubated for 30 min at 50°C with:

      30 μl Proteinase K
      15 μl 10% SDS,

followed by a phenol/chloroform extraction and ethanol precipitation with 30 μl RNase-free 5 M NH$_4$Ac, 100 mM EDTA solution (Ambion) and 10 μg/ml linear acrylamide (Ambion) as carrier molecule. All centrifugation steps were for 15 min, 4°C, at 14.000 rpm. The pellet was eluted in 30 μl nuclease-free water, and the OD$_{260}$ determined.

2.8.2   *In vitro* transcription to generate double-stranded RNA

To produce dsRNA, 1 μg of each linearized plasmid of each gene was transcribed in a single reaction using the MEGAscript T7 Kit (Ambion). The Ambion protocol was used with the following changes:

1.)   the *in vitro* transcription was extended from 2 hours to over night,

2.)   after DNase I digestion and phenol/chloroform extraction, the RNA was precipitated with 1 volume of isopropanol and 10 μg/ml linear acrylamide (Ambion) as co-precipitant,

3.)   at the end of the procedure the RNA was dissolved in 100 μl nuclease-free water, heated for 10 min at 65ºC and the RNA annealed by allowing the solution to cool to room temperature.

The dsRNA concentration was determined at OD_{260} using an Eppendorf BioPhotometer. Typically, a 1:100 or 1:200 dilution of an aliquot of the reaction mixture gave an absorbance reading in the linear range of the spectrophotometer.

The dsRNA integrity was also checked by running an aliquot on a standard agarose gel (Figure 13), and then shock frozen in liquid nitrogen and stored at -80ºC.
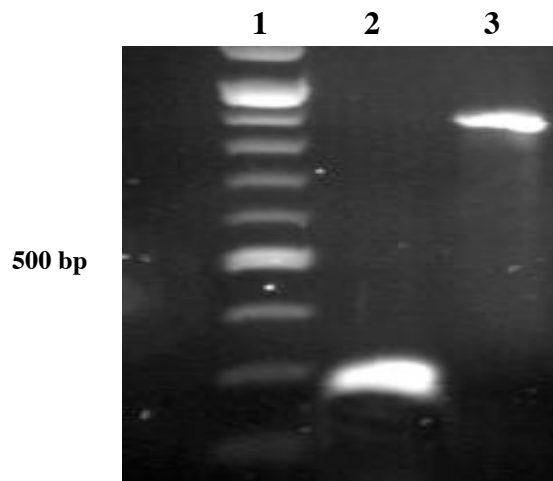
Figure 13. **The dsRNA integrity was confirmed on a standard agarose gel.**

Lane 1: molecular weight marker (100 bp DNA ladder; Fermentas), lane 2: *Ls-act* dsRNA, and lane 3: *Ce-rme-2* dsRNA.

Note: The *in vitro* transcribed dsRNA on a native gel runs at a higher molecular weight than dsRNA (charge difference).

2.8.3 Soaking *L. sigmodontis* in dsRNA

Adult *L. sigmodontis* worms (depending on the experiment, 6 to 10 months old) were recovered by flushing the thoracic cavity of naturally infected cotton rats with PBS. The nematodes were washed in RPMI 1640, 1% penicillin/streptomycin (PAA Lab., Coelbe, Germany) preheated to 37ºC. Only vigorously moving worms were used in the experiments.

RNA interference was carried out with a few important modifications to the procedure described by Aboobaker et al. (2003). Briefly, five groups of three adult female worms for each treatment were placed in 300 μl culture medium A (no FCS), containing RPMI 1640, 1% penicillin/streptomycin, 1 mM spermidine (Sigma-Aldrich) and *Ls-act* dsRNA in serial dilutions ranging from 0.035 μM to 35 μM in domed cap PCR tubes with the domed tops removed (see also Figure 14 for the experimental setup). Nematodes of the control groups were incubated in culture medium A with either 3.5 μM *Ce-rme-2* dsRNA (negative control) or cultured in dsRNA-free medium A (100% control). The tubes were then covered with a single layer of dialysis tubing (molecular weight cut-off 15 kDa), closed and placed in a beaker containing 500 ml pre-warmed culture medium B (contained FCS). The nematodes were incubated for 24 hours at 37ºC under 5% CO_2. After 24 hours, the nematodes were transferred from the PCR tubes to culture dishes with 5 ml dsRNA-free medium B and cultured for another 24 or 48 hours. Nematodes were collected after 24, 48 and 72 hours to determine phenotypes (adult phenotype and microfilarial release) and for RNA extraction.

Culture medium A (–FCS)
(was used to soak the nematodes during the first 24 hours in the micro-volume system)

> 300 μl RPMI 1640/tube
> 1%   penicillin/streptomycin
> 1 mM spermidine (Sigma-Aldrich)
> +/- dsRNA

Culture medium B (+FCS)
(dsRNA-free; medium was used i) during the first 24 hours as medium that the PCR tubes were in and ii) during the following 48 hours after removal of the nematodes from the micro-volume system)

> 500 ml RPMI 1640
> 1%   penicillin/streptomycin
> 10%   FCS (fetal calf serum)

The micro-volume dialysis system

cap, domes top removed

dialysis membrane

PCR tube

nematodes

cultur medium A
∓ dsRNA

1) Serial dilution of dsRNA

35 μM   17.5 μM   3.5 μM   0.35 μM   0.035 μM

2) Soaking nematodes in dsRNA

500 ml
culture medium B
+ 10% FCS

300 μl
culture medium A
+ dsRNA

24h
37°C/5% CO₂

4) RNA extraction from isolated nematodes and RT-qPCR

24, 48 or 72h
37°C,/5% CO₂

3) Transfer into dsRNA-free medium

5 ml dsRNA-free
culture medium B

nematodes

Figure 14. The experimental setup of the RNAi experiments.

2.8.4   Phenotype assessment

2.8.4.1   Video documentation of the worm movements

The adult phenotype was scored at each time point by videotaping the nematodes in culture dishes for 30 to 60 seconds. A digital video camcorder SONY®-PC 120E Handy cam (Sony Corporation, Japan) was used to document worm movements/ behavior. Subsequently, the videos were edited using Final Cut Pro 3.0 for Macintosh. After recording worm movements, the nematodes were washed two times in PBS, snap frozen in liquid nitrogen, and stored at –80ºC for RNA extraction.

2.8.4.2   Evaluation of the microfilarial release

The microfilariae released from 3 females/tube were collected after 24 and 48 hours. The microfilariae were centrifuged for 5 min at 1300 rpm (250× g) at room temperature. Then all but 20 μl of the supernatant was removed. To the remaining 20 μl, an equal volume of Hinkelmann's solution was added and the contents mixed (Al-Qaoud, 1997). After 30 min incubation at room temperature, the total numbers of microfilariae (from 3 nematodes/tube, n = 5) were counted for each time point using a light microscope (Leitz Diaplan, Wetzlar, Germany) at 10× magnification.

Hinkelmann's solution (Korenaga, 1991)

     0.5% w/v eosin Y (2.5 g)

     0.5% v/v phenol (2.5 ml)

     0.185% v/v formaldehyde (0.925 ml)

     ad 500 ml distilled water

2.9   Statistical test used

The nonparametric Mann-Whitney U-test was performed to determine the statistical differences between the control group and the treatment group of each experiment (Graphpad Prism 4.0 for Mac). P values ≤ 0.05 were considered significant.

Some of the results were log-transformed to meet the parametric assumptions.

3 Results

3.1 Altered gene expression after anti-*Wolbachia* treatment

The mutualistic living *Wolbachia* endobacteria, found in most filarial nematodes, are essential for embryogenesis and required for proper larval development into adults (Hoerauf, 1999). Therefore, *Wolbachia* represent new targets for antifilarial drug development. These insights led to the innovative use of tetracycline antibiotics to deplete the *Wolbachia* in the animal model filaria *L. sigmodontis* (Hoerauf, 2000c) and *B. pahangi* (Chirgwin, 2003), as well as in the human parasite *B. malayi* (McGarry, 2004)*, O. volvulus* (Hoerauf, 2003c; Hoerauf, 2008) and *W. bancrofti* (Hoerauf, 2003b). Still, very little is known about the molecular mechanism of the symbiotic interaction between *Wolbachia* and their filarial nematode hosts. Therefore, nematode genes that respond to anti-*Wolbachia* antibiotic treatment may play important roles in the symbiosis and were investigated (see section 3.2).

In field studies, ochocerciasis patients from Ghana were treated with doxycycline for 6 weeks at 100 mg/day to eliminate the *Wolbachia*. The absence of the *Wolbachia* in *O. volvulus* after antibiotic treatment has been previously monitored by immuno-histochemistry using specific antisera against bacterial *Y*-HSP60 protein (*Yersinia enterocolitica*) and *Bm*-WSP (*Wolbachia* surface protein of *B. malayi*) (Hoerauf, 1999). On the other hand, an apparent up-regulation of the mitochondrial HSP60 protein after *Wolbachia* depletion was also noticed (see section 3.1.2). Therefore, it was necessary to investigate whether a differentiation between *Wolbachia* bacteria and mitochondria is feasible.

3.1.1 *Wolbachia* and mitochondria localize in different zones of the hypodermis and are morphologically different

To confirm the specificity of the anti-*Y*-HSP60 serum for the endobacteria and mitochondria, the antiserum was used for staining ultra-thin sections of worms in onchocercomata, extirpated from an untreated patient.

Detailed electron micrographs were generated from untreated female *O. volvulus* worms with anti-*Y*-HSP60 serum. The typical localization pattern of *Wolbachia* and mitochondria was detected. As demonstrated in Figure 15A, the hypodermis can be divided into three zones.

Starting from the cuticle of the nematode, an area that contains only mitochondria, but no *Wolbachia,* was found. Next is a middle zone where the mitochondria become sparser and *Wolbachia* bacteria are also found. The innermost region of the hypodermis is almost exclusively free of mitochondria, containing just *Wolbachia*.

The anti-*Y*-HSP60 serum appeared to detect *Wolbachia* more intensely than the mitochondria. Apparently, the antiserum did not react with other organelles, such as lysosomes, granular structures also located in the middle zone of the hypodermis or the cytoplasm. The specific distribution of *Wolbachia* and mitochondria was even more pronounced when oocytes were examined. *Wolbachia* were detected near one or both ends of the oocyte, whereas the mitochondria were localized to the rest of the *Wolbachia*-free cytoplasm surrounding the chromosomes (Pfarr, 2008).

Additionally, histological examinations at a higher magnification showed the distinct morphology of *Wolbachia* and mitochondria. *Wolbachia* bacteria are larger and occur within a nematode-derived membrane (Figure 15B). These vacuoles often contain clusters of *Wolbachia* bacteria.
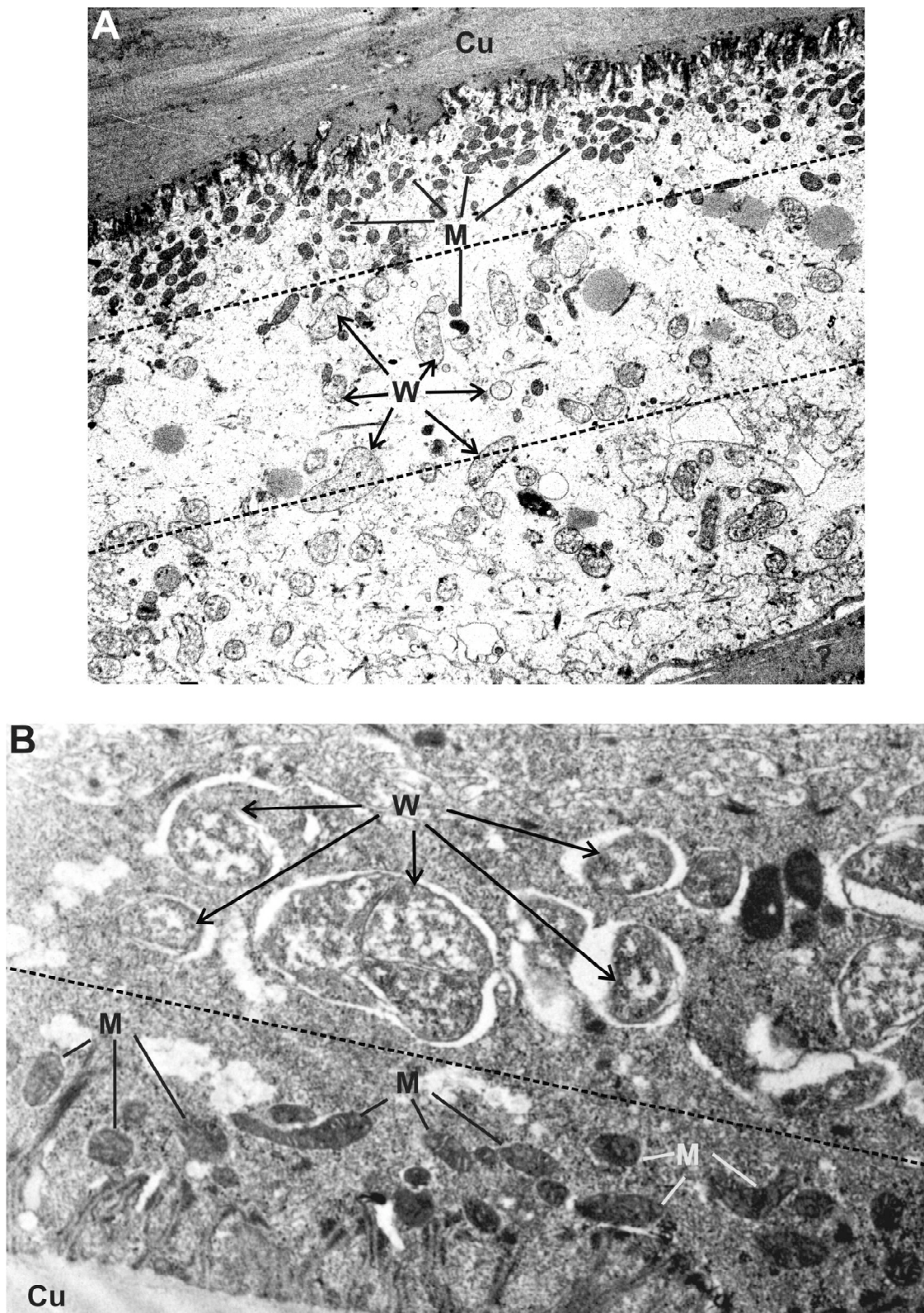
Figure 15. **Electron micrographs of a female *O. volvulus* worm detailing the localization of *Wolbachia* and mitochondria in the hypodermis.**

(A) The hypodermis was divided into three zones (dashed lines) based on the distribution of mitochondria (lines) and *Wolbachia* (arrows). (B) Higher magnification shows the different morphologies of mitochondria (lines) and *Wolbachia* (arrows). The *Wolbachia* were often seen in clusters of several bacteria in one membranous structure. Cu=cuticle; M=mitochondria; W=*Wolbachia* (Pfarr, 2008).

Immunohistochemical staining of an untreated *O. volvulus* female worm with specific anti-*Y*-HSP60 serum shows the location of *Wolbachia*. The *Wolbachia* endobacteria were predominantly found in the hypodermal cells of the lateral chords of both sexes, in oocytes, developing embryos, and all larval stages (Figure 16). The muscles, the epithelia of the digestive and genital tracts are devoid of *Wolbachia*, as well as the reproductive system (sperm) of male worms.
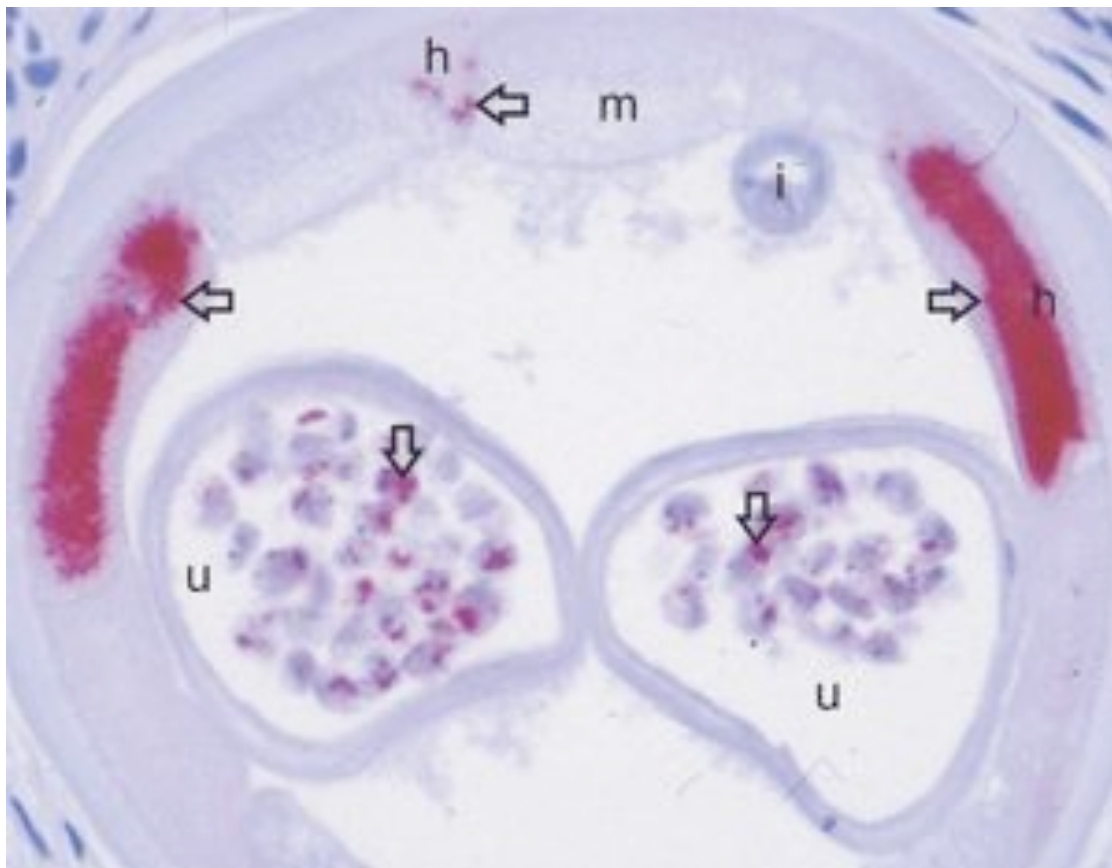
Figure 16. **Localization of *Wolbachia* in an untreated female *O. volvulus* worm.**

Immunohistochemical staining of HSP60 in *Wolbachia* endobacteria using specific anti-*Yersinia*-HSP60 antibodies. The bacteria are located in the hypodermis and oocytes of the nematode (open arrows).
h, hypodermis; i, intestine; m, muscle; u, uterus.
(Photo: D. W. Büttner, Institute for Tropical Medicine, Hamburg, Germany)

3.1.2 Anti-*Y*-HSP60 labeling is increased in *O. volvulus* upon doxycycline treatment

The *Wolbachia* endobacteria were detectable in the tissues of *L. sigmodontis* by antisera against *Ov-Wolbachia* HSP60 (Hoerauf, 1999) or *Yersinia enterocolitica* HSP60 (Taylor, Hoerauf, 1999; Hoerauf, 2000a). These antibodies also label *Wolbachia* in *O. volvulus* (Hoerauf, 2000b) and in *W. bancrofti* (unpublished data).

In female *O. volvulus* worms that were not exposed to doxycycline, a granular staining of *Wolbachia* was also seen in the innermost zone of the hypodermis, in oocytes, and all developing embryonic stages within the uteri (morulae, coiled and stretched microfilariae) (Figure 17, A-C open arrows).

Using antisera against HSP60 of *Yersinia* and of humans (Clone A57-E4, Dianova, Hamburg, Germany), mostly weak staining, representing nematode mitochondrial HSP60, was also seen in untreated worms or worms that were exposed to ivermectin (Figure 17A). Nevertheless, the different localization of *Wolbachia* and mitochondria within the nematode made it possible to distinguish between the two organelles.

Diffuse staining, indicating mitochondrial HSP60, was found in the outer zone of the hypodermis (Figure 17A and C, closed arrows), the epithelia of the intestine (Figure 17A), genital tracts, muscle cells of the body wall (Figure 17A), uterus and oocytes (Figure 17B), and embryos and sperm (data not shown). The intensity varied greatly, being strongest in portions of the filaria where no bacteria are present and often in moribund worms, such as those with neoplastic cells in the pseudocoeloma (Figure 17C; (Duke, 2002).

Examination of sections from onchocerciasis patients treated for 6 weeks with doxycycline showed that the hypodermis, oocytes, and embryos are devoid of *Wolbachia* (Figure 17D-F; Figure 18A and B). Interestingly, these worms showed a noticeable increase of mitochondrial HSP60 labeling in tissues which were normally unstained or only lightly stained in untreated worms, especially in oocytes, and embryos (Figure 17E and F). The mitochondria appeared as small dots or diffuse staining that were distinct from the granular, ring-like structures of *Wolbachia*. The diffuse staining was probably due to the labeled outer membrane folding of the hypodermis (lamellae). Tissues that were unstained or only slightly stained in untreated worms also showed an increased mitochondrial HSP60 expression after doxycycline therapy (Figure 17D-F).
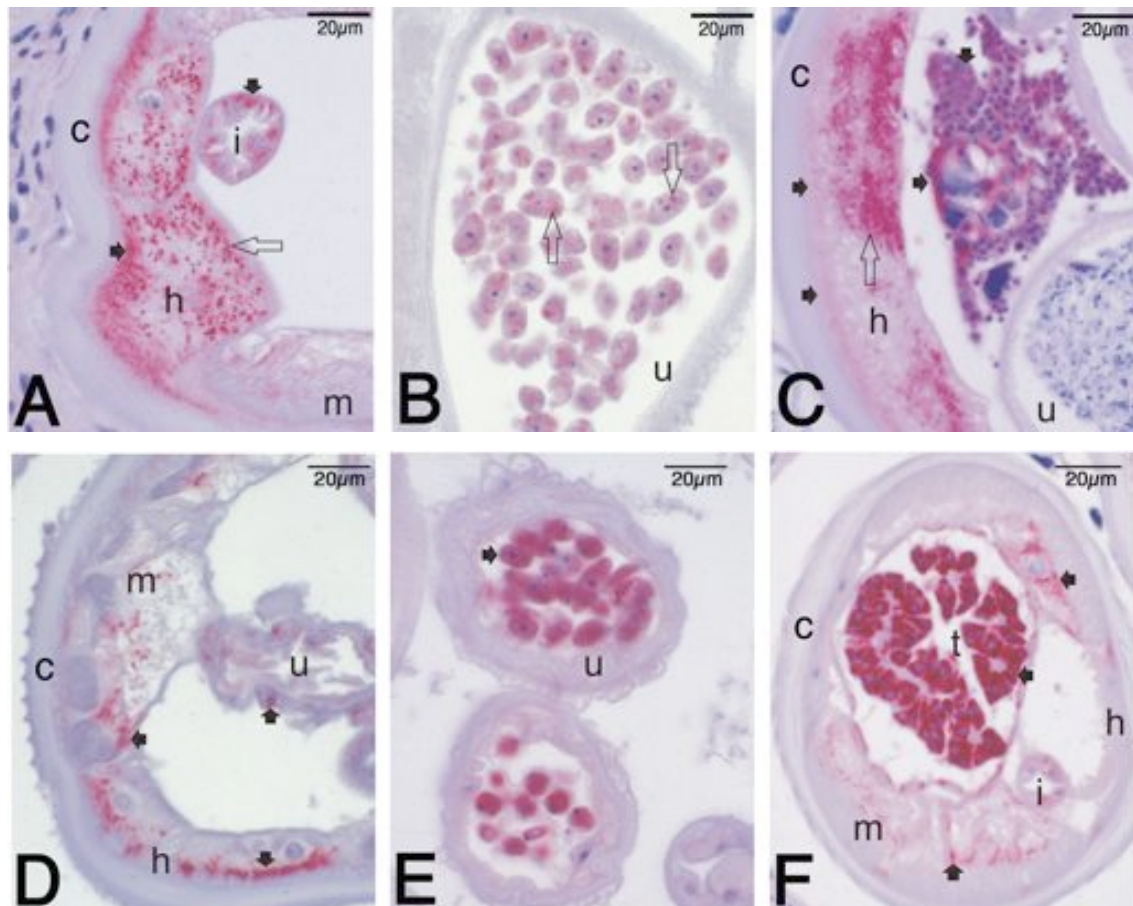
Figure 17. **Mitochondrial HSP60 in filarial tissues is increased after depletion of *Wolbachia* endobacteria.**

(A-C) Female *O. volvulus* after treatment with ivermectin (A, 20 months) or untreated showing granular endobacteria in the hypodermis (open arrows; A and C) and in oocytes in the uterus (open arrows, B). The mitochondria of the filaria are weakly labeled in the outer zone of the hypodermis, in the intestine (filled arrows, A), and in neoplastic cells in the pseudocoeloma (filled arrows, C). Stronger labeling of the intestinal mitochondria after ivermectin (A) is often seen.

(D-E) Female *O. volvulus* collected 5 months, and (F) male *O. volvulus* collected 19 months after treatment with 100 mg doxycycline per day for 6 weeks showing increased labeling of filarial HSP60 in the outer zone of the hypodermis (filled arrows; D), muscles of the body wall (filled arrows; D, F) muscle cells of the uterus (D), the entire oocytes (E, in comparison to the granular staining seen in B), and developing spermatozoa in the testis (F).

c, cuticle; h, hypodermis; i, intestine; m, muscles; t, testis; u, uterus.

3.1.3   Evidence for *Wolbachia* depletion by staining with *Bm*-WSP antiserum

The HSP60 staining seen in doxycycline-treated *O. volvulus* was not due to the *Wolbachia*. Using consecutive sections, the anti-*Y*-HSP60 serum specifically labeled the muscles in worms from patients who had received doxycycline (Figure 18A). However, serial sections from these worms were also labeled with antiserum against *B. malayi*-*Wolbachia* surface protein (*Bm*-WSP), which is specific for bacteria. It does not stain filarial tissues. This antiserum clearly showed that the *Wolbachia* were depleted from the doxycycline-treated worms (Figure 18B), indicating that the staining detected using the anti-*Y*-HSP60 serum indeed represented the filarial mitochondria. The comparison of consecutive sections labeled using the anti-*Y*-HSP60 but not the *Bm*-WSP serum demonstrated the specificity of the antibody probes (Figure 18A, B). The increase in mitochondrial HSP60 was not a direct effect of the antibiotic treatment of the nematode itself but rather due to the depletion of *Wolbachia* as there was no change in HSP60 expression after antibiotic treatment in a filaria devoid of *Wolbachia* (see also section 3.1.4). Furthermore, after administration of doxycycline for only 2 weeks, a treatment that does not deplete *Wolbachia*, increased staining of the mitochondria was not detected at any time point up to 30 months after treatment.
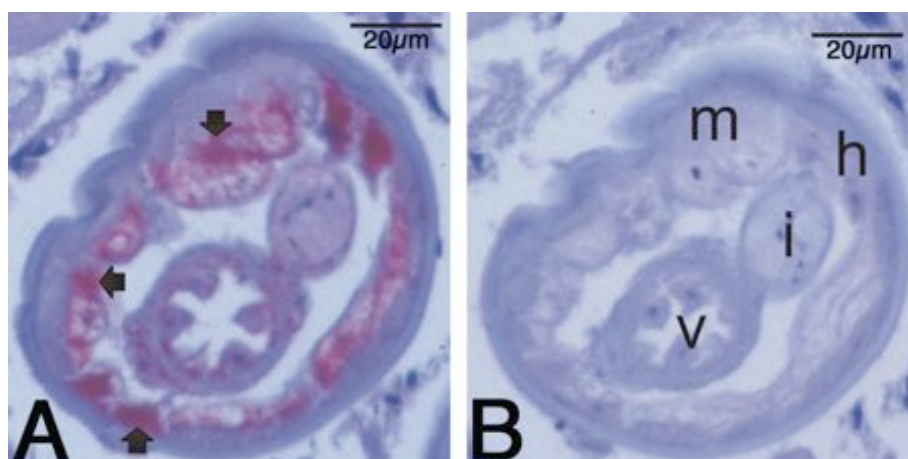
Figure 18. **The bacteria-specific *Bm*-WSP antiserum confirmed *Wolbachia* depletion in doxycycline treated *O. volvulus*.**

Immunohistochemical labeling of HSP60 in *Wolbachia* endobacteria and in filarial tissues. Primary antibodies against *Y*-HSP60 (A) and *Bm*-*Wolbachia* surface protein (B) were detected using anti-rabbit mouse monoclonal antibodies as described. (A, B) Female *O. volvulus* collected 19 months after treatment with 100 mg doxycycline per day for 6 weeks showing increased labeling of filarial HSP60 in the hypodermis and muscles of the body wall (filled arrows; A). Consecutive sections of the respective worms stained with anti-*Bm*-WSP serum demonstrated that *Wolbachia* endobacteria were absent (B). h, hypodermis; i, intestine; m, muscles; v, vagina.

3.1.4 No alteration in HSP60 expression in the *Wolbachia*-free nematode *Acanthocheilonemea viteae*

A. viteae belongs to the subfamily of Onchocercinae and is one of a few filariae that do not harbor *Wolbachia* endobacteria (Hoerauf, 1999). Comparing sections from untreated (Figure 19A) and tetracycline-treated *A. viteae* (Figure 19B), there was no detectable increase in HSP60 staining in the worms. The staining in the oocytes, the muscles and the gut was equivalent between both groups. This experiment supports the hypothesis that an increased labeling of HSP60 in the mitochondria of *O. volvulus* is due to the depletion of *Wolbachia*.
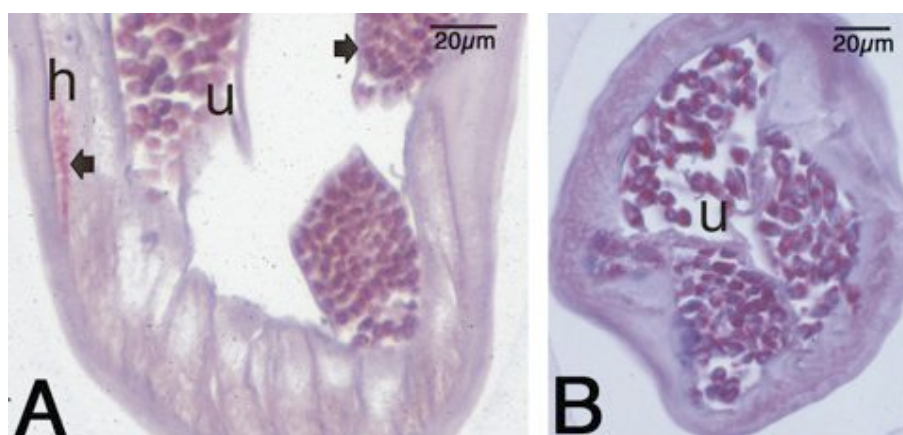
Figure 19. Comparable HSP60 expression in untreated and tetracycline-treated *A. viteae*.
(A, B) No difference is seen in the labeling of filarial HSP60 in untreated (closed arrows; A) and treated (B) females of *A. viteae*, a species without *Wolbachia* (after 70 days treatment of *Mastomys coucha* hosts with 25 mg/kg/day tetracycline). h, hypodermis; u, uterus.

3.1.5 Quantification of *hsp60* transcription following *Wolbachia* depletion

One argument for the increase in nematode mitochondrial HSP60 staining after doxycycline treatment could be that the anti-*Y*-HSP60 antibodies are more specific for the bacterial HSP60 and therefore stain weakly for the filarial HSP60 until the *Wolbachia* are depleted. To address this issue, *hsp60* gene expression was measured in onchocercomata extirpated from untreated and doxycycline-treated patients 5 months after start of the doxycycline regimen to demonstrate that the increase in mitochondrial

HSP60 is also reflected at the level of transcription. The primers used for the *hsp60* gene had no similarity to the *hsp60* gene of *Wolbachia*, as determined by BLAST analysis. The primers for *actin* were also tested on human cDNA and did not amplify the human gene (see Figure 20).
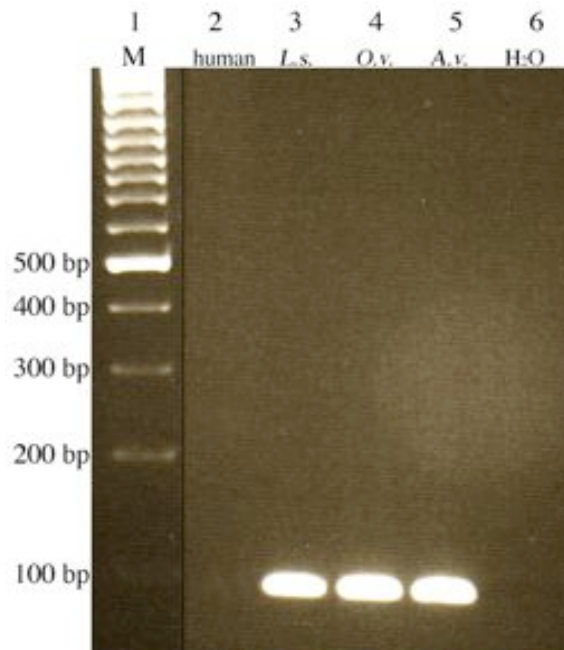
Figure 20. The *actin* primers used for normalization are nematode specific.

The *actin* primers were tested in PCR with human cDNA and cDNAs of three different nematode species. The amplified products were separated on a 2% agarose gel. Lane 1: 100 bp Marker (Fermentas); lane 2: human cDNA as template; lane 3: *L. sigmodontis*; lane 4: *O. volvulus*; lane 5: *A. viteae*; lane 6: water control. The *actin* primers are nematode specific, as no signal was detectable for the human material.

It should be noted that 8 out of 16 controls, and 7 out of 23 doxycycline-treated patients also received a single dose of ivermectin, a medication with microfilaricidal effects. According to the immunochemichal stainings of ivermectin-exposed nematodes that sometimes also show an increase of mitochondrial HSP60 (as seen in Figure 17A), we have split the groups to distinguish between these different treatment groups (Figure 21).
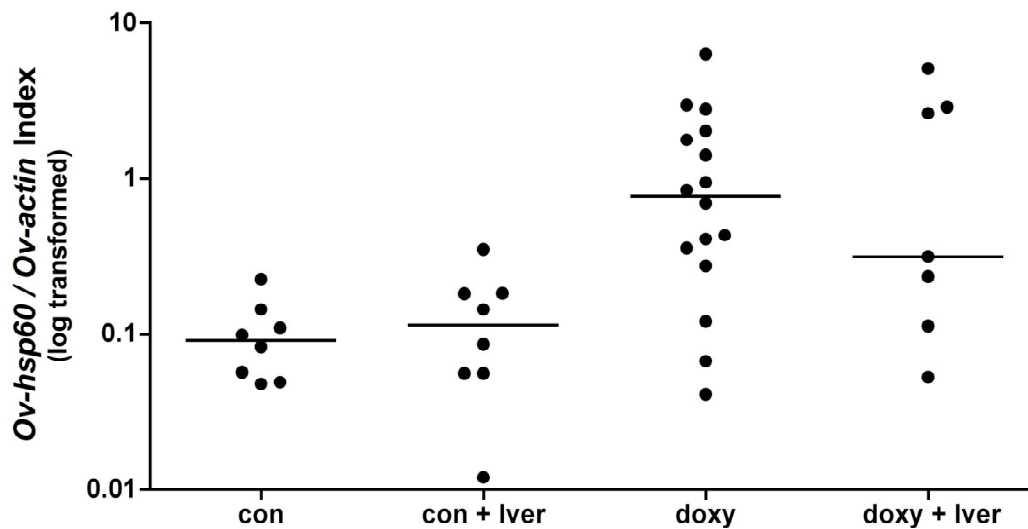
Figure 21. **Influence of ivermectin on the *hsp60* expression in onchocercomata.**

Side-by-side comparison shows that patients that received ivermectin (+Iver) have no difference in *hsp60* expression compared to patients that had not received ivermectin. Marginal differences in *hsp60* were only seen if the patients had received doxycycline.

No significant differences were detected between the groups that received ivermectin and the doxycycline-treated or untreated control group. Henceforth, all controls and doxycycline-treated patients, no matter if they have been exposed to ivermectin or not, were combined to a single group each. The resulting data are displayed in Figure 22.

The normalized *hsp60/actin* index generated by quantitative PCR (qPCR) showed a significant increase in *hsp60* transcript levels after the *Wolbachia* had been depleted by doxycycline (Figure 22A). In comparison to the untreated controls, the doxycycline-treated patients produced a 7.7 fold increase in *hsp60* expression. Additionally, the absence of *Wolbachia* bacteria in *O. volvulus* nodules after doxycycline treatment was confirmed by qPCR, measuring *ftsZ*, a gene for a bacterial cell cycle protein. As shown

in Figure 22B, the determined *ftsZ* levels were drastically reduced (median value = 0) after doxycycline treatment.
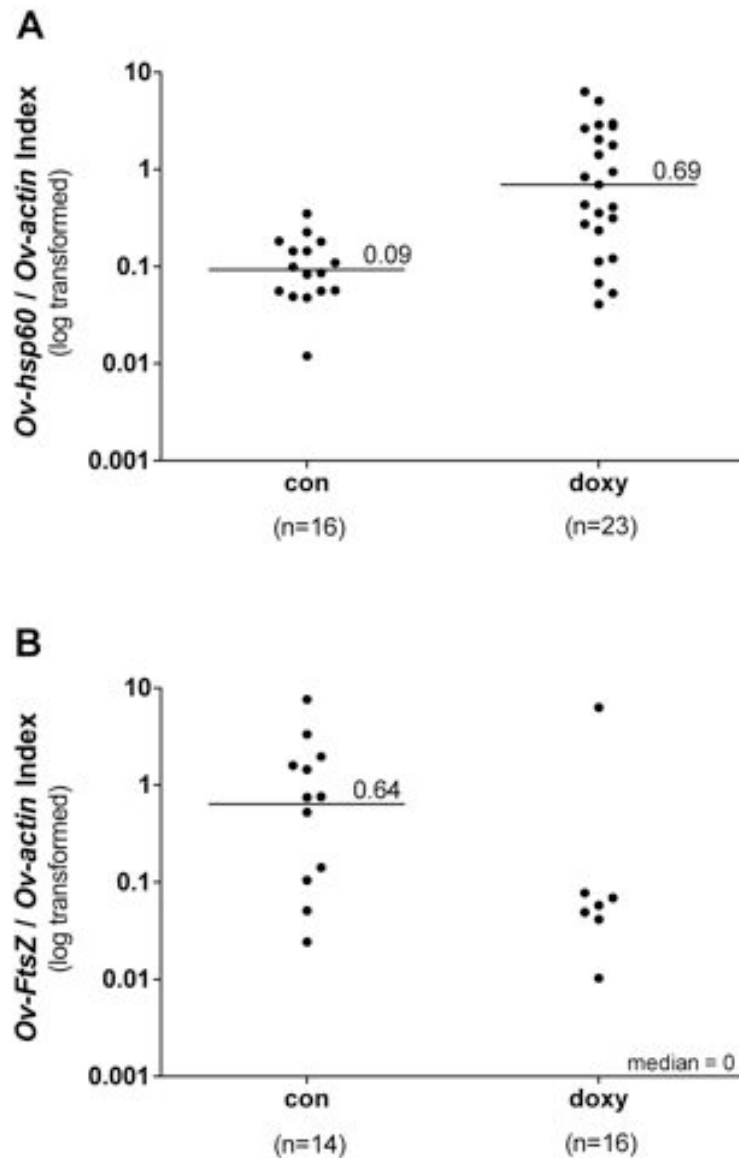
Figure 22. **Filarial *hsp60* and bacterial *ftsZ* levels before and after depletion of *Wolbachia* endosymbionts from *O. volvulus*.**

Five months after the start of the treatment, nodules were excised from patients taking part in studies on the effect of doxycycline on *O. volvulus* in Ghana. (A) Up-regulation of filarial *hsp60* by a factor of 7.7 was demonstrated using the ratio of filarial *Ov-hsp60* to *Ov-actin* transcription levels ($P = 0.0002$). The transcription levels for each gene (copies/μl) were determined by comparing crossing point data to a gene-specific standard curve included in every run. Median values are indicated. (B) The *ftsZ*/*Ov-actin* Index was significantly reduced after doxycycline treatment, demonstrating successful depletion of *Wolbachia* bacteria from *O. volvulus* ($P = 0.004$). Statistical differences were determined by Mann-Whitney *U* test using GraphPad Prism 4.02 (Graphpad Software, San Diego, CA, USA).
PCR data for *ftsZ* were generated by Anna Albers (then a diploma student at IMMIP).

65

3.1.6 Spearman Rank Correlation

To test whether the up-regulation of the mitochondrial *hsp60* is directly correlated with depletion of *Wolbachia* endobacteria, the Spearman Rank test was performed. The linear regression blot (*Ov-hsp60* versus *Ov-ftsZ* levels) shows a weak but positive correlation of these two parameters examined, which is indicated by positive R-($R = 0.18$) and P-values ($P = 0.0448$) (Figure 23).

The assumption that the increased expression of *hsp60* after the loss of *Wolbachia* upon tetracycline antibiotics is due to an interruption of the homeostasis of the endosymbiosis could hereby be strengthened.
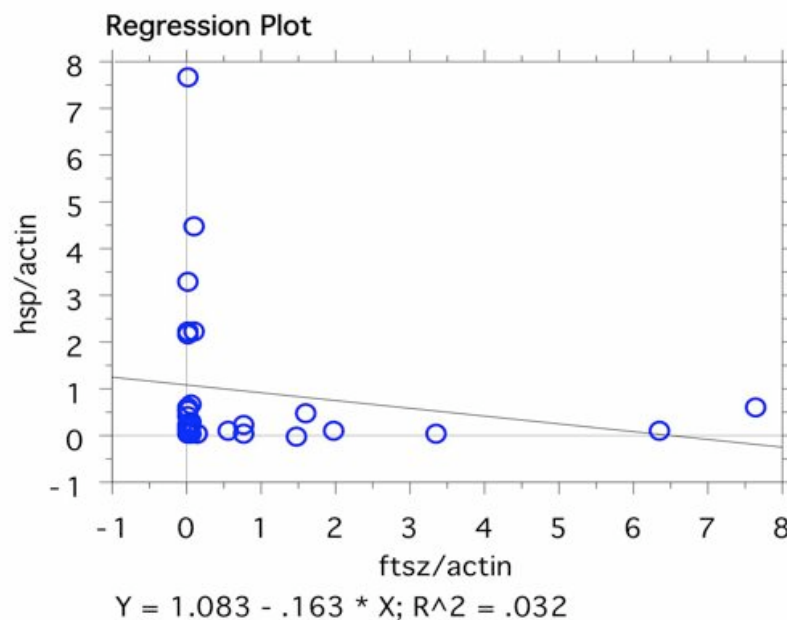
Figure 23. **High *hsp60* levels correlate with low *ftsZ* levels.**

The linear regression blot of a Spearman Rank test shows a positive correlation (*R* value = 0.18) between increasing in *Ov-hsp60* transcript levels after doxycycline treatment and decreasing *Ov-ftsZ* levels upon doxycycline treatment, due to the depletion of the *Wolbachia* endobacteria. The correlation was calculated using Statview 5.0 for Macintosh ($P \leq 0.05$).

3.2 Screening for *L. sigmodontis* genes affected by tetracycline treatment

3.2.1 Differential display

We used differential display PCR (DD PCR) followed by Reverse Northern blot to screen for cDNA fragments that truly represent differentially expressed mRNAs after tetracycline treatment in the rodent filaria *L. sigmodontis*.

Complex expression patterns were observed by DD PCR with the 14 different primer sets used. A representative area of a differential display gel identifying several bands that appeared to be differentially expressed is shown in Figure 24. Many down-regulated fragments were identified, but cloning and sequencing of a number of these products showed that they were all of *Wolbachia* origin, and thus indicate likely genomic contamination (Figure 24C). Several fragments only displayed a short up-regulation directly after the beginning of the treatment (Figure 24B), and may represent responses to the stress induced by tetracycline. Therefore, only transcripts up-regulated for two or more time points were considered to be responding to *Wolbachia* depletion (Figure 24A).
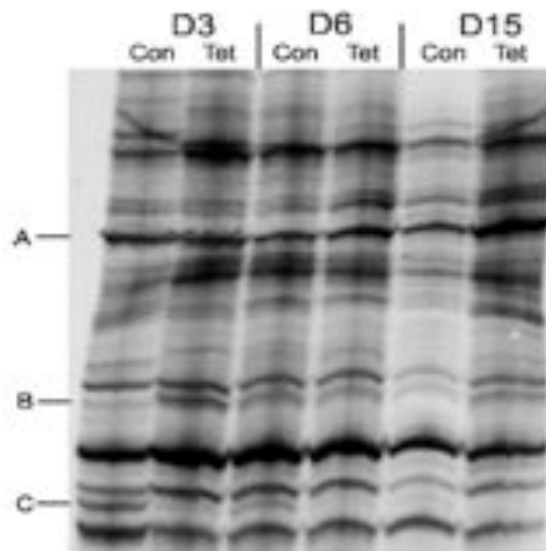
Figure 24. **A representative autoradiogram from Differential Display PCR.**

The differential display of mRNA from untreated control (con) and tetracycline-treated (tet) *L. sigmodontis* on days 3, 6 and 15 of treatment using the arbitrary primer set H-AP-8 and anchored primer HT$_{11}$G (both from GenHunter) is shown. The indicated bands show: (A) *Ls-ppe-1*, a gene that is consistently up-regulated and was therefore considered for further analysis; (B) a gene that is up-regulated only at day 3, and therefore not further investigated; (C) a gene which is down-regulated. Cloning and sequencing of these fragments showed they were of *Wolbachia* origin, indicating genomic DNA contamination.

As part of the effort to apply differential display to identify genes that are up-regulated after tetracycline treatment, PCR products from control and tetracycline-treated animals over 36 days of treatment time were compared side-by-side, and yielded 12 up-regulated candidates (in a range of 80 to 700 bp) from four different DD PCR primer sets (see Table 5). These were cloned for later validation.

Table 5. **Fragments differentially expressed upon tetracycline treatment.**

Fragment	3' primer	5' primer	Size [bp]
DD-1	A	9	180
DD-2	C	9	330
DD-3	C	9	120
DD-4	C	11	450
DD-5	G	11	150
DD-6	G	11	150
DD-7	G	11	150
DD-8	A	13	400
DD-9	G	8	700
DD-10	G	8	80
DD-11	A	8	100
DD-12	A	8	300

Note: 3'primers refer to GenHuter anchored primers H-T$_{11}$G, H-T$_{11}$A, or H-T$_{11}$C.
5'primers refer to GenHunter arbitrary primers H-AP-1 to -14.

3.2.2   Confirmation assays

Several methods were used to confirm the up-regulation of the 12 fragments cloned after DD PCR. The standard protocol recommends the use of re-amplified cDNA directly as a probe for Northern blot verification (Liang, 1993). This was especially difficult under circumstances where the amount of RNA samples was limited. Thus, we used the Reverse dot blot technique for which equal portions of the individual plasmids corresponding to the candidate genes were applied to duplicate nylon membranes. The blots were then hybridized with labeled cDNA probes (separately for control and tetracycline treatment) generated from amplified antisense RNA (aRNA).

3.2.2.1 Reverse dot blot with fluorescein labeled probes

In order to omit radioactivity, fluorescein-labeled probes made from aRNA (see section 2.4.1) were used for the dot blot hybridization (Figure 25). The results lead to the suggestion that all candidates applied in lane 3, i.e. DD-9 alias *Ls-ppe-1* (indicated in red), DD-10, DD-11, and DD-12, are clearly up-regulated on day 36, the end of the tetracycline treatment. The *hsp60* gene, that is known to be up-regulated upon antibiotic therapy (Figure 22A), was here used as an internal positive control, and indeed showed an increasing expression in the tetracycline-probed blot. As expected, the expression of the housekeeping gene *EE4*, which encodes for the *60S* ribosomal protein of *Brugia pahangi* (Devaney, 1996), was not altered in comparison to the control blot. However, these results could not be consistently repeated by this method.
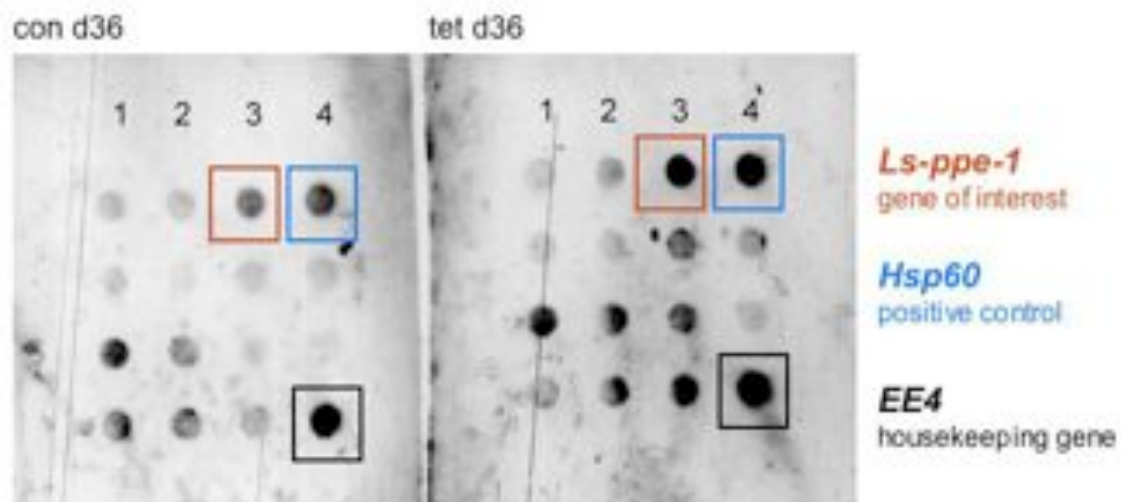
Figure 25. **Fluorescein labeled cDNA probes are not reliable in reverse dot blots.**

6 μg plasmid containing each candidate gene were spotted on nylon membranes and hybridized overnight with labeled cDNAs from control and tetracycline treated worms from day 36 of the treatment trial. The 12 candidate genes were applied top down as follows: lane 1: DD-1, 2, 3, 4; lane 2: DD-5, 6, 7, 8; lane 3: DD-9 (*Ls-ppe*-1, red frame), 10, 11, 12; lane 4: *hsp-60* (blue frame), calponin homology domain-1, calponin homology domain-2, *EE4* gene (black frame).

3.2.2.2 Reverse dot blot with radioactive labeled probes

Since fluorescein labeled cDNA probes could not be used to confirm the up-regulation of the selected genes, radioactive labeling of cDNA probes was accomplished. Therefore, we first determined that we could detect a signal over the entire spectrum from weak to strong gene expression using cDNA probes generated from aRNA and labeled with either 100 μCi (Figure 26A) or 50 μCi (Figure 26B) of α-^{32}P dCTP per reaction in comparison to the 500 μCi in the original method (Poirier, Erlander, 1998).
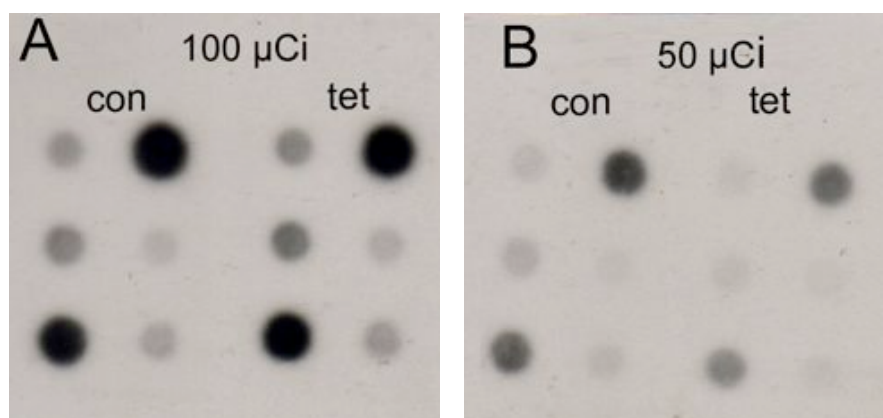
Figure 26. **Confirmation of signal detection with low amounts radioactivity.**

Plasmids containing different gene fragments from DD PCR of control and tetracycline treated samples (d15) were spotted onto nylon membranes and hybridized with (A) 100 μCi or (B) 50 μCi labeled probes generated from aRNA. The applied plasmids correspond to genes with weak to strong gene expression.

Additionally, plasmids transferred onto nylon membranes in quantities ranging from 6 μg to 60 ng per spot and hybridized with radioactive labeled cDNA probes derived from aRNA showed that the probes were always in excess.
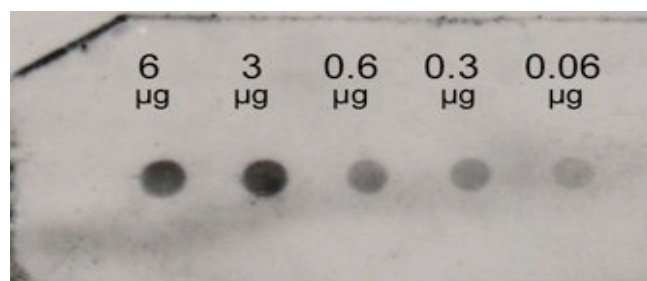
Figure 27. **Reverse dot blot.**

A plasmid was serially diluted (6 μg – 0.06 μg), applied on a nylon membrane, and hybridized with radioactive labeled probes made from aRNA. Even at the highest plasmid concentration, the probe is still in excess.

Whereas reverse dot blots hybridized with the fluorescein labeled cDNA probes (ECL kit) made from aRNA (day 36) could not deliver reliable results, radioactive α-^{32}P dCTP-labeled cDNA probes confirmed then the up-regulation of the 12 DD PCR fragments with a range of 0.5 to 3.2 compared to the controls (Table 6).

For this purpose, cDNA probes made from aRNA of day 15 post treatment were used. This earlier time point was chosen, since it is conceivable that genes are up-regulated only for a short period after treatment, and that day 36 might be too late for verification. We decided to follow up the three fragments with greater than 1.5-fold up-regulation (arbitrary decision), which were clones DD-1, DD-9, and DD-10.

Table 6. **Reverse dot blot analysis on day 15 after tetracycline treatment.**

Fragment	Factor up-regulation
DD-1	1.73
DD-2	1.28
DD-3	1.30
DD-4	1.11
DD-5	0.48
DD-6	0.81
DD-7	0.91
DD-8	0.62
DD-9	3.21
DD-10	1.56
DD-11	0.59
DD-12	0.66

3.2.2.3 Reverse dot blot with radioactive labeled DD PCR products

In parallel, another method with fewer enzymatic steps than aRNA amplification was used to independently confirm the up-regulation of the candidate genes. For this, radioactive-labeled DD PCR products generated from independent reactions were used as a probe to detect genes by dot blot hybridization (Coetzer, 2003). This technique confirmed the up-regulation by a factor of >1.5 of only one of the three remaining genes (data not shown). Fragment DD-9 was the only one out of the 12 candidate genes that could be confirmed to be up-regulated after tetracycline treatment by a factor >1.5 by all methods used.

3.3 Identification of *Litomosoides sigmodontis* phosphate permease (*Ls-ppe-1*) as a tetracycline up-regulated gene

The single DD PCR fragment that had passed the rigorous screening (DD-9) was sequenced, yielding ~700 bp with an open reading frame of 112 amino acids. This fragment was significantly similar by BLAST to the C-terminal region of a family of *C. elegans* phosphate permeases and is hereafter termed *L. sigmodontis* phosphate permease 1 (*Ls-ppe-1*).

3.3.1 Full-length cloning of *Ls-ppe-1* and identification of transcript variants

In order to more fully characterize *Ls-ppe-1*, the missing 5' and 3' sequences were generated by RLM-RACE PCR, subsequently cloned and sequenced. Finally, three transcript variants were identified: *Ls-ppe-1*_1 (AY644700), *Ls-ppe-1*_2 (DQ211815), and *Ls-ppe-1*_3 (DQ211816), but all have the same coding sequence. Three different spliced variants were confirmed by Northern blot analysis (Figure 28B).
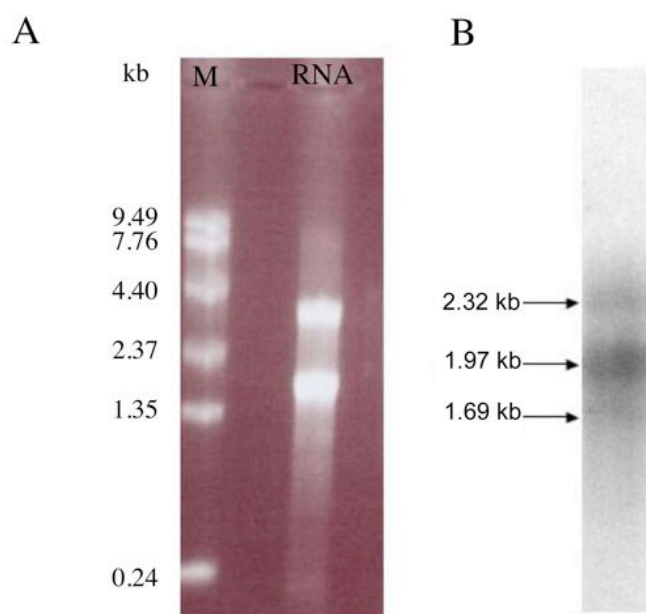
Figure 28. **Northern blot to identify three transcript variants of *Ls-ppe-1*.**

(A) The RNA gel (1.2%) showed no degradation of the RNA (2 μg/lane). On the left-hand side the RNA Marker was applied. (B) The Northern blot was hybridized with radioactive-labeled probes for *Ls-ppe-1*, using the initial Differential Display clone. Three spliced variants of *Ls-ppe-1* could be identified and show up as discrete bands.

All three variants are full-length, as each has the spliced leader sequence (SL1: AAAGGTTTAATTACCCAAGTTTGAG) at its 5' end and terminates in a polyA signal (signaling pattern at nucleotide position 1714: TGACTAAAAA) (Figure 29A).

The SL1 sequence is added to the 5'end of more than 70% of the RNAs in filarial nematodes (Blaxter, Liu, 1996; Liu, 1996). Variants 2 and 3 have an additional 78 nucleotides between the SL1 and the start methionine. The 3 variants differ only in the 3' untranslated region after the polyA signal. Variant 2 has 85 additional nucleotides beginning at nucleotide position 1716 of variant 1. Variant 3 has 284 additional nucleotides from nucleotide position 1716 of variant 1 (Appendix A).

The full-length cDNA of *Ls-ppe-1*-1 is 1729 base pairs and has an open reading frame of 523 amino acids (Figure 29).

A

>*Ls-ppe-1_1* (1729nt)

```
AAAGGTTTAATTACCCAAGTTTGAGGTTAACTGAGAAATAAAGGAAGATGTCAACATTGACAGTAACTACGCTAATGCCATCCTCTTC
TACAATGTCAGAAGCATTCATAGCCGCCTTTCGGAATGATGTATTATGGGCATTAATATGTGGTGTAATTTTGGCTTTTGTGCTTGGT
TTTGCGATGGGTGCAAATGACGTTGCAAATGCTTTTGGTACATCGGTTGGTAGCAAAGTGCTGACATTACGGCAAGCTTATATACTTG
CAGTAATTTTTGAAACACTTGGAGCACTGCTTATCGGTTACAACGTAACGGATACGGTACGTAAAGGTGTCATCGATCTGACGTTATA
TGAAGATAAACCAAAAGAGATTTTCATTGGGCAAATCGCCATTCTTGGAGGTTGCTCATTATGGTTATTAATTGCTACACTTGCGCGT
CTACCTGTATCATCAACTCATAGTGTCACTGGAGCTACTGTAGGATTTGGCTTGATGACACGAGGTGTTGCTGGAATACAATGGAAAA
AAATTGCTCATATTGTTGCTTCATGGTTTTTATCACCGATATTGTCTGGCGTCGTGTCAGCCGTTCTGTACATTATTGTTGACCATTC
AGTTCTCAGACGGAAGGATCCATTTCGTTGTGGTTTGAGAGCTTTGCCAATATTTTACTGGTTTTGTATCGCATTTAATATTTTCACC
GCTAGCTATCAAGGATTGAAATTACTTCGCCTGTCAAAGTTGCCGTTGTGGTTGAGCTCATTAGTGAGTATTGGATGTGCAACAGTTG
GCTCCATCGCTATTTACTTTTTGCTCTTGCCGAGGCTGAAAATCTGGATAAACAATTCACTTGGCAGTAATACAGCTAGAGACGATTC
GTTTGAAGTGCAGACTATAAGTAATGCGGTTCAATTGGAGGGAAATGTGATAAATCAAAAATGTCAAGCATCGAAGACAGAAATGTT
GAGAGTTCAACTGTTATCAAAAGCGATAGCAAATCATCGAGAGTATGGCGAAAAAGGGTGAAGAAAAGAAACTAACCGATAATACAG
TAATGAAGTTCATTCGTTGGATATTGCCGACTGATAATAGAGCAACGGACAATAGAACAATGAAAATATTTAGTTCGATACAAGCTTT
TACCGCGTGCTTTGCTGGATTTGCGCATGGCGCTAATGACGTCGGGAATGCAATAGCTCCGCTGACAGCATTGATATCGATTTACAGT
AATCTGGATGTTCGACAACGAAGTGAAACACCGATCTATGTGTTACTGTACGGCGTACTTGCAATATGTGTTGGACTTGTGGTACTTG
GACATCACGTAATACAAACTATTGGTACTGATATGTCTACGACTCAATGCTGCTAGCGGTTTTACAATCGGTGCAGCGGTAAC
TTCACTAACAGCCAGTAAACTTGGCCTACCAATTAGTACAACCCATTCATTGGTGGGAAGCGTGGTATTCGTTGGAATGGTGCGTGCC
AAGAAAGGTGTCCAGTGGTTAATATTCCGAAACATTGCCTTATCGTGGATTTTAACGTTGCCTATTTCAGGTCTTTTGGCAATGGGTT
TGACGTTAATCCTCAAGTTTTCACTTTGAGAGTGTAGTTGGACATTTATTTTTTCTTGTACATTTGTTACTTTGTTGTATATTTTCAT
CAGTTCACCCATTCTCATCTTTGTTTACTTTAATTTTTTTGACTAAAAAAAAAAAAAA
```

B

>*Ls_PPE-1* (523aa)

```
RKMSTLTVTT LMPSSSTMSE AFIAAFRNDV LWALICGVIL AFVLGFAMGA NDVANAFGTS
VGSKVLTLRQ AYILAVIFET LGALLIGYNV TDTVRKGVID LTLYEDKPKE IFIGQIAILG
GCSLWLLIAT LARLPVSSTH SVTGATVGFG LMTRGVAGIQ WKKIAHIVAS WFLSPILSGV
VSAVLYIIVD HSVLRRKDPF RCGLRALPIF YWFCIAFNIF TASYQGLKLL RLSKLPLWLS
SLVSIGCATV GSIAIYFLLL PRLKIWINNS LGSNTARDDS FEVQTISNAV QLEGNVINQK
CQASKTENVE SSTVIKSDSK IIESMAKKGE EKKLTDNTVM KFIRWILPTD NRATDNRTMK
IFSSIQAFTA CFAGFAHGAN DVGNAIAPLT ALISIYSNLD VRQRSETPIY VLLYGVLAIC
VGLVVLGHHV IQTIGTDMST INAASGFTIE FGAAVTSLTA SKLGLPISTT HSLVGSVVFV
GMVRAKKGVQ WLIFRNIALS WILTLPISGL LAMGLTLILK FSL
```

Figure 29. Sequence information of *Ls-ppe-1_1*

(A) The nucleotide sequence of *Ls-ppe-1*_1 (1729 nucleotides) is shown. The SL1 sequence is framed, the Start codon (ATG) and the Stop codon (TGA) are indicated in bold, and the underlined nucleotides indicate the polyA signal. (B) The predicted protein sequence of the Ls-PPE-1 has an open reading frame (ORF) of 523 amino acids.

The translated protein *Ls*-PPE-1 was predicted to have an amino-terminal signal peptide with a predicted cleavage site between amino acid positions 49 and 50. The signal peptide was predicted by Signal*P* and Target*P* (Center for Biological Sequence Analysis) that used neural networks (NN) and hidden Markov models (HMM) trained on eukaryotes (Bendtsen, 2004b). These two different neural networks were used to predict the actual signal peptide and the most likely cleavage site (Figure 30).
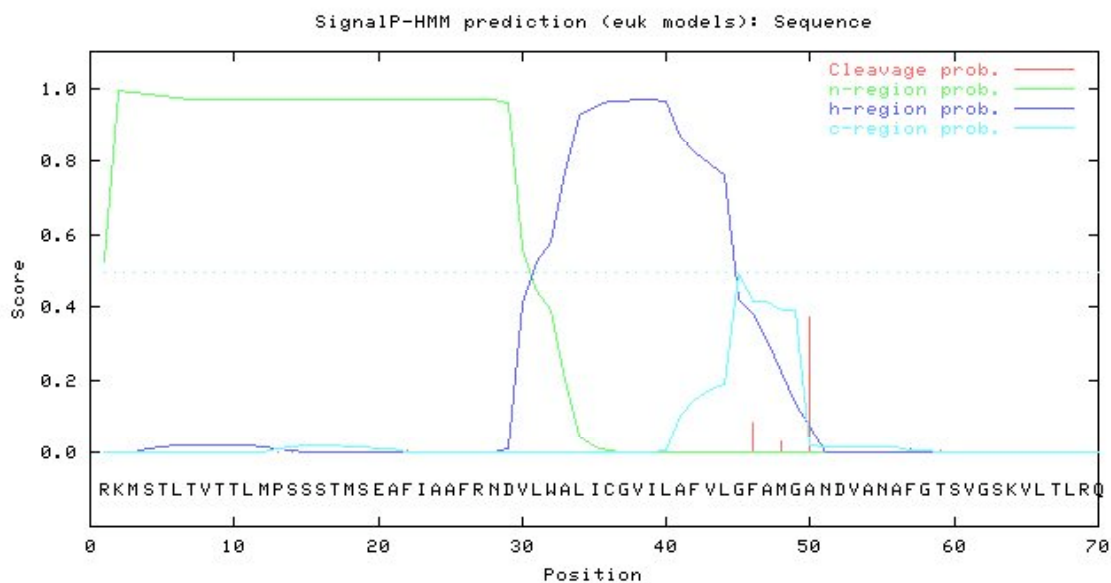
Figure 30. Signal peptide prediction for *Ls*-PPE-1 using Signal*P*.

A signal peptide for *Ls*-PPE-1 was detected with a potential cleavage site between amino acids 49 and 50.

The program PredictProtein, PHDhtm (Rost, 1996) detected 10 hydrophobic, transmembrane helices for *Ls*-PPE-1, which are connected to each other by hydrophilic loops (Figure 31).

Signal peptides have a common structure: a short, positively charged amino-terminal region (n-region); a central hydrophobic region (h-region); and a more polar carboxy-terminal region (c-region) containing the site that is cleaved by the signal peptidase (Figure 30). The highly variable h-region is helical, whereas the c-region must be in an extended conformation to be accessible for cleavage (von Heijne, 1998). It is known from the literature that many signal peptides are misidentified as a transmembrane segment (Tusnady, Simon, 1998; Zhou, Zhou, 2003). This might also be the case for *Ls*-PPE-1 since the potential cleavage site was indicated after the first membrane-spanning segment. Therefore, it could be possible that *Ls*-PPE-1 has only 9 membrane spanning

helices and the first detected helix most likely belongs to the signal peptide. The cellular compartment the signal peptide will localize *Ls*-PPE-1 is unknown since consensus sequences exist for very few systems.
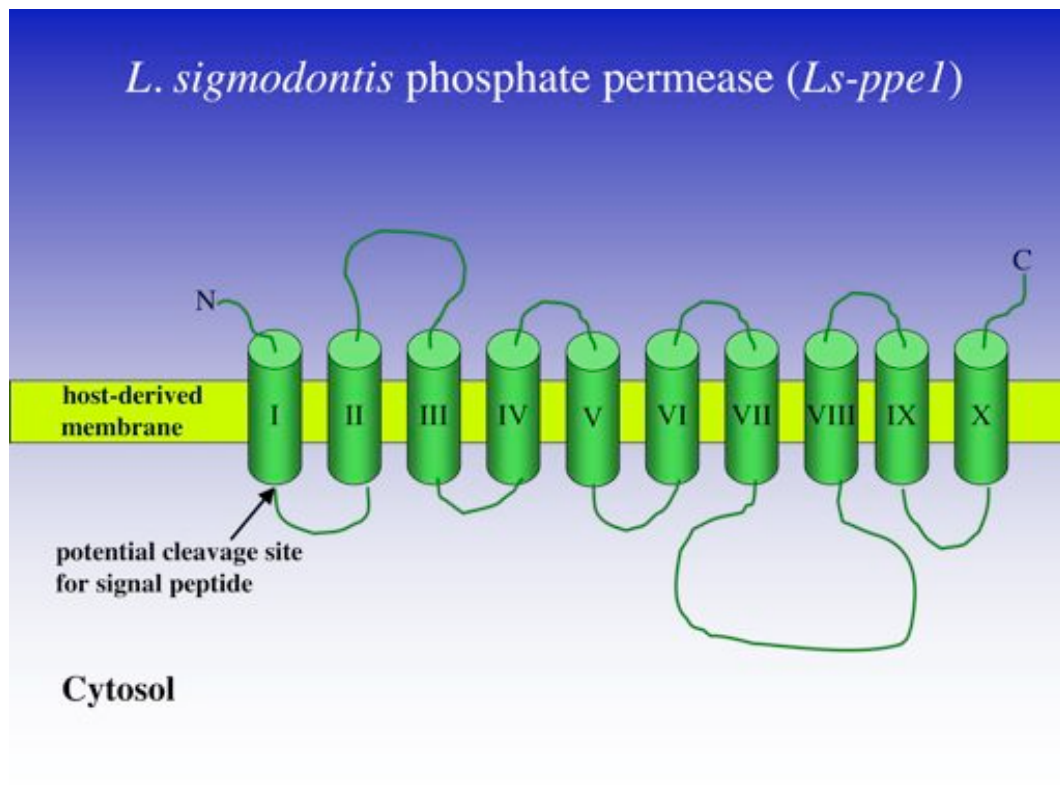
Figure 31. **Structural model of *Ls*-PPE-1.**

The program PHDhtm (PredictProtein) detected 10 transmembrane helices for the best model (I-X, counted from N- to C-terminus). The predicted cleavage site for the signal peptide is indicated (black arrow). The first helical transmembrane region (I) belongs most likely to the signal peptide.

3.3.2   Phylogenetic analysis of nematode homologues of *Ls-ppe-1*

Ls-ppe-1 was identified as a phosphate permease by similarity to homologues from *C. elegans* and other species (analysis by M. Blaxter, Institute of Evolutionary Biology, University of Edinburgh, UK) (Heider, 2006). While peptides from other taxa were also identified in these searches, it was most similar to the nematode members of the phosphate permease family (InterPro domain IPR001204). The extensive nematode EST datasets available in NemBase (Parkinson et al., 2004) were also searched. Three matching genes were identified: from *Onchocerca volvulus* (OVC00569), *Globodera rostochiensis* (GRC01656; a potato cyst nematode) and *Xiphine index* (XIC02915; a plant ectoparasite). While *O. volvulus* OVC00569 matches the N-terminal portion of the permease, the ESTs from the plant parasites matched only the very C-terminus. No *B. malayi* ESTs were identified, but the emerging genome sequence for this filarial parasite (Ghedin, 2004) yielded two putative permease matches. One was apparently complete (TIGR gene model 14967 n01567) while the other, on a small (3000 bp) contig, only contains some of the 5' exons of a permease gene (TIGR model 13026 m00037). For both of these *B. malayi* homologues we reviewed the gene models and re-predicted their structure based on matches to the *Caenorhabditis* (Consortium, 1998; Stein, 2003) and *L. sigmodontis* proteins. An *Ls-ppe-1* orthologue was amplified by reverse transcriptase PCR from cDNA of *A. viteae* using primers designed to quantify *Ls-ppe-1* expression by qPCR. The amplified *A. viteae* product (DQ211814) matched the C-terminus of *Ls-ppe-1*, and was therefore not included in the phylogenetic analysis. *Ls-ppe-1* is most similar to a subset of caenorhabditid homologues, lacking an N-terminal insertion, and having a relatively extended expansion in the C-terminal half (Appendix B). The plant parasitic ESTs both match a C-terminal conserved domain, but do not overlap with *O. volvulus* OVC00569 or the partial *B. malayi* gene 13026 m00037. Several of the sequences are slightly 5' truncated. *O. volvulus* OVC00569 starts just after the end of the signal peptide, and *B. malayi* 13026 m00037 ends at a splice acceptor site in a similar position (no upstream exon was found in the short genomic contig). No genome sequence likely to correspond to the C-terminal (3') half of *B. malayi* 13026 m00037 was found in the whole genome shotgun data, which is known to be incomplete (Ghedin, 2004).

The phylogenetic analysis was carried out using just the N-terminal portion of the alignment (residues 49 to 180 in the alignment of Appendix B). Both maximum parsimony and neighbor joining analyses agree on the linking of most of the caenorhabditid proteins in pairs of orthologues (Figure 32). The one exception is the triplet Cb_CBP19533/Ce_B0222_2/ Ce_B0222_3, where two *C. elegans* proteins are co-orthologues to the *C. briggsae* protein. As the *C. elegans* genes are present as a tandem duplication it is likely that this pattern arose through duplication in the *C. elegans* lineage. The filarial permease homologues are all most closely related to the Ce_C48A7_2/Cb_CBP01602 orthologue pair. Notably, *Ls*-PPE-1 and its *B. malayi* orthologue have apparently arisen by gene duplication unique to the filarial nematodes.
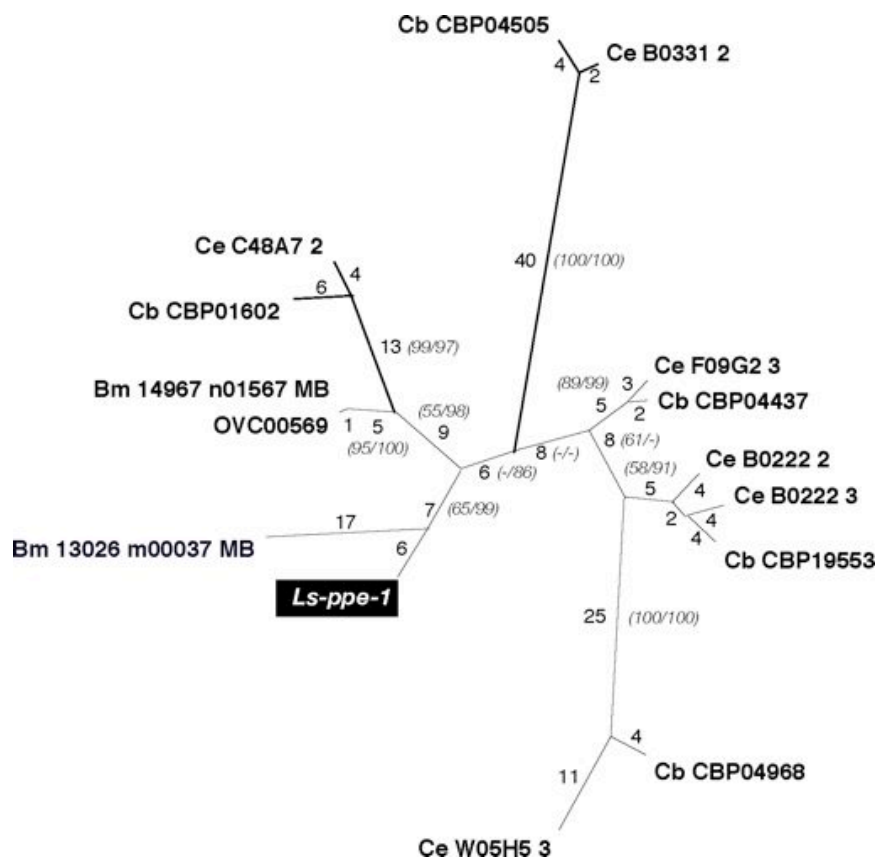
Figure 32. Phylogenetic analysis of nematode homologues of *Ls-ppe-1*

An unrooted phylogram showing the inferred relationships of the permease homologues from nematodes based on maximum parsimony bootstrap analysis of 131 aligned residues. The inferred length, under maximum parsimony is given next to each branch, with, in brackets, the bootstrap support under maximum parsimony followed by support under neighbour joining. Bootstrap support values less than 60% are indicated by a '-'. The *X. index* and *G. rostochiensis* representatives were not included because available sequence does not overlap with the OVC00569 or *B. malayi* 13026 m00037 fragments: they are most closely related to Ce_B0331_2/Cb_CBP04505, although this relationship is weakly supported in the case of GRC01656. Analysis by Mark Blaxter (Heider, 2006)

3.3.3 Quantification of *Ls-ppe-1* expression after tetracycline treatment

3.3.3.1 Northern blot analysis

To avoid artifacts resulting from the use of aRNA or differential display PCR products as probes, a Northern blot analysis was performed to confirm up-regulation of *Ls-ppe-1* after tetracycline treatment. By this method, *Ls-ppe-1* is up-regulated by factor 2.8 on day 15 of the tetracycline treatment. The results confirmed those determined by reverse dot blot (Table 7).

Table 7. **Confirmation of *Ls-ppe-1* up-regulation by three distinct methods on day 15 after tetracycline treatment.**

Ls-ppe-1	Northern Blot [1]	Reverse Northern [2]	Real Time PCR [3]
control	1.0	1.0	1.0
tetracycline	2.8	3.2	2.0

Note: The data were normalized to 1: *Ov*-5S rRNA in the Northern blot analysis, 2: to the untreated controls in the reverse dot blot, and 3: to *Ls-act* gene expression in the RT-qPCR.

3.3.3.2 Real time-quantitative PCR

RT-qPCR was used to quantify the kinetics of *Ls-ppe-1* mRNA expression over the treatment trial of 36 days. The *Ls-ppe-1* expression levels were significantly higher by day 3 to 6 in tetracycline treated female nematodes (Figure 33A). Significantly increased expression was maintained from days 3 to 36, though there was a slight but significant dip in fold expression on day 15. Day 15 expression was nevertheless significantly up-regulated compared to controls. *Ls-ppe-1* was up-regulated by a factor of 3.3 at the end of treatment on day 36. The same bimodal expression pattern with peaks on days 6 and 36 through day 70 was obtained from three different treatment trials of infected mice. In contrast to these results, *Ls-ppe-1* expression in tetracycline treated male nematodes did not have a bimodal expression pattern, being significantly elevated starting after day 15 and remaining up-regulated through day 70 (Figure 33B). Here, it should be noted that the *Ls-ppe-1* expression index is not increased as a result of falling actin levels.
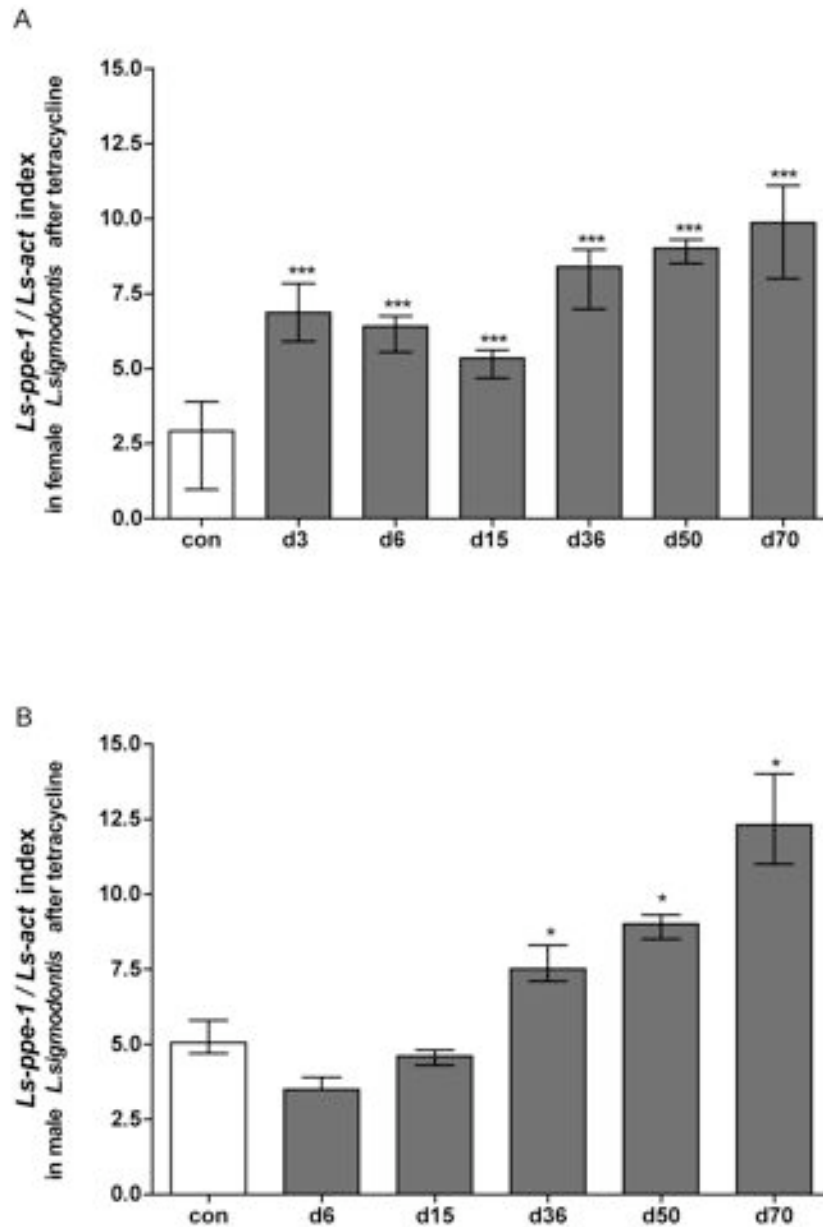
Figure 33. *Ls-ppe-1* **is up-regulated in response to loss of** *Wolbachia* **in female and male worms.**

(A) *Ls-ppe-1* has a bimodal expression pattern during *Wolbachia* depletion by tetracycline treatment of female *L. sigmodontis*. *Ls-ppe-1* and *Ls-act* copy numbers were determined for each time point by quantitative PCR. *Ls-ppe-1* copy numbers were then normalized to the transcript levels of actin to produce the *Ls-ppe-1/Ls-act* index. PCR reactions were performed in triplicate and reproduced twice.
(B) *Ls-ppe-1* expression in male *L. sigmodontis* shows a steady increase beginning on day 36 and continuing through day 70. Significance was calculated by the Mann-Whitney *U* Test (P ≤ 0.05).

3.3.4 Up-regulation of *Ls-ppe-1* is specific to *Wolbachia* depletion

3.3.4.1 *Ls-ppe-1* remains elevated after the end of the tetracycline treatment

In another three independent trials with tetracycline for 36 days, *Ls-ppe-1* transcript levels were measured on days 50 and 70, which represent 14 and 34 days after the end of treatment, respectively. *Ls-ppe-1* expression remained enhanced, and tended to increase even one month after the treatment had been stopped (Figure 33A). These data support the hypothesis that the up-regulation of *Ls-ppe-1* is not simply a direct side effect of tetracycline treatment, but rather is related to the loss of *Wolbachia*.

3.3.4.2 Gentamicin treatment of *L. sigmodontis* has no effect on *Ls-ppe-1*

To further test this, gentamicin, an antibiotic that is known to be ineffective against *Wolbachia*, was used according to the tetracycline regimen for 36 days. No significant difference could be observed in *Ls-ppe-1* expression between untreated controls and gentamicin treated *L. sigmodontis* (Figure 34).
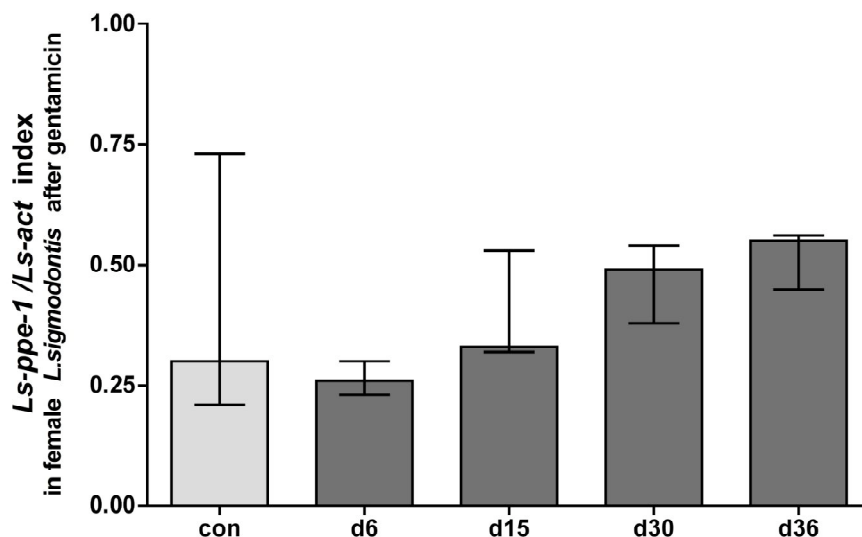
Figure 34. **No change in *Ls-ppe-1* expression after gentamicin treatment.**

Ls-ppe-1 expression in female *L. sigmodontis* treated for 36 days with gentamicin, an antibiotic ineffective against *Wolbachia*, showed no significant alteration over the whole treatment time. The bars represent the median values with error bars for the range.

3.3.4.3 Tetracycline treatment of *A. viteae* has no effect on *Ls-ppe-1*

An *Ls-ppe-1* orthologue was amplified by reverse transcriptase PCR from cDNA of *A. viteae* (DQ211814) using primers designed to quantify the *L. sigmodontis* sequence. *A. viteae* is a filarial nematode that is free of *Wolbachia*. Compared to untreated controls, no significant differences in expression could be detected in *A. viteae* after tetracycline treatment (Figure 35). Thus, the tetracycline treatment itself does not cause an increase in expression of the nematode phosphate transporter in this related species.
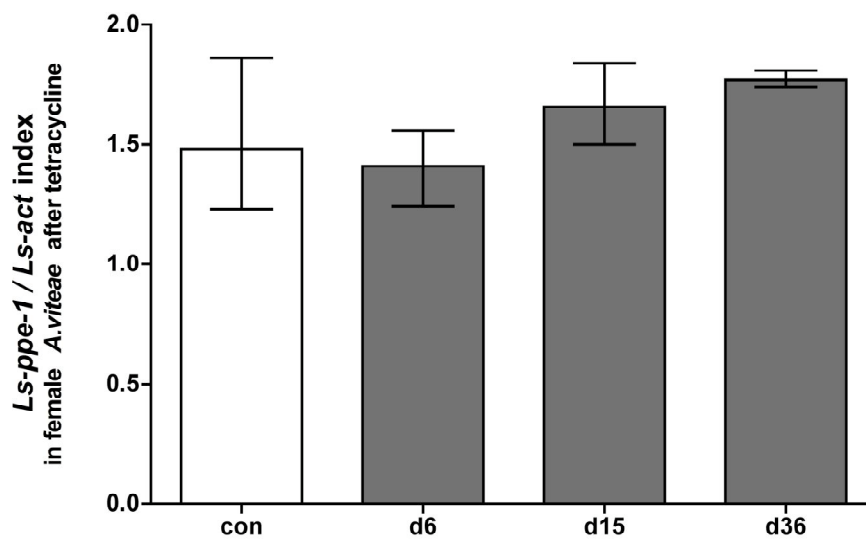
Figure 35. *Ls-ppe-1* **is not altered in** *A. viteae* **after tetracycline treatment.**

Ls-ppe-1 expression remains the same in *A. viteae* (devoid of *Wolbachia*) by tetracycline treatment for 36 days. A representative experiment with median values and error bars indicating the range is shown.

3.3.4.4 *Ls-ppe-1* is not induced upon oxidative stress and heat shock

In order to exclude the possibility that up-regulation of *Ls-ppe-1* was simply a stress response to tetracycline treatment, naïve *L. sigmodontis* were exposed to three different oxidative stress stimuli: paraquat and plumbagin, which generate an internal oxidative stress by redox cycling within the parasite, and xanthine-xanthine oxidase, which produces oxygen radicals in the medium surrounding the nematode. In all three experiments, no significant differences in *Ls-ppe-1* expression were detected compared to unstressed nematodes (Figure 36). In contrast, and as expected, *Ls-hsp-60* expression was increased 3-fold.

In parallel, heat shock (42°C) applied for 2 hours did not increase *Ls-ppe-1* expression compared to controls (Figure 36).
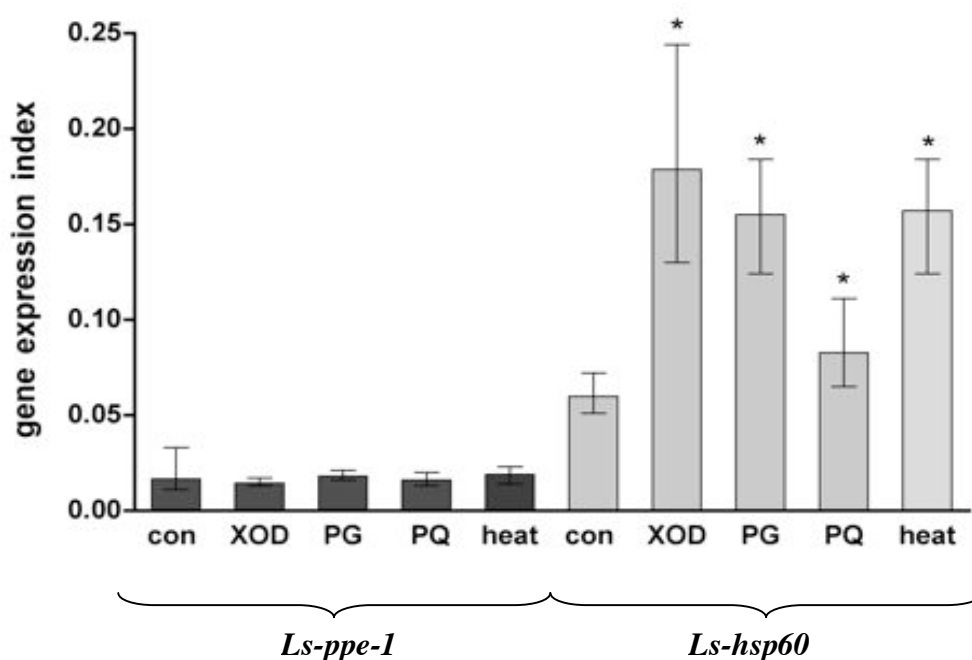
Figure 36. **No up-regulation of *Ls-ppe-1* in response to oxidative stress and heat shock.**

qPCR results for *Ls-ppe-1* from *Wolbachia*-containing *L. sigmodontis* after exposure to xanthine-xanthine oxidase (XOD), plumbagin (PG), paraquat (PQ) and heat shock at 42°C (heat) in comparison to *Ls-hsp60*. Normalizing the copy numbers to copies of *Ls-act* generated the respective gene expression index. Median values with error bars indicating the range of a representative experiment are shown. The PCRs were performed in triplicate and reproduced once. The black bars indicate the *Ls-ppe-1* index after the different oxidative stress stimuli and heat shock. The gray bars indicate the *Ls-hsp60* index. *Ls-hsp60* was significantly increased by all four treatments in comparison to controls. Significance was calculated by the nonparametric Mann-Whitney *U* test ($P \leq 0.05$).

3.4 Quantification of other candidate genes

Reverse dot blot hybridization (Table 6) confirmed the up-regulation of DD-1, DD-9, and DD-10 on day 15 post treatment, thus primers for real time PCR were designed to quantify these genes.

The fragment DD-1 identified as U small nuclear RNA, which is an important component in RNA processing and splicing, was quantified over the treatment duration of 36 days by RT-qPCR, although it was rejected at a later time point (see 3.2.2.3). The results show a short-term up-regulation of DD-1 transcripts during the first 15 days of the tetracycline regime with the peak on day 6, followed by a decreased expression after 30 days, a level comparable to the controls (Figure 37). These data suggest that DD-1 expression reflects either a general stress response to the antibiotic itself or a possible embryonic-specific expression, as the embryos were always affected first by the anti-*Wolbachia* treatment. U RNA is needed for the expression of all genes as part of the processing of RNA into mRNA, but is not necessarily specific to the *Wolbachia* symbiosis.
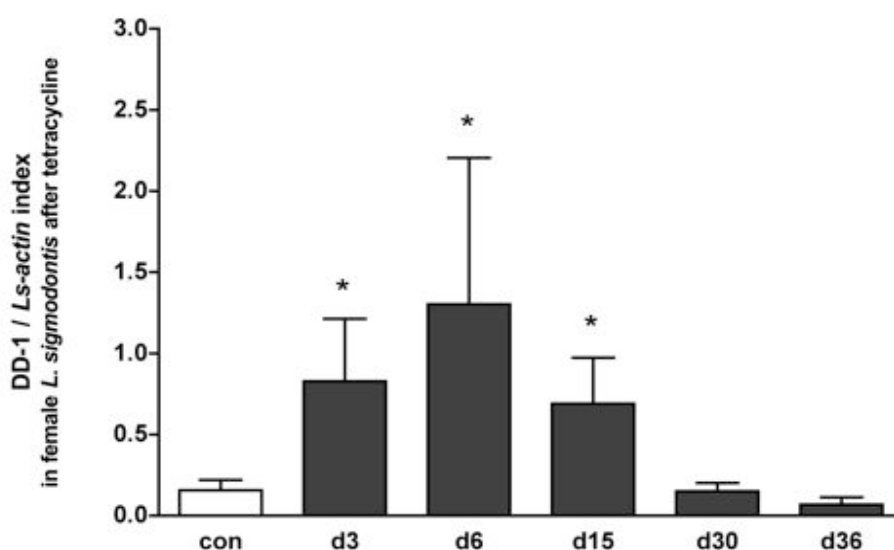
Figure 37. **Short-term up-regulation of DD-1 indicates either a stress response to tetracycline treatment or an embryonic-specific expression.**

The fragment DD-1 shows a significant up-regulation during the first 15 days of the treatment with a peak on day 6. Afterwards, DD-1 transcript level decline and reach levels comparable to the control group. DD-1 and *Ls-act* copy numbers were determined for each time point by RT-qPCR. The DD-1 copy numbers were normalized to the transcript level of *Ls-act* to produce the DD-1/*Ls-act* index. PCR reactions were performed in triplicate and reproduced in 3 independent experiments. A representative experiment with median values and error bars indicating the range are shown. Significance was calculated by the Mann-Whitney *U* Test. Asterisks denote a significant difference between tetracycline treated *L. sigmodontis* and untreated controls ($P \leq 0.05$).

The fragment DD-10 was an inappropriate candidate for quantitative PCR. Because of its short sequence length of only 80 base pairs and the sequence composition, it was impossible to generate adequate primers for real time PCR. For this reason, candidate gene DD-10 was also excluded from further investigations.

3.5 Establishment of RNAi for *Ls-act* in adult *L. sigmodontis*

To establish RNAi in *L. sigmodontis* the actin gene (*Ls-act*) was chosen because, as an important housekeeping gene, a phenotype could be expected from knockdown of its expression. As a negative control, the *Caenorhabditis elegans* yolk receptor, *Ce-rme-2*, was chosen. *Ce-rme-2* is a non-filarial gene that has no homology in the genome of *Brugia malayi* (no significant hits of 22 bp by BLAST search in the TIGR *B. malayi* database), making it suitable as a negative dsRNA control. To compare gene expression of the genes measured, the median copies/μl of the dsRNA-free medium control group was set as 100% in all experiments, and the relative expression of the experimentally treated groups was calculated. In all cases, the median values were used to limit the effects of outliers.

3.5.1 RNAi is dependent on the dsRNA concentration

Serial dilutions of *Ls-act* dsRNA were tested to determine the lowest effective concentration needed to specifically knockdown gene expression in *L. sigmodontis* without generating off-target effects. The nematodes were soaked as described for *B. malayi* for 24 hours in medium containing dsRNA at final concentrations of 35 μM, 17.5 μM, 3.5 μM, 0.35 μM, and 0.035 μM. While all concentrations tested significantly inhibited *Ls-act* expression to less than 10% ($P \leq 0.0001$) as determined by RT-qPCR (Figure 38), the 3.5 μM dsRNA concentration was used in subsequent experiments because it consistently reduced *Ls-act* expression with the low variation and caused no significant differences in *Ls-hsp60* and *Ls-gst2* transcript levels (Figure 39A and B). After 24 hours incubation with 3.5 μM dsRNA *Ls-act* transcripts were reduced to 11.8%

(data not shown), and the inhibition decreased further to 3.1% in dsRNA-free medium quantified after 48 hours (Figure 38).
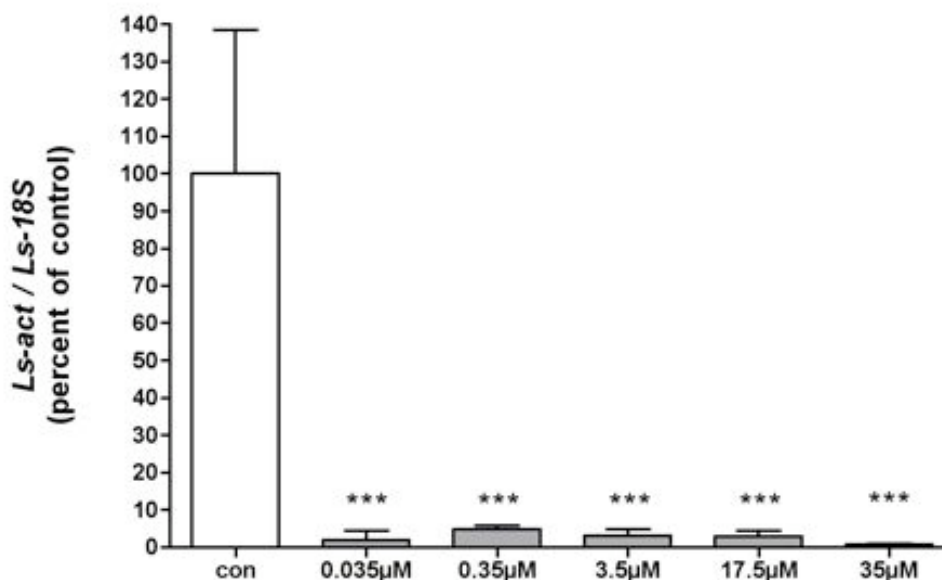
Figure 38. **Determination of the most effective dsRNA concentration for silencing *Ls-act*.**

Nematodes (five groups of three adult females) were soaked for 24 hours in dsRNA-free medium (con) or in the presence of different concentrations of *Ls-act* dsRNA (0.035 – 35 μM). After 24 hours incubation, the worms were transferred into dsRNA-free medium. Forty-eight hours after the start of the experiment, *Ls-act* transcript levels were determined by RT-qPCR and then normalized to *Ls-18S* rRNA gene expression to produce the *Ls-act/Ls-18S* index. The median value of the control group was set to 100%, and the relative reduction of the experimentally treated groups was calculated accordingly. The expression of *Ls-act* was significantly inhibited after incubation of the nematodes with *Ls-act* dsRNA (grey bars) in comparison to control worms (white bar). The same results were seen in three different experiments, one of which is presented here. RT-qPCR was performed in triplicate. The error bars indicate the inter-quartile range. Asterisks denote a significant difference between RNAi-treated nematodes and untreated medium controls (Mann-Whitney *U* Test, $P \leq 0.0001$).

3.5.2 RNAi of *Ls-act* is gene specific

3.5.2.1 Quantification of non-targeted genes: *Ls-hsp60* and *Ls-gst2*

To demonstrate that the inhibitory effect mediated by the dsRNA was specific for *Ls-act*, the *Ls-hsp60* and *Ls-gst2* genes were also measured by RT-qPCR. All tested concentrations of dsRNA showed no significant reduction of *Ls-hsp60* (Figure 39A) and *Ls-gst2* (Figure 39B) transcript levels. The expression of *Ls-hsp60* was significantly increased at concentrations of 17.5 μM and 35 μM (Figure 39A), suggesting that these high dsRNA concentrations cause stress in the nematodes. All dsRNA concentrations lower than 17.5 μM showed no significant differences in *Ls-hsp60* expression. No significant differences were detectable in *Ls-gst2* expression (Figure 39B) despite the higher variation in comparison to *Ls-hsp60* expression (Figure 39A).
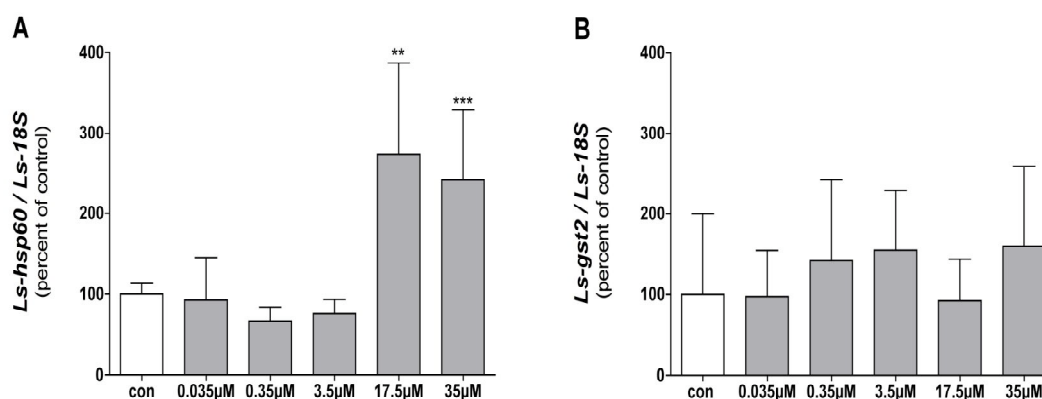
Figure 39. Soaking in *Ls-act* dsRNA does not inhibit the expression of *Ls-hsp60* or *Ls-gst2*.

After 48 hours, two non-related genes were quantified by RT-qPCR as a measure for off-target effects of soaking the nematodes in *Ls-act* dsRNA (0.035 – 35 μM). (A) Normalized *Ls-hsp60* expression was presented as percent inhibition relative to the control group. The *Ls-hsp60* levels were not significantly reduced compared to the dsRNA-free medium control. The two highest dsRNA concentrations showed a significant increase in *Ls-hsp60* expression, indicating that the worms are stressed with such high concentrations of dsRNA. (B) Normalized *Ls-gst2* levels were presented as percent inhibition relative to the control group. *Ls-gst2* expression was not inhibited by soaking in *Ls-act* dsRNA. *Ls-hsp60* and *Ls-gst2* copy numbers were normalized to *Ls-18S* rRNA to generate the RNA/*Ls-18S* index. The median values of the controls were set to 100%, and the relative reduction of the experimentally treated groups was calculated accordingly. The same results were seen in three different experiments, one of which is presented here. RT-qPCR was performed in duplicate. The error bars indicate the inter-quartile range. Asterisks denote a significant difference between RNAi-treated nematodes and untreated medium controls (Mann-Whitney *U* Test, $P \leq 0.05$).

3.5.2.2 Testing a non-filarial gene from *C. elegans* as negative control

The specificity of RNAi was further shown using *Ce-rme-2* dsRNA as a negative control. Soaking of *L. sigmodontis* with *Ce-rme-2* did not reduce *Ls-act* expression at 24 hours (Figure 40A) and 48 hours (Figure 40D). *Ls-hsp60* (Figure 40B, E) and *Ls-gst2* (Figure 40C, F) expression remained the same after soaking in *Ce-rme-2* dsRNA compared to medium controls, further demonstrating that the reduction in *Ls-act* was specific and not due to toxicity of dsRNA or off-target effects.
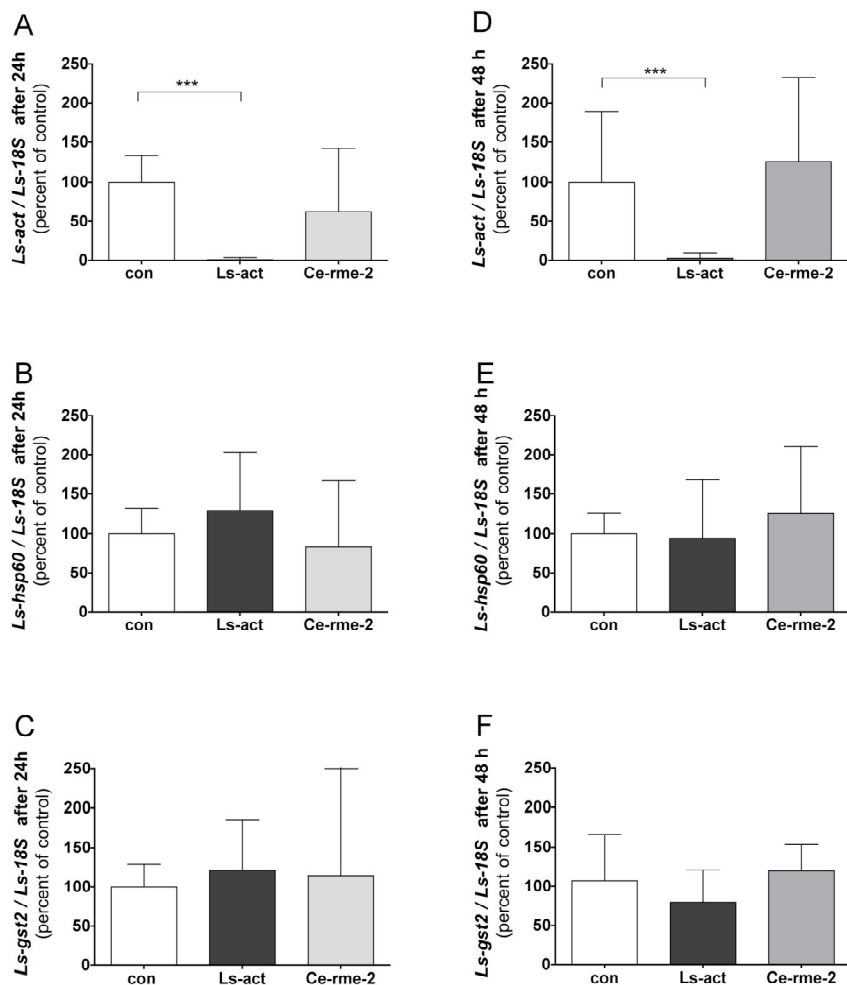
Figure 40. **Soaking *L. sigmodontis* in dsRNA from a non-filarial gene does not inhibit *Ls-act* expression.**

Nematodes were soaked for 24 hours in 3.5 μM dsRNA of *Ls-act* (black bars), 3.5 μM dsRNA of *Ce-rme-2* (gray bars) or dsRNA-free control medium (white bars). *Ls-act*, *Ls-hsp60* and *Ls-gst2* levels were quantified by RT-qPCR 24 hours (A, B, C) and 48 hours (D, E, F) after the start of the experiment and normalized to *Ls-18S*. The median values for the expresson index were presented in the graphs as percent of control (set to 100%). (A+D) *Ls-act* dsRNA specifically inhibited *Ls-act* transcripts to ~3% of control worms. No significant change was seen in the nematodes incubated with *Ce-rme-2* dsRNA. (B+E) *Ls-hsp60* and (C+F) *Ls-gst2* expression levels were not affected by *Ls-act* or *Ce-rme-2* dsRNA treatment. The same results were seen in two experiments, one of which is presented her. Significance was calculated by Mann-Whitney *U* Test, $P \leq 0.0001$.

3.5.3   Persistence of the RNAi effect in the absence of dsRNA

A key hallmark of RNAi is the persistence of gene knockdown after the removal of the dsRNA. To test this in *L. sigmodontis*, the nematodes were removed from the dsRNA after 24 hours and transferred into a larger volume of dsRNA-free medium. The worms were then monitored for an additional 48 hours. In the absence of dsRNA, *Ls-act* gene expression remained low and was even significantly reduced at 48 hours (7%) and 72 hours (3%) (Figure 41). The percent reduction after 48 hours was equivalent to that shown in Figure 38. Longer time points were not tested to avoid adverse effects of long-term culturing of *L. sigmodontis* causing non-specific stress on the worms.
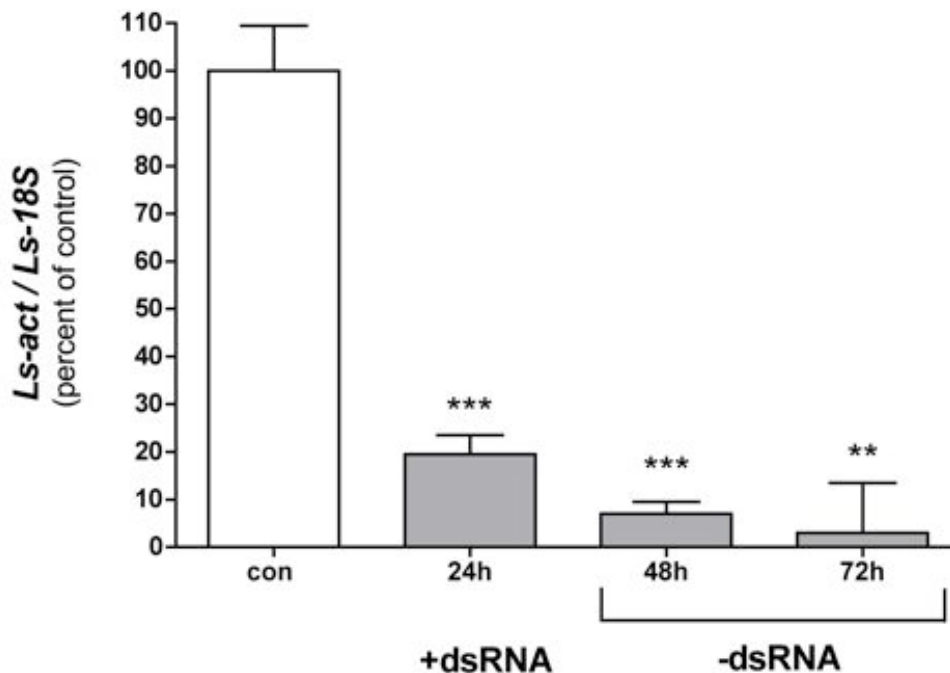
Figure 41. Inhibition of *Ls-act* expression persists in the absence of *Ls-act* dsRNA.

Female *L. sigmodontis* (five groups of three worms/tube) were soaked for 24 hours in the presence of 3.5 μM *Ls-act* dsRNA or in dsRNA-free control medium. The nematodes were then transferred to dsRNA-free medium and incubated for an additional 48 hours. The *Ls-act/Ls-18S* index was determined by RT-qPCR, the median value of the control group was set to 100% and the inhibition of the dsRNA treated groups calculated. *Ls-act* expression was reduced to 19% of the controls after the first 24 hours with dsRNA (+dsRNA). The *Ls-act* transcript levels were further reduced in the absence of dsRNA (-dsRNA) to 7% after 48 hours, and 3% after 72 hours. RT-qPCR was performed in triplicate. The graph presents one experiment from multiple experiments (3 or more, depending on the time point). The same results were seen in all experiments. The error bars represent the inter-quartile range. Asterisks denote a significant difference between RNAi-treated nematodes and untreated medium controls (Mann-Whitney *U* Test, $P \leq 0.05$).

3.5.4   Silencing *Ls-act* produced visible phenotypes in *L. sigmodontis*

3.5.4.1   Reduced motility after RNAi treatment

Adult *L. sigmodontis* were soaked in serial dilutions of dsRNA (0.035-35 μM) for 24 hours as described for *B. malayi* (Aboobaker, Blaxter, 2003). The nematodes of the three different treatment groups (control, *Ls-act*, and *Ce-rme-2*) showed no deleterious effects after removal from the microvolume dialysis system (after 24 hours) and transfer into dsRNA-free culture medium, as indicated by their vigorous movement. A visible phenotype was then clearly seen with *Ls-act* dsRNA 48 and 72 hours after the start of the experiment (i.e. 24 and 48 hours after changing the worms to dsRNA-free culture medium). The nematodes incubated with dsRNA of *Ls-act* had visibly reduced motility or were fully elongated rather than being coiled (Movie 1). This phenotype was consistently observed in all *Ls-act* treated worms 48 and 72 hours after the start of the experiment. Nematodes that were soaked in dsRNA-free medium (Movie 2) or in *Ce-rme-2* dsRNA (Movie 3) showed no change in motility.

The enclosed CD contains the original movies.

Pictures of the recorded worm movements after RNAi treatment were presented here.

Movie 1. *Ls-act* dsRNA treatment results in paralysis of adult worms.
L. sigmodontis were soaked for 24 hours in *Ls-act* dsRNA in a small volume dialysis system and then transferred to a larger volume of dsRNA-free medium. After incubating for another 24 hours, the worms were examined for changes in movement by videotaping for 30-60 s. In comparison to the medium control (Movie 2) and *Ce-rme-2* negative control (Movie 3) the *Ls-act* treated nematodes consistently showed signs of paralysis or were stretched out, indicative of moribund worms. The phenotype shown in the selected movie was seen in all *Ls-act* dsRNA treated worms.

Movie 2. Control nematodes soaked in medium without dsRNA.
L. sigmodontis were soaked in dsRNA-free medium in a small volume dialysis system and then transferred to a larger volume of dsRNA-free medium. After incubating for another 24 hours, the worms were examined for changes in movement by videotaping for 30-60 s. No change in movement was seen when the worms were observed at 24 hours after transfer into a larger volume of medium. The selected movie is representative of all
RNAi experiments.

Movie 3. *Ce-rme-2* dsRNA does not cause paralysis in *L. sigmodontis*.
L. sigmodontis were soaked for 24 hours in *Ce-rme-2* dsRNA in a small volume dialysis system and then transferred to a larger volume of dsRNA-free medium. After incubating for another 24 hours, the worms were examined for changes in movement by videotaping for 30-60 s. No change in movement was seen when compared to control worms (Movie 2). The selected movie is representative of all RNAi experiments treated
with dsRNA of *Ce-rme-2*.

3.5.4.2 Reduced release of microfilariae after RNAi treatment

Microfilarial release was determined by counting released microfilariae from control and RNAi-treated nematodes directly after removal of the adult worms from the low volume dialysis system and after 24 hours in dsRNA-free culture medium. The total number of released microfilariae was significantly lower in *Ls-act* treated parasites than those of control nematodes after 24 (Figure 42A) and 48 hours (Figure 42B). In contrast, there was no significant decrease in the number of released microfilariae from *Ce-rme-2* treated or control worms. Comparing just the medium controls from each time point showed no significant difference in the number of released microfilariae (Mann-Whitney *U* Test, $P \le 0.05$). The same was true for the *Ce-rme-2* treated nematodes. Thus, the significant reduction in microfilarial release was specific for *Ls-act* dsRNA and not the culturing conditions.
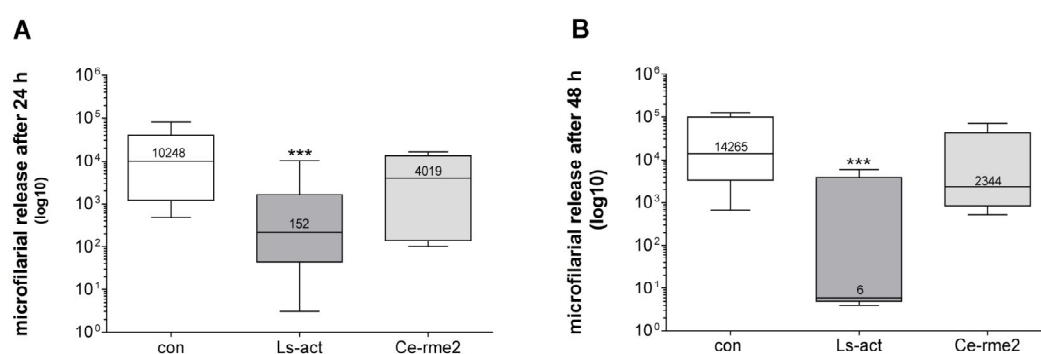
Figure 42. **Inhibition of *Ls-act* expression leads to a reduction in microfilarial release from female *L. sigmodontis* in culture.**

L. sigmodontis (five groups of three worms/tube) were soaked for 24 hours in 3.5 μM dsRNA (*Ls-act, Ce-rme-2*) or in medium-alone (con). The worms were then transferred to dsRNA-free medium and incubated for an additional 24 hours. The microfilariae were collected 24 hours (A) and 48 hours (B) after the start of treatment. The collected microfilariae were stained with Hinkelmann's solution and all microfilariae were counted using a light microscope (10× magnification). Treatment of nematodes with *Ls-act* dsRNA lead to a significant reduction in the number of microfilariae released from the worms at both collection time points. No significant difference was seen from nematodes soaked in *Ce-rme-2*.
The line in the box represents the median value; the error bars represent the minimum and maximum values; the top and bottom of the box represents the 75th and 25th quartiles. The median number of microfilarae released is given in the box. Each graph presents one experiment from multiple experiments (3 or more, depending on the time point). The same results were seen in all experiments. Asterisks denote a significant difference between RNAi-treated nematodes and untreated medium controls (Mann-Whitney *U* Test, $P \le 0.05$).

4   Discussion

Filarial infections are a major health problem in more than 80 developing countries. In endemic areas, mainly in the tropics, an estimated 200 million people are affected, and over one billion are at risk of infection. The current control regimens aim to interrupt the transmission by reducing the levels of microfilariae in infected individuals. Since adult worms can survive up to 15 years (e.g. *O. volvulus*), chemotherapy to control the microfilariae requires annual treatments for many years. In regard to this, worm resistance to the currently administered drugs cannot be excluded. Therefore, a goal for the World Health Organization is the development of new therapeutics that work in a shorter treatment time, and that either lead to an efficient long-lasting block of microfilariae production to control the pathology-inducing worm stages in onchocerciasis (sterilization) or lead to macrofilaricidal effects (killing). The discovery that in addition to the many animal filarial species, most of the human pathogenic filariae also harbor mutualistic *Wolbachia* endobacteria (Taylor, Hoerauf, 1999) opened up new strategies for therapy.

In animal studies, administering tetracycline antibiotics (anti-Rickettsiales) depleted the *Wolbachia* bacteria from the nematodes and caused embryos to degenerate, resulting in the reduction of microfilariae released and finally producing sterility of female worms (Hoerauf, 1999; Hoerauf, 2000c). In the case of bovine onchocerciasis, also macro-filaricidal effects of tetracycline treatment were reported (Langworthy, 2000).

The results of trials with doxycycline in humans infected with *O. volvulus* (6 weeks at 100 mg/day) or LF patients infected with *W. bancrofti* (6-8 weeks at 200 mg/day) also demonstrated the depletion of *Wolbachia*, accompanied by a significant reduction of microfilariae (the main cause of onchocercal disease), followed by amicrofilaremia which persisted for almost two years. These data suggest that the *Wolbachia* do not return, once they are eliminated or depleted below a threshold.

For onchocerciasis patients a significant macrofilaricidal effect was also observed (Hoerauf, 2008). Doxycycline treatment reduced the adult worms to 70% in contrast to multiple rounds of IVM treatment that reduced the adult worms to only 30%. Similarly, a clear macrofilaricidal effect of doxycycline was demonstrated for LF patients (Taylor, 2005b; Supali, 2008).

The pharmacological efficiency of doxycyline is undisputable but the length of the treatment and the known contraindications (not to be given to children under 9 years of age and pregnant or breast-feeding women) make this treatment currently unsuitable for mass chemotherapy. Doxycycline treatment alone (sterility of adult female worms) or in combination with ivermectin (elimination of microfilariae) can thus far improve on the condition of individual patients, and interrupt the transmission of the disease as long as a new infection can be excluded. Recent studies showed as well that doxycycline, either alone or in combination with DEC and albendazole, leads to a decrease in microfilaremia and reduces adverse reactions to antifilarial treatment in *B. malayi*-infected individuals (Supali, 2008).

Doxycycline might be used as a reserve drug in case the suspected resistance to IVM does further develop (Awadzi, 2004a; Awadzi, 2004b). Resistance of *Wolbachia* to doxycycline can theoretically not be excluded, but is unlikely, since *Wolbachia*, being endosymbionts contained in a vacuole behind several membranes inside the nematodes, are not accessible to plasmid or transposon exchange as is the case with free-living bacteria. Also, with other Rickettsiales, there has been no clear resistance development to doxycycline for more than 50 years (Branger, 2004).

In order to find new possibilities to block the transmission or even kill the adult nematodes and then to develop suitable treatment approaches, the aim of this thesis was the screening for nematode genes that might be involved in the symbiosis between *Wolbachia* and their filarial hosts and that play an important role when the bacteria were removed by antibiotic treatment.

4.1   Filarial HSP60 is up-regulated in *O. volvulus* after *Wolbachia* depletion but not directly involved in the symbiosis

The elimination of *Wolbachia* upon antibiotic treatment was repeatedly monitored by immunohistochemistry and electron microscopy using antibodies against bacterial proteins as *Y*-HSP60 and *Bm*-WSP (Hoerauf, 2001). In these studies, an up-regulation of filarial HSP60 was reported in sections from nodules excised 2, 5, 11, 19, and 24 months after the start of doxycycline treatment, being strongest in portions of the filariae where usually no bacteria are present. A weak staining of filarial HSP60 has also been seen in worms from untreated patients (Figure 17C) but these latter worms

have been classified as moribund or dead, as the worms were either old, damaged, or contained neoplastic cells in the pseudocoeloma (Duke, 2002). These signs of pleomorphic neoplasms may partly account for the macrofilaricidal effect of the doxycycline treatment.

One reason for the detected increase in filarial HSP60 could be that the used *Y*-HSP60 antibodies are more specific to the bacterial HSP60 and stain only weakly for the filarial HSP60 until the *Wolbachia* are entirely depleted, as shown by staining consecutive sections of *O. volvulus* with *Bm*-WSP antibodies, specific for bacteria.

To rule this out we decided to quantify the *hsp60* expression of onchocercomata extirpated from untreated and doxycycline treated patients. Specific primers for the filarial *hsp60* gene were designed and tested for specificity by BLAST search as well as in PCR with cDNA of *O. volvulus, L. sigmodontis, A. viteae,* and human material. The BLAST search revealed no hits for bacteria, and the PCR results demonstrated that the primers were clearly nematode specific, as no signal was detectable in human material. The same was true for the *actin* gene, which was used to generate the gene expression index. The advantage of using RT-qPCR is the exactly quantification of mRNA transcripts by the use of an external, defined specific standard curve. Any contamination with genomic DNA would be detectable by this technique running a melting curve after each PCR run, which was not the case in the reported experiments.

In comparison to semi-quantitative PCR (*16S/5S* index), which was used in earlier studies to calculate the decline of *Wolbachia* (Hoerauf, 2003c; Volkmann, 2003b) at the DNA level, RT-qPCR is a more sensitive and precise method, and not as time consuming, as no competitors have to be generated and introduced into the PCR. Additionally, with the earlier semi-quantitative PCR it was impossible to distinguish between living or dead organisms since gDNA was measured and would therefore detect remnant endobacteria present in the samples.

A successful elimination of *Wolbachia* from patients infected with *O. volvulus* by antibiotic treatment could be confirmed by quantification of the bacterial *ftsZ* mRNA transcripts. The median value of the doxycycline treated samples was zero. In contrast, the filarial *hsp60* transcripts of the same samples were up regulated by a factor of 7.7 after doxycycline treatment. A direct association between increasing *hsp60* transcripts and *Wolbachia* reduction was demonstrated when filarial *hsp60* index was plotted against bacterial *ftsZ* index in the Spearman Rank test (Statview 5.0). The linear regression plot shows a weak but positive correlation. A way to support this direct

association between *Wolbachia* depletion and increased *hsp60* expression might be better shown with greater sample numbers and samples extirpated from several earlier time points, when *Wolbachia* levels are not near zero.

For the reasons mentioned above, it is believed that the transcriptional up-regulation of filarial mitochondrial *hsp60* is not just a reaction to the stress of accumulating many dead *Wolbachia* bacteria. Rather, the up-regulation may indicate efforts by the filarial cells to compensate for an interruption in some cell process, which the *Wolbachia* provide to the nematode. This interruption may lead to a buildup of proteins which require HSP60 for proper folding, i.e. the unfolded protein response. Such a response has been described for mitochondria in mammalian cells and in *Caenorhabditis elegans* (Yoneda, 2004). In *C. elegans*, the accumulation of unfolded proteins leads to the up-regulation of HSP60 specifically in the mitochondria and is associated with proteins imported into the mitochondria, which subsequently form multi-protein complexes. Therefore we conclude that the resulting up-regulation of HSP60 in the mitochondria is not from other stresses such as reactive oxygen species (Zhao, 2002; Yoneda, 2004).

In summary, the depletion of *Wolbachia* from filarial worms leads to increased mitochondrial *hsp60* expression at the level of transcription and translation, and this increase is not a direct effect of the antibiotic treatment since in *A. viteae*, a filarid that is devoid of *Wolbachia*, no increase in *hsp60* expression upon tetracycline treatment was detectable. Since this up-regulation lasts up to 24 months, and hopefully longer, it demonstrates that doxycycline treatment has a long lasting effect on the metabolism of *O. volvulus*.

4.2   *Wolbachia*, targets for a new chemotherapy against filarial infections

Nematode genes that respond to an anti-wolbachial treatment might be important in the symbiosis and thus represent targets for new chemotherapeutical approaches. The development of new drugs is indeed needed since issues of drug resistance, especially for the currently used mass drugs DEC and IVM, have emerged (Awadzi, 2004a).

Efforts in the *Wolbachia* community lead to the sequencing and annotation of the complete *Wolbachia* genome of *B. malayi* (*w*Bm), and revealed important insights into genes that have been kept by the *Wolbachia* and genes that have been lost during this symbiosis (Foster, 2005; Pfarr, Hoerauf, 2005). Additionally, the draft genome of

B. *malayi* (Ghedin, 2007) provided evidence for adaptations of *B*. *malayi* to niches in its human and vector hosts and into the molecular basis of a mutualistic interaction with its *Wolbachia* endosymbiont. As 9 of 10 enzymes required for the *de novo* purine synthesis, 6 of 7 genes required for heme biosynthesis, and all 5 enzymes required for *de novo* riboflavin biosynthesis are absent from the *B*. *malayi* genome (Ghedin, 2007), the worm may be forced to meet requirements for these key metabolites by active uptake of mammalian host-supplied molecules or through reliance on *w*Bm, which has retained the ability to make all but one amino acid, nucleotides, and purine, heme, and riboflavin synthesis pathways. All these metabolites may be provided by the endobacteria to the nematode as part of the symbiosis. Exploitation of this wealth of information is just beginning.

4.3 Screening for genes involved in the symbiosis between *Wolbachia* and its filarial host

The identification of filarial genes that are up-regulated in response to the loss of their endosymbiotic bacteria due to anti-wolbachial treatment was proposed. In our animal model, IL-5-deficient Balb/c mice infected with *L. sigmodontis* were treated with tetracycline at levels known to deplete endosymbiotic *Wolbachia* bacteria. Differential display PCR of mRNA generated from tetracycline treated and untreated nematodes revealed many fragments that had changed in expression. Many down-regulated fragments were identified, but after sequencing all were found to be of *Wolbachia* origin, indicating genomic DNA contamination. Therefore, we focused on up-regulated genes only, and found 12 potential candidates (Table 5).

These candidates were rigorously tested to confirm that they were up-regulated, and further to eliminate false-positives. This was done by Reverse dot blot and Northern blot. In the first, we used a non-radioactive variant of aRNA generated hybridization probes that were fluorescein labeled with the ECL kit. Unfortunately, the results were not reproducible, probably due to the multiple enzymatic steps needed to amplify the small amounts of RNA extractable from small numbers of worms. These included three transcription steps (reverse transcription from RNA to cDNA; *in vitro* transcription to aRNA; and reverse transcription of aRNA into single stranded cDNA that was subsequently used for fluorescein labeling). Therefore, we switched to radioactive

hybridization probes, which allowed a more "direct" labeling of the aRNA since only two steps were needed between RNA extraction and labeled probe, thus limiting the introduction of error. In Reverse dot blots with these radioactive hybridization probes made from aRNA, 3 out of the 12 candidate genes had an up-regulation of factor ≥1.5 at day 15 post treatment (Table 6), our arbitrarily chosen cut-off. The candidates that passed this screening were DD-1, DD-9, and DD-10.

Sequence analysis of the DD-1 gene fragment revealed BLAST hits corresponding to the small nuclear RNA U6 gene (U snRNA) of *Ascaris lumbricoides*, another parasitic nematode (Shambaugh, 1994). In nematodes, nuclear pre-messenger RNAs are processed by *cis-* and *trans*-splicing. Usually, the catalysis of the splicing process depends on the participation of several snRNAs in the form of ribonucleoprotein particles (U snRNPs) (Nilsen, 1993). The U6 snRNA is required for both *cis-* and *trans*-splicing. Therefore, the clone DD-1 was further investigated by qPCR, but had just a short-term up-regulation during the first two weeks of the treatment trial (Figure 37), suggesting that the raised expression might be due to a general stress response regarding the tetracycline treatment. On the other hand, the short-term up-regulation might also be embryonic-specific expression since it is known that the antibiotic treatment affects the embryos first (Langworthy, 2000). Nevertheless, since this was a gene associated with a general process, RNA transcription, DD-1 was excluded from further investigations.

Candidate DD-10 (an 80 bp fragment) could not be confirmed by Reverse dot blot hybridized with radioactive labeled DD PCR products and was also rejected.

Only one gene out of these three candidate genes, DD-9, passed the rigorous screening.

4.4 Identification of a *L. sigmodontis* phosphate permease

The candidate designated as DD-9, identified by BLAST as a phosphate permease of *L. sigmodontis* (*Ls-ppe-1*), was verified to have a 2-3 fold up-regulation by Reverse Northern blot using radioactively labeled aRNA and DD PCR products and was therefore chosen for additional confirmation and quantification by Northern blot and quantitative PCR.

Using quantitative PCR, *Ls-ppe-1* was shown to be up-regulated in female nematodes in a bimodal pattern while male nematodes only showed a linear increase in expression. This 3-fold over-expression remained at its peak level up to one month (day 70) after

the tetracycline treatment has been stopped, demonstrating a long-term alteration in the transcriptional state of the gene. These data also suggest that *Wolbachia* do not return, once they are eliminated from the nematode.

Experiments in cattle demonstrating killing of adult *O*. *ochengi* by tetracycline showed that the embryos are the first stage to die within 3 months post treatment, followed later by death of the adult nematodes after 6 months (Langworthy, 2000). The kinetic of *Ls-ppe-1* expression was consistent with a similar pattern in *L. sigmodontis*. The first peak in expression of adult female worms between days 3 and 6 after the start of tetracycline treatment could result from an increased expression of *Ls-ppe-1* in embryos trying to compensate for the lack of *Wolbachia,* accompanied with decreased delivery of nucleotides or other metabolites usually provided to the nematode (see also 4.5.4).

The decreased expression on day 15, which is still significantly higher than in control nematodes, could represent the loss of embryonic expression as embryos are more sensitive to anti-wolbachial treatment. At this time, a detectable up-regulation in the adult nematodes is just beginning. In contrast, male nematodes show linearly increasing *Ls-ppe-1* expression beginning on day 6 of treatment with a significant peak on day 36, the end of the treatment.

Investigation of the dynamics of embryo and adult death, and of the pattern of *Ls-ppe-1* expression in pre-fertile females (which would not be expected to show the early peak) would address this hypothesis.

4.5   Characterization and potential function of *Ls-ppe-1*

4.5.1   Identification of three *Ls-ppe-1* sequence variants

RLM-RACE PCR was used to obtain the full-length sequence of three variants of the phosphate permease: *Ls-ppe-1*-1, *Ls-ppe-1*-2 and *Ls-ppe-1*-3. These three transcripts have the same coding sequence and differ only in their 5' and 3' untranslated regions.

The predicted *Ls*-PPE-1 protein was most similar to four phosphate permeases in *C*. *elegans* (B0222_3, B0222_2, F09G2_3 and C48A7_2). The Ce_C48A7_2 phosphate permease is expressed in adult nematodes and larvae and shows a severe phenotype in RNAi experiments (embryonic lethality, sterility of adult nematodes, and other, undescribed growth and morphological defects) (Maeda, 2001). The two genes on cosmid B0222 were also tested as part of large-scale RNAi screens by two groups,

using different methods: feeding (Kamath, Ahringer, 2003) or microinjection (Sonnichsen, 2005). Both approaches produced no visible phenotype. However, the same two groups also did not see a phenotype when testing the sequence for Ce_C48A7_2, whereas Maeda *et al*. did see a phenotype by soaking the nematodes in dsRNA. The differences in the techniques may be a source of the different results. It is also possible that phenotypes may have been missed, since the large scale RNAi screenings looked only at early development stages and lethality. More subtle phenotypes could have been missed in these screens. The results from Maeda's group are relevant to *Ls-ppe-1* since the knock down in *C. elegans* has a phenotype similar to that observed in nematodes depleted of *Wolbachia* upon tetracycline treatment, namely embryonic death and female sterility.

4.5.2   Phylogenetic studies of nematode homologues of *Ls-ppe-1*

Phylogenetic analysis (Heider, 2006) using available *Caenorhabditis* (The *C. elegans* Genome Sequencing Consortium, 1998; Stein, 2003), the *B. malayi* genome sequence (Ghedin, 2004) and other nematode EST datasets (Parkinson, 2004) shows that the *Ls-ppe-1* gene is not unique to *L. sigmodontis* but has an orthologue in another filarial nematode *B. malayi*. No other orthologues were detected. However, closely related paralogues were found in *O. volvulus, B. malayi* and the two *Caenorhabditis* species (Appendix B).

O. volvulus OVC00569 and *B. malayi* 14967 n01567 are significantly more similar to these caenorhabditid orthologues than are *Ls-ppe-1* and *B. malayi* 13026 m00037, which have no orthologous caenorhabditid proteins (Figure 32). Indeed, in the portion of the protein available for comparison, *Ls-ppe-1* and *B. malayi* 13026 m00037 are more divergent than any of the caenorhabditid orthologue pairs, and are as distant from each other as *O. volvulus* OVC00569/*B. malayi* 14967 n01567 are from their caenorhabditid orthologues. We interpret this pattern to suggest that the *Ls-ppe-1* gene arose from duplication in a lineage predating the *L. sigmodontis–B. malayi* split, and that it has undergone accelerated evolution since then in matching the biology and needs of the *Wolbachia* symbionts. It will be informative to isolate and complete the sequence of *B. malayi* 13026 m00037 and compare its biology and regulation to *Ls-ppe-1*.

4.5.3 *Ls-ppe-1* does not respond to stress stimuli

Even though the loss of *Wolbachia* causes stress in the filarial nematodes, *Ls-ppe-1* is probably not a general stress-response gene. Exposure to oxidative stress and heat shock did not induce a rise in *Ls-ppe-1* transcript levels whereas an increase in *Ls-hsp-60* expression could be measured after both stresses. It was not possible to test all possible sources of stress (e.g. nutrition, cold, etc.), but as all three chemicals used to generate oxidative stress and an elevated temperature induced *Ls-hsp-60* expression but not *Ls-ppe-1*, it is likely that other physical stresses would not lead to an up-regulation in *Ls-ppe-1*. Secondly, treatment with gentamicin, an antibiotic that does not deplete *Wolbachia* from the nematode (Taylor, 2000; Mohanty, 2001), had no effect on *Ls-ppe-1* expression. Finally, and of greater importance, the *Wolbachia*-free filarid *A. viteae* displayed no increased expression of the orthologue after tetracycline treatment. The up-regulation of *Ls-ppe-1* steady state mRNA levels observed with tetracycline treatment likely reflects a role for the protein product of this gene in the physiological interaction between the nematode and *Wolbachia*.

4.5.4 The hypothetical function of *Ls-ppe-1* in the symbiosis

The role of *Ls-ppe-1* in the symbiosis between *Wolbachia* and their filarial hosts may relate to a possible involvement in nucleotide metabolism. The genome of the *Wolbachia* from the filarial nematode *B. malayi* (*w*Bm) has been completely sequenced (Foster, 2005). The *w*Bm genome contains a type IV secretion system that in other intracellular bacteria is used to export molecules to host cells. In contrast to most endosymbiotic bacteria, *w*Bm is able to make only one amino acid *de novo*, but has retained all genes necessary to synthesize nucleotides. *w*Bm may provide nucleotides or nucleotide precursors to its host for processes such as embryogenesis (Foster, 2005; Pfarr, Hoerauf, 2005).

Database searches (motif.genome.jp/) for the *Ls*-PPE-1 protein revealed that apart from the signal peptide only a PHO4 motif is present (amino acid position: 48-512). PHO4 is belongs to a phosphate transporter family (NCBI GenomeNet database Pfam; InterPro domain IPR001204) that includes PHO4 from the filamentous fungus *Neurospora crassa* (Versaw, Metzenberg, 1995). Phosphate uptake by PHO4 in *N. crassa* was stimulated 85-fold by the addition of Na+, which supported the idea that PHO4 is a

Na(+)-phosphate symporter. The sequence difference between *Ls-ppe-1* and PHO4 did not allow a direct comparison and phosphate uptake by *Ls-ppe-1* was not examined. Thus, *Ls-ppe-1* is supposed to transport phosphate, and there is no hint for an antiport/symport mechanism or other function yet.

Phosphate is an essential molecule for nucleotide synthesis. As *Wolbachia* are contained within a vesicle in the nematode cells, they do not have direct access to either extracellular or cytoplasmic phosphate. If *Ls-ppe-1* were located in the vesicle surrounding the *Wolbachia* it would be well placed to transport phosphate from the nematode cell to the *Wolbachia*. This is supported by the presence of a signal sequence that could potential lead to transport of *Ls-ppe-1* to the membrane around the *Wolbachia* endobacteria. According to this hypothesis, the loss of *Wolbachia* after tetracycline treatment would then lead to a deficiency of nucleotides, or some other metabolite provided by the endobacteria, in the nematode cell. The cell would then attempt to compensate for the lack of nucleotides by increasing the expression of *Ls-ppe-1*, thereby providing more phosphate to *Wolbachia* (Figure 43).

Evidence for such a feedback interaction can be inferred from the bimodal regulation of *Ls-ppe-1* expression (see section 4.4). In this scenario, the *Wolbachia* do not need to provide the worm cell with nucleotides, but the inability of the endobacteria to synthesize needed nucleotides would lead to death of the *Wolbachia* and therefore deplete the molecules that are provided to the worm by their endosymbionts.
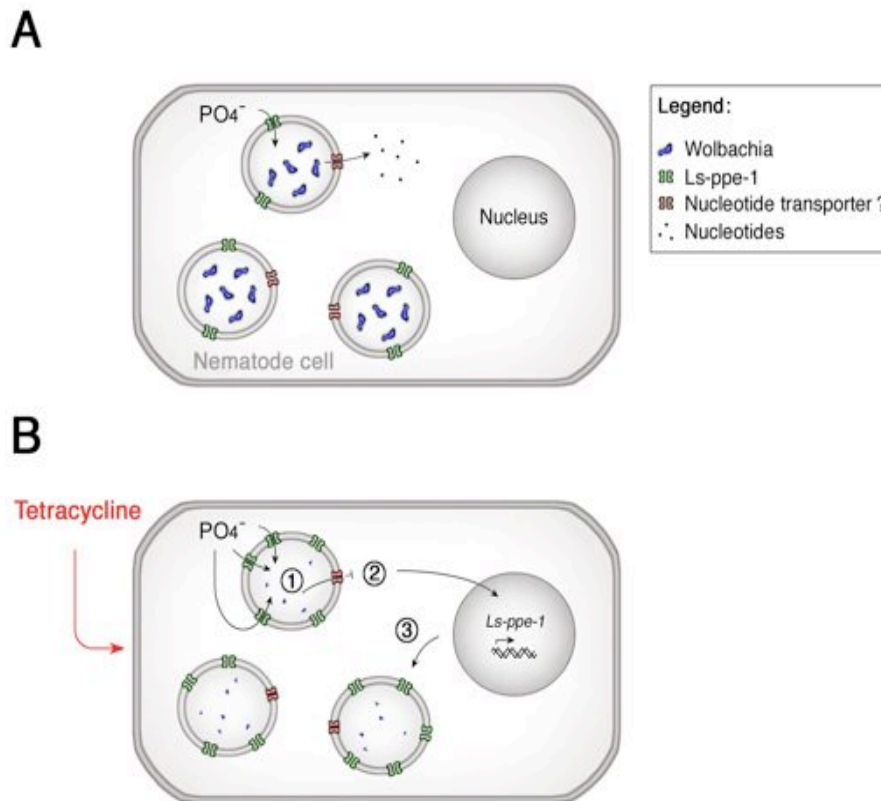
Figure 43. The hypothetical function of *Ls-ppe-1*.

(A) The steady state of a nematode cell is shown A nematode-derived vesicle contains *Wolbachia* producing metabolites that are delivered to the host cell. (B) *Wolbachia* depleted by tetracycline (step 1) leads to a deficiency of the provided metabolites. The cell senses the imbalance and signals the nucleus (step 2). Then the nematode cells try to compensate for the loss by increasing *Ls-ppe-1* (step 3) thereby pumping more phosphate into the vesicle.

4.5.5 Prospects

RNAi can be suggested as a way to produce a functional knock down of the phosphate permease in *L. sigmodontis* and *B. malayi* to demonstrate that the phosphate transport is an important feature for embryonic development. To further investigate the function of *ppe-1*-like genes, the *C. elegans* phosphate permease orthologues could be knocked down and a thorough analysis of the resulting phenotypes could be performed. This would set the groundwork for recovering phosphate permease activity in *C. elegans* using *Ls-ppe-1* and orthologues from *B. malayi* and *O. volvulus*. Since it is possible that related *C. elegans* genes could compensate for one another, a knock down of two genes through double-target RNAi would need to be performed (Reichhart, 2002). Analysis of the ultrastructural location of *Ls*-PPE-1 will test the hypothesis of co-localization with the vesicle surrounding the *Wolbachia*.

4.6   Implementation of RNAi in the model organism *L. sigmodontis*

The knockdown experiments accomplished in this thesis showed that a housekeeping gene such as *Ls-actin* could be efficiently silenced, demonstrating that parts of the RNAi machinery are also present in the rodent filaria *L. sigmodontis*.

4.6.1   The characteristics of silencing *Ls-act*

The efficiency of RNAi depends on the concentration of dsRNA in the medium with the best effect seen using a ten-fold lower concentration of dsRNA (for *Ls-act*) than that reported in the original method of Aboobaker (Aboobaker, Blaxter, 2003) for adult *B. malayi*. A concentration of 3.5 μM dsRNA mediated the specific knockdown of *Ls-act* gene expression in *L. sigmodontis* to less than 10% of controls. Concentrations lower than 3.5 μM were also effective, but not as consistent between experiments.

This knockdown of *Ls-act* persisted for at least two days after the removal of the worms from the dsRNA. This is a key feature of RNAi described also in other systems (Montgomery, Fire, 1998; Correnti, 2005). To avoid any adverse effects due to long term culturing of the worms in medium, adult nematodes could be implanted into naïve *Meriones unguiculatus*. By this method, the nematodes can then be removed as late as 60 days post implantation and it could be determined how long the RNAi effect persists as has been shown in *Schistosoma mansoni* (Correnti, 2005).

The silencing of *Ls-act* by RNAi resulted in visible phenotypes: it reduced the motility of adult worms and led to a significant reduction in the number of larvae released into the medium. Not all worms were affected to the same extent as can be seen by the large variation in the number of microfilariae released (see the boxes and range bars in Figure 42A and B). Clearly some nematodes make no larvae while others still release a large number. Such variation is consistent with results reported in other organisms including *Drosophila*, *C. elegans, Trypanosoma brucei* and *S. mansoni* (Grant, Hirsh, 1999; Simmer, 2003; Hashmi, 2004; Ullu, 2004; Correnti, 2005).

4.6.2 Additional control for off-target effects

Another improvement over the original protocol and the methods used for *T. colubriformis* (Issa, 2005) is the establishment of controls for off-target effects. Delivery of dsRNA molecules into organisms can have cytotoxic effects, presumably mediated by acidification of the medium due to high dsRNA concentrations (Huppi, 2005). Off-target-effects such as rapid dying of nematodes and a decrease in expression of non-targeted genes have been avoided in other systems by lowering the concentration of dsRNA (Yang, 2000; Persengiev, 2004; Huppi, 2005).

We controlled for off-target effects in two ways:

    1) monitoring the expression levels of *Ls-hsp60* and *Ls-gst2*; and

    2) including a dsRNA negative control.

The 3.5 μM dsRNA concentration that reduced *Ls-act* expression was shown not to reduce the expression of *Ls-hsp60* or *Ls-gst2*. Not unexpectedly, 17.5 μM and 35 μM dsRNA caused an increase in *Ls-hsp60* expression, showing that these high concentrations of dsRNA were stressful to the worms. The normally low transcript abundance of *Ls-gst2* in the samples (Liebau, 2000) led to a late signal in the RT-qPCR (between 35 and 40 cycles) and caused high variation in the copy number measured, even in the control worms. The apparent increase as high as 200% in *Ls-gst2* is therefore not biologically significant. The reduction in *Ls-act* expression was further shown to be gene specific and not due to cytotoxicity of dsRNA by incubating worms with a non-filarial dsRNA from *C. elegans. Ce-rme-2,* used at the same concentration as *Ls-act,* did not significantly inhibit the expression levels of all three genes measured (Figure 40). *Ce-rme-2* dsRNA at 3.5 μM, like *Ls-act*, did not significantly increase the expression of *Ls-hsp60* and *Ls-gst2*.

4.6.3 The differences between different model organisms

Although Aboobaker et al. (2003) demonstrated in adult *B. malayi* worms that FITC-labeled dsRNA is localized to the hypodermis and digestive and uterine tracts, the exact method of uptake in filarial nematodes, whether passive or active, is not known. Differences in the thickness of the cuticle between individual worms could therefore contribute to an inefficient uptake of dsRNA from the surrounding medium, especially if uptake is strictly passive. Additionally, differences between *L. sigmodontis* and *B. malayi* may account for the differences in the amount of dsRNA needed to produce an RNAi effect in these two species. In addition to the ease of maintaining the life cycle of *L. sigmodontis*, the apparent requirement for lower concentrations of dsRNA by *L. sigmodontis* to produce a phenotype without off-target effects supports the use of this model organism for further functional studies by RNAi. However, we have tested only one gene. Further experiments with other genes need to be performed to support this conclusion.

In contrast to Aboobaker (Aboobaker, Blaxter, 2003) who were unable to deliver FITC-labeled β-tubulin dsRNA into sheathed and exsheathed first stage larvae, Lustigman *et al.* (Lustigman, 2004) could demonstrate successful delivery of dsRNA for two cysteine proteases into *O. volvulus* third stage larvae by soaking. This group used ~1.5 μM dsRNA to knockdown the gene expression in *O. volvulus* larvae.

In our present study with adult *L. sigmodontis*, we found the best effect with 3.5 μM of dsRNA for the *Ls-act* gene. We also observed that concentrations as low as 0.035 μM significantly reduced *Ls-act* transcript levels, confirming that only a few molecules dsRNA per cell are required to produce RNAi (Fire, 1998). Thus, *Ls-act* dsRNA concentrations lower than 17.5 μM (see Figure 39 and Figure 40) are optimal for RNAi in *L. sigmodontis* without causing off-target effects. However, each gene should be empirically tested to determine the best concentration that reduces gene expression without off-target effects.

Recently, limited reliability and efficiency of RNAi in parasitic nematodes of plants and animals has been reported (Issa, 2005; Geldhof, 2006; Visser, 2006). To understand these variable outcomes, the available preliminary parasite genomes of *H. contortus* (95% coverage) and *B. malayi* (98% coverage), and expressed sequence tag (EST) datasets were searched for genes that are known to be involved in the RNAi pathway in

C. elegans (Zawadzki, 2006; Knox, 2007). Both groups were unable to identify the following genes (Table 8) that were thought to be essential for a functional and systemic RNAi pathway:

Table 8. Unidentified genes essential for a functional RNAi pathway

C. elegans gene name	Protein function
Rde-4	RNA binding in dicer complex
Rde-2	siRNA accumulation
Sid-2	Systemic RNAi
Rsd-2	Systemic RNAi

These observations were crucial since *C. elegans*, with mutations in the *rde-4* gene are deficient in RNAi induced by dsRNA but not by siRNA, which shows the essential role of RDE-4 in siRNA generation. It is possible that an *rde-4* homologue has yet to be sequenced from parasitic nematodes or that *rde-4* is considerably divergent from *C. elegans rde-4* and the *Drosophila melanogaster* homologue *r2d2* (Liu, 2003). It is not known whether the function of RDE-4 is undertaken by a different protein or *rde-4* has been lost during evolution. If this were the case, how would one explain the increasing number of reports describing successful RNAi in parasitic nematodes? One possibility is that standard dsRNA preparations, which are used at relatively high concentrations, contain contaminating partially degraded dsRNA, aRNA or siRNAs at a concentration sufficient to induce RNAi downstream of the interaction of RDE-4 and Dicer (Knox, 2007). The other possibility would be an alternative pathway.

If the *sid-2* and *rsd-2* genes were indeed absent, this would infer that the RNAi effect would not systemically spread throughout the worm. In this case, the effects would only be observed in areas of the worms that were directly accessible to the dsRNA such as the outer surface, the gut and the reproductive tract (Geldhof, 2007).

Nevertheless, it has been clearly demonstrated that RNAi is possible in helminths under certain conditions (delivery mode of dsRNA, developmental stage targeted).

4.6.4 Prospects

The reduction in the dsRNA concentration used for the soaking method makes RNAi possible in filarial nematodes without incurring extremely high material costs. Lower dsRNA concentrations could also be tried with electroporation so that an alternative method to introduce dsRNA might be developed for those cases where soaking fails. This is a valid concern as has been demonstrated in the sheep parasite *T. colubriformis* (Issa, 2005). In this system, electroporation lead to a better reduction in *T. colubriformis* ubiquitin (*Tc ubq-1*) expression compared to feeding or soaking with dsRNA. Also to be tested is whether siRNA could be used for filarial nematodes. Again, Issa *et al*. (Issa, 2005) showed successful reduction in *Tc ubq-1* expression using a 22 bp synthetic dsRNA (siRNA). The authors showed that *Tc ubq-1* siRNA works better by soaking than the corresponding full length dsRNA, and that the *Tc ubq-1* knockdown with siRNA is even more efficient by electroporation. Our own experiments demonstrated that a short dsRNA (99 bp) lead to efficient RNAi in adult *L. sigmodontis*. Our results with dsRNA of 99 bp and those of Issa *et al*. (Issa, 2005) with siRNA suggest that shorter dsRNAs may be better for RNAi in parasitic nematodes and should be examined formally in more parasitic nematodes, especially filarial nematodes, with more genes. The similarity of many genes in filarial nematodes (Blaxter, 2002) allows for functional testing of unique genes identified from the *B. malayi* genome in the rodent filaria *L. sigmodontis*. Using *L. sigmodontis* for RNAi studies is advantageous because it may require, as shown here with *Ls-act*, lower concentrations of dsRNA, and any long-term RNAi effect can be monitored by implantation of the nematodes into a natural host.

5   Summary

Filariasis is a vector-borne disease that affects 200 million individuals in the tropics, a large number of them seriously, where the disease leads to blindness (onchocerciasis) or elephantiasis (lymphatic filariasis). The prevalence of infections with lymphatic filariasis is declining but for onchocerciasis newer data revealed an additionally 20 million cases (Basanez, 2006). Despite intensive efforts, it may be impossible to eradicate filariasis by conventional therapies (Stolk, 2006). The *Wolbachia*, which are mutualistic endobacteria of most filarial nematodes, are essential for embryogenesis and larval development into adults and were thus identified as new target for anti-filarial drug development. Tetracycline antibiotics deplete *Wolbachia* in the animal model filariae *Litomosoides sigmodontis* and *Brugia pahangi*, as well as in the human parasites *Brugia malayi*, *Onchocerca volvulus* and *Wuchereria bancrofti*. Still, very little is known about the molecular details of the symbiosis between *Wolbachia* and its filarial host but nematode genes that respond to an anti-*Wolbachia* treatment may play important roles in the symbiosis. Therefore, the aim of this thesis was first to screen for such genes that might be involved in the symbiosis, and second to establish RNAi in the rodent filaria *L. sigmodontis* to study the function of filarial genes.

Differential display PCR was used to detect several candidate genes that are up-regulated upon antibiotic treatment. One of these genes, *Ls-ppe-1*, was similar to a family of phosphate permeases, and had putative orthologues in *O. volvulus* and *B. malayi*. *Ls-ppe-1* mRNA levels were elevated by day 3 to 36 of treatment and remained elevated through to 70 days post infection, one month after the treatment had been stopped, demonstrating a long-term alteration in the transcriptional state of the gene (Heider, 2006). In *Caenorhabditis elegans*, the knockdown of a homologous phosphate permease results in embryonic lethality, with the production of degenerating embryos, a phenotype that is also seen in filarial nematodes after the depletion of *Wolbachia* with tetracycline. The role of *Ls-ppe-1* in the symbiosis may relate to a possible direct or indirect involvement in nucleotide metabolism. In contrast to other endosymbionts that have undergone gene reduction, *Wolbachia* has retained the ability to synthesize nucleotides (in addition to other metabolites). Potentially the phosphate permease provides the *Wolbachia* with phosphate as part of the mutualistic symbiosis.

The mitochondrial HSP60 was found to be up-regulated in immunohistochemical stained sections of *O. volvulus* after the depletion of *Wolbachia* by doxycycline treatment. The anti-HSP60 serum binds specifically to this protein in both *Wolbachia* and mitochondria but the distinct localization of *Wolbachia* bacteria and mitochondria allows for the differentiation of the two. Immunohistochemistry data showed an up-regulation of filarial HSP60 after *Wolbachia* depletion. This could have been the result of the antiserum that binds preferentially to *Wolbachia* when they are present. To address this question, the mRNA levels of filarial *hsp60* in *O. volvulus* were measured. After depletion of *Wolbachia*, the *hsp60* transcripts were significantly increased compared to untreated control worms (Pfarr, 2008). The results lead to the hypothesis that the increased expression of HSP60 is due to a disruption of the homeostasis of metabolic pathways for which *Wolbachia* may be needed.

RNAi in adult worms of the rodent filaria *L. sigmodontis* was established and optimized. The actin gene of *L. sigmodontis* was successfully knocked-down, whereas the transcript levels of *Ls-hsp60* and *Ls-gst2,* used as controls to measure off-target effects, were not reduced (Pfarr, 2006). Soaking of nematodes with dsRNA coding for the *C. elegans yolk receptor* (*Ce-rme-2*), which has no orthologues in filaria, did not affect *Ls-act* transcription, demonstrating that the reduction of *Ls-act* is specific and not due to toxicity of dsRNA or off-target effects. The inhibition of *Ls-act* persisted for 72 hours, the length of the observation time. Two additional phenotypes were seen: first, the adult nematodes observed 48 and 72 hours after the beginning of the experiment showed paralysis by being stretched out and having slower movements, second, the release of microfilariae was significantly inhibited after soaking with dsRNA.

The use of lower concentrations of dsRNA than those previously reported for RNAi in *B. malayi* as well as the establishment of proper controls for off-target effects could make RNAi a possibility to study the function of filarial genes. However, there are issues with RNAi in filarial nematodes and other parasitic nematodes, namely that their genomes appear to lack the genes to allow spreading of the dsRNA signal from cell to cell, indicating that the process is still hit-or-miss, depending on the gene to be silenced and/or the method of delivery.

6 References

Aboobaker, A.A., Blaxter, M.L., (2003) Use of RNA interference to investigate gene function in the human filarial nematode parasite *Brugia malayi*. *Mol Biochem Parasitol* 129: 41.

Al-Qaoud, K.M., Pearlman, E., Hartung, T., Klukowski, J., Fleischer, B., Hoerauf, A., (2000) A new mechanism for IL-5-dependent helminth control: neutrophil accumulation and neutrophil-mediated worm encapsulation in murine filariasis are abolished in the absence of IL-5. *Int Immunol* 12: 899.

Al-Qaoud, K.M., Taubert, A., Zahner, H., Fleischer, B., Hoerauf, A., (1997) Infection of BALB/c mice with the filarial nematode *Litomosoides sigmodontis*: role of CD4+ T cells in controlling larval development. *Infect Immun* 65: 2457.

Allen, J.E., Adjei, O., Bain, O., Hoerauf, A., Hoffmann, W.H., Makepeace, B.L., Schulz-Key, H., Tanya, V.N., Trees, A.J., Wanji, S., Taylor, D.W., (2008) Of mice, cattle, and humans: the immunology and treatment of river blindness. *PLoS neglected tropical diseases* 2: e217.

Anderson, C.L., Karr, T.L., (2001) *Wolbachia*: evolutionary novelty in a rickettsial bacteria. *BMC evolutionary biology* 1: 10.

Awadzi, K., Attah, S.K., Addy, E.T., Opoku, N.O., Quartey, B.T., Lazdins-Helds, J.K., Ahmed, K., Boatin, B.A., Boakye, D.A., Edwards, G., (2004a) Thirty-month follow-up of sub-optimal responders to multiple treatments with ivermectin, in two onchocerciasis-endemic foci in Ghana. *Annals of tropical medicine and parasitology* 98: 359.

Awadzi, K., Boakye, D.A., Edwards, G., Opoku, N.O., Attah, S.K., Osei-Atweneboana, M.Y., Lazdins-Helds, J.K., Ardrey, A.E., Addy, E.T., Quartey, B.T., Ahmed, K., Boatin, B.A., Soumbey-Alley, E.W., (2004b) An investigation of persistent microfilaridermias despite multiple treatments with ivermectin, in two onchocerciasis-endemic foci in Ghana. *Annals of tropical medicine and parasitology* 98: 231.

Awadzi, K., Edwards, G., Opoku, N.O., Ardrey, A.E., Favager, S., Addy, E.T., Attah, S.K., Yamuah, L.K., Quartey, B.T., (2004c) The safety, tolerability and pharmacokinetics of levamisole alone, levamisole plus ivermectin, and levamisole plus albendazole, and their efficacy against *Onchocerca volvulus*. *Annals of tropical medicine and parasitology* 98: 595.

Baldo, L., Werren, J.H., (2007) Revisiting *Wolbachia* supergroup typing based on WSP: spurious lineages and discordance with MLST. *Current microbiology* 55: 81.

Bandi, C., Anderson, T.J., Genchi, C., Blaxter, M.L., (1998) Phylogeny of *Wolbachia* in filarial nematodes. *Proceedings* 265: 2407.

Bandi, C., Dunn, A.M., Hurst, G.D., Rigaud, T., (2001a) Inherited microorganisms, sex-specific virulence and reproductive parasitism. *Trends Parasitol* 17: 88.

Bandi, C., Trees, A.J., Brattig, N.W., (2001b) *Wolbachia* in filarial nematodes: evolutionary aspects and implications for the pathogenesis and treatment of filarial diseases. *Vet Parasitol* 98: 215.

Basanez, M.G., Pion, S.D., Churcher, T.S., Breitling, L.P., Little, M.P., Boussinesq, M., (2006) River blindness: a success story under threat? *PLoS Med* 3: e371.

Baugh, L.R., Hill, A.A., Brown, E.L., Hunter, C.P., (2001) Quantitative analysis of mRNA amplification by *in vitro* transcription. *Nucleic Acids Res* 29: E29.

Bendtsen, J.D., Jensen, L.J., Blom, N., Von Heijne, G., Brunak, S., (2004a) Feature-based prediction of non-classical and leaderless protein secretion. *Protein Eng Des Sel* 17: 349.

Bendtsen, J.D., Nielsen, H., von Heijne, G., Brunak, S., (2004b) Improved prediction of signal peptides: SignalP 3.0. *Journal of molecular biology* 340: 783.

Benton, B., Bump, J., Seketeli, A., Liese, B., (2002) Partnership and promise: evolution of the African river-blindness campaigns. *Annals of tropical medicine and parasitology* 96 Suppl 1: S5.

Blaxter, M., Daub, J., Guiliano, D., Parkinson, J., Whitton, C., (2002) The *Brugia malayi* genome project: expressed sequence tags and gene discovery. *Trans R Soc Trop Med Hyg* 96: 7.

Blaxter, M., Liu, L., (1996) Nematode spliced leaders--ubiquity, evolution and utility. *Int J Parasitol* 26: 1025.

Bordenstein, S., Rosengaus, R.B., (2005) Discovery of a novel *Wolbachia* super group in Isoptera. *Current microbiology* 51: 393.

Borsboom, G.J., Boatin, B.A., Nagelkerke, N.J., Agoua, H., Akpoboua, K.L., Alley, E.W., Bissan, Y., Renz, A., Yameogo, L., Remme, J.H., Habbema, J.D., (2003) Impact of ivermectin on onchocerciasis transmission: assessing the empirical evidence that repeated ivermectin mass treatments may lead to elimination/eradication in West-Africa. *Filaria J* 2: 8.

Bouchon, D., Rigaud, T., Juchault, P., (1998) Evidence for widespread *Wolbachia* infection in isopod crustaceans: molecular identification and host feminization. *Proceedings* 265: 1081.

Branger, S., Rolain, J.M., Raoult, D., (2004) Evaluation of antibiotic susceptibilities of *Ehrlichia canis, Ehrlichia chaffeensis,* and *Anaplasma phagocytophilum* by real-time PCR. *Antimicrobial agents and chemotherapy* 48: 4822.

Britton, C., Murray, L., (2002) A cathepsin L protease essential for *Caenorhabditis elegans* embryogenesis is functionally conserved in parasitic nematodes. *Mol Biochem Parasitol* 122: 21.

Britton, C., Murray, L., (2004) Cathepsin L protease (*CPL-1*) is essential for yolk processing during embryogenesis in *Caenorhabditis elegans*. *J Cell Sci* 117: 5133.

Brownlie, J.C., Adamski, M., Slatko, B., McGraw, E.A., (2007) Diversifying selection and host adaptation in two endosymbiont genomes. *BMC evolutionary biology* 7: 68.

Büttner, D.W., Wanji, S., Bazzocchi, C., Bain, O., Fischer, P., (2003) Obligatory symbiotic *Wolbachia* endobacteria are absent from *Loa loa*. *Filaria J* 2: 10.

Casiraghi, M., Bain, O., Guerrero, R., Martin, C., Pocacqua, V., Gardner, S.L., Franceschi, A., Bandi, C., (2004) Mapping the presence of *Wolbachia pipientis* on the phylogeny of filarial nematodes: evidence for symbiont loss during evolution. *Int J Parasitol* 34: 191.

Chirgwin, S.R., Coleman, S.U., Porthouse, K.H., Nowling, J.M., Punkosdy, G.A., Klei, T.R., (2003) Removal of *Wolbachia* from *Brugia pahangi* is closely linked to worm death and fecundity but does not result in altered lymphatic lesion formation in Mongolian gerbils (*Meriones unguiculatus*). *Infect Immun* 71: 6986.

Chomczynski, P., Mackey, K., (1995) Substitution of chloroform by bromo-chloropropane in the single-step method of RNA isolation. *Analytical biochemistry* 225: 163.

Christie, P.J., Atmakuri, K., Krishnamoorthy, V., Jakubowski, S., Cascales, E., (2005) Biogenesis, architecture, and function of bacterial type IV secretion systems. *Annual review of microbiology* 59: 451.

Chuang, C.F., Meyerowitz, E.M., (2000) Specific and heritable genetic interference by double-stranded RNA in *Arabidopsis thaliana*. *Proc Natl Acad Sci U S A* 97: 4985.

Coetzer, D.R.M.a.T.L., (2003) Reverse Slot Blot for the Verification of cDNAs Identified through Differential Display. *BioTechniques* 34: 270.

Correnti, J.M., Brindley, P.J., Pearce, E.J., (2005) Long-term suppression of cathepsin B levels by RNA interference retards schistosome growth. *Mol Biochem Parasitol* 143: 209.

Dale, C., Moran, N.A., (2006) Molecular interactions between bacterial symbionts and their hosts. *Cell* 126: 453.

Debrah, A.Y., Mand, S., Marfo-Debrekyei, Y., Batsa, L., Pfarr, K., Buttner, M., Adjei, O., Buttner, D., Hoerauf, A., (2007) Macrofilaricidal effect of 4 weeks of treatment with doxycycline on *Wuchereria bancrofti*. *Trop Med Int Health* 12: 1433.

Debrah, A.Y., Mand, S., Specht, S., Marfo-Debrekyei, Y., Batsa, L., Pfarr, K., Larbi, J., Lawson, B., Taylor, M., Adjei, O., Hoerauf, A., (2006) Doxycycline reduces plasma VEGF-C/sVEGFR-3 and improves pathology in lymphatic filariasis. *PLoS pathogens* 2: e92.

Dedeine, F., Vavre, F., Fleury, F., Loppin, B., Hochberg, M.E., Bouletreau, M., (2001) Removing symbiotic *Wolbachia* bacteria specifically inhibits oogenesis in a parasitic wasp. *Proc Natl Acad Sci U S A* 98: 6247.

Dernburg, A.F., Zalevsky, J., Colaiacovo, M.P., Villeneuve, A.M., (2000) Transgene-mediated cosuppression in the *C. elegans* germ line. *Genes Dev* 14: 1578.

Devaney, E., Martin, S.A., Thompson, F.J., (1996) Stage-specific gene expression in lymphatic filarial nematodes. *Parasitol Today* 12: 418.

Dillin, A., (2003) The specifics of small interfering RNA specificity. *Proc Natl Acad Sci U S A* 100: 6289.

Duke, B.O., Marty, A.M., Peett, D.L., Gardo, J., Pion, S.D., Kamgno, J., Boussinesq, M., (2002) Neoplastic change in *Onchocerca volvulus* and its relation to ivermectin treatment. *Parasitology* 125: 431.

Emanuelsson, O., Nielsen, H., Brunak, S., von Heijne, G., (2000) Predicting subcellular localization of proteins based on their N-terminal amino acid sequence. *Journal of molecular biology* 300: 1005.

Esterre, P., Plichart, C., Sechan, Y., Nguyen, N.L., (2001) The impact of 34 years of massive DEC chemotherapy on *Wuchereria bancrofti* infection and transmission: the Maupiti cohort. *Trop Med Int Health* 6: 190.

Evans, D.B., Gelband, H., Vlassoff, C., (1993) Social and economic factors and the control of lymphatic filariasis: a review. *Acta tropica* 53: 1.

Feinberg, E.H., Hunter, C.P., (2003) Transport of dsRNA into cells by the transmembrane protein SID-1. *Science* 301: 1545.

Fenn, K., Blaxter, M., (2004) Are filarial nematode *Wolbachia* obligate mutualist symbionts? *http://www.sciencedirect.com/science/journal/01695347* 19: 163.

Fenn, K., Blaxter, M., (2006) *Wolbachia* genomes: revealing the biology of parasitism and mutualism. *Trends Parasitol* 22: 60.

Fire, A., Xu, S., Montgomery, M.K., Kostas, S.A., Driver, S.E., Mello, C.C., (1998) Potent and specific genetic interference by double-stranded RNA in *Caenorhabditis elegans*. *Nature* 391: 806.

Fischer, P., Bamuhiiga, J., Buttner, D.W., (1997) Treatment of human *Mansonella streptocerca* infection with ivermectin. *Trop Med Int Health* 2: 191.

Ford, L., Guiliano, D.B., Oksov, Y., Debnath, A.K., Liu, J., Williams, S.A., Blaxter, M.L., Lustigman, S., (2005) Characterization of a novel filarial serine protease inhibitor, Ov-SPI-1, from *Onchocerca volvulus*, with potential multifunctional roles during development of the parasite. *J Biol Chem* 280: 40845.

Foster, J., Ganatra, M., Kamal, I., Ware, J., Makarova, K., Ivanova, N., Bhattacharyya, A., Kapatral, V., Kumar, S., Posfai, J., Vincze, T., Ingram, J., Moran, L., Lapidus, A., Omelchenko, M., Kyrpides, N., Ghedin, E., Wang, S., Goltsman, E., Joukov, V., Ostrovskaya, O., Tsukerman, K., Mazur, M., Comb, D., Koonin, E., Slatko, B., (2005) The *Wolbachia* genome of *Brugia malayi*: endosymbiont evolution within a human pathogenic nematode. *PLoS Biol* 3: e121.

Geldhof, P., Murray, L., Couthier, A., Gilleard, J.S., McLauchlan, G., Knox, D.P., Britton, C., (2006) Testing the efficacy of RNA interference in *Haemonchus contortus*. *Int J Parasitol* 36: 801.

Geldhof, P., Visser, A., Clark, D., Saunders, G., Britton, C., Gilleard, J., Berriman, M., Knox, D., (2007) RNA interference in parasitic helminths: current situation, potential pitfalls and future prospects. *Parasitology* 134: 609.

Genchi, C., Sacchi, L., Bandi, C., Venco, L., (1998) Preliminary results on the effect of tetracycline on the embryogenesis and symbiotic bacteria (*Wolbachia*) of *Dirofilaria immitis*. An update and discussion. *Parassitologia* 40: 247.

Ghedin, E., Wang, S., Foster, J.M., Slatko, B.E., (2004) First sequenced genome of a parasitic nematode. *Trends Parasitol* 20: 151.

Ghedin, E., Wang, S., Spiro, D., Caler, E., Zhao, Q., Crabtree, J., Allen, J.E., Delcher, A.L., Guiliano, D.B., Miranda-Saavedra, D., Angiuoli, S.V., Creasy, T., Amedeo, P., Haas, B., El-Sayed, N.M., Wortman, J.R., Feldblyum, T., Tallon, L., Schatz, M., Shumway, M., Koo, H., Salzberg, S.L., Schobel, S., Pertea, M., Pop, M., White, O., Barton, G.J., Carlow, C.K., Crawford, M.J., Daub, J., Dimmic, M.W., Estes, C.F., Foster, J.M., Ganatra, M., Gregory, W.F., Johnson, N.M., Jin, J., Komuniecki, R., Korf, I., Kumar, S., Laney, S., Li, B.W., Li, W., Lindblom, T.H., Lustigman, S., Ma, D., Maina, C.V., Martin, D.M., McCarter, J.P., McReynolds, L., Mitreva, M., Nutman, T.B., Parkinson, J., Peregrin-Alvarez, J.M., Poole, C., Ren, Q., Saunders, L., Sluder, A.E., Smith, K., Stanke, M., Unnasch, T.R., Ware, J., Wei, A.D., Weil, G., Williams, D.J., Zhang, Y., Williams, S.A., Fraser-Liggett, C., Slatko, B., Blaxter, M.L., Scott, A.L., (2007) Draft genome of the filarial nematode parasite *Brugia malayi*. *Science* 317: 1756.

Gilbert, J., Nfon, C.K., Makepeace, B.L., Njongmeta, L.M., Hastings, I.M., Pfarr, K.M., Renz, A., Tanya, V.N., Trees, A.J., (2005) Antibiotic chemotherapy of onchocerciasis: in a bovine model, killing

of adult parasites requires a sustained depletion of endosymbiotic bacteria (*Wolbachia* species). *The Journal of infectious diseases* 192: 1483.

Grant, B., Hirsh, D., (1999) Receptor-mediated endocytosis in the *Caenorhabditis elegans* oocyte. *Mol Biol Cell* 10: 4311.

Grishok, A., Tabara, H., Mello, C.C., (2000) Genetic requirements for inheritance of RNAi in *C. elegans*. *Science* 287: 2494.

Hashmi, S., Zhang, J., Oksov, Y., Lustigman, S., (2004) The *Caenorhabditis elegans* cathepsin Z-like cysteine protease, Ce-CPZ-1, has a multifunctional role during the worms' development. *J Biol Chem* 279: 6035.

Heider, U., Blaxter, M., Hoerauf, A., Pfarr, K.M., (2006) Differential display of genes expressed in the filarial nematode *Litomosoides sigmodontis* reveals a putative phosphate permease up-regulated after depletion of *Wolbachia* endobacteria. *Int J Med Microbiol* 296: 287.

Hoerauf, A., (2000a) Targeting of *Wolbachia* endobacteria in *Litomosoides sigmodontis*: comparison of tetracyclines with chloramphenicol, macrolides and ciprofloxacin. *Trop Med Int Health* 5: 275.

Hoerauf, A., (2006) New strategies to combat filariasis. *Expert review of anti-infective therapy* 4: 211.

Hoerauf, A., Buttner, D.W., Adjei, O., Pearlman, E., (2003a) Onchocerciasis. *Bmj* 326: 207.

Hoerauf, A., Mand, S., Adjei, O., Fleischer, B., Buttner, D.W., (2001) Depletion of *Wolbachia* endobacteria in *Onchocerca volvulus* by doxycycline and microfilaridermia after ivermectin treatment. *Lancet* 357: 1415.

Hoerauf, A., Mand, S., Fischer, K., Kruppa, T., Marfo-Debrekyei, Y., Debrah, A.Y., Pfarr, K.M., Adjei, O., Buttner, D.W., (2003b) Doxycycline as a novel strategy against bancroftian filariasis-depletion of *Wolbachia* endosymbionts from *Wuchereria bancrofti* and stop of microfilaria production. *Med Microbiol Immunol (Berl)* 192: 211.

Hoerauf, A., Mand, S., Volkmann, L., Buttner, M., Marfo-Debrekyei, Y., Taylor, M., Adjei, O., Buttner, D.W., (2003c) Doxycycline in the treatment of human onchocerciasis: Kinetics of *Wolbachia* endobacteria reduction and of inhibition of embryogenesis in female *Onchocerca* worms. *Microbes Infect* 5: 261.

Hoerauf, A., Nissen-Pahle, K., Schmetz, C., Henkle-Duhrsen, K., Blaxter, M.L., Buttner, D.W., Gallin, M.Y., Al-Qaoud, K.M., Lucius, R., Fleischer, B., (1999) Tetracycline therapy targets intracellular bacteria in the filarial nematode *Litomosoides sigmodontis* and results in filarial infertility. *J Clin Invest* 103: 11.

Hoerauf, A., Specht, S., Buttner, M., Pfarr, K., Mand, S., Fimmers, R., Marfo-Debrekyei, Y., Konadu, P., Debrah, A.Y., Bandi, C., Brattig, N., Albers, A., Larbi, J., Batsa, L., Adjei, O., Buttner, D.W., (2008) *Wolbachia* endobacteria depletion by doxycycline as antifilarial therapy has macrofilaricidal activity in onchocerciasis: a randomized placebo-controlled study. *Medical microbiology and immunology* 197: 295.

Hoerauf, A., Volkmann, L., Hamelmann, C., Adjei, O., Autenrieth, I.B., Fleischer, B., Buttner, D.W., (2000b) Endosymbiotic bacteria in worms as targets for a novel chemotherapy in filariasis. *Lancet* 355: 1242.

Hoerauf, A., Volkmann, L., Nissen-Paehle, K., Schmetz, C., Autenrieth, I., Buttner, D.W., Fleischer, B., (2000c) Targeting of *Wolbachia* endobacteria in *Litomosoides sigmodontis*: comparison of tetracyclines with chloramphenicol, macrolides and ciprofloxacin. *Trop Med Int Health* 5: 275.

Hong, J., Wei, N., Chalk, A., Wang, J., Song, Y., Yi, F., Qiao, R.P., Sonnhammer, E.L., Wahlestedt, C., Liang, Z., Du, Q., (2008) Focusing on RISC assembly in mammalian cells. *Biochemical and biophysical research communications* 368: 703.

Huigens, M.E., de Almeida, R.P., Boons, P.A., Luck, R.F., Stouthamer, R., (2004) Natural interspecific and intraspecific horizontal transfer of parthenogenesis-inducing *Wolbachia* in *Trichogramma* wasps. *Proceedings* 271: 509.

Huigens, M.E., Luck, R.F., Klaassen, R.H., Maas, M.F., Timmermans, M.J., Stouthamer, R., (2000) Infectious parthenogenesis. *Nature* 405: 178.

Huppi, K., Martin, S.E., Caplen, N.J., (2005) Defining and assaying RNAi in mammalian cells. *Mol Cell* 17: 1.

Hurst, G.D., Graf von der Schulenburg, J.H., Majerus, T.M., Bertrand, D., Zakharov, I.A., Baungaard, J., Volkl, W., Stouthamer, R., Majerus, M.E., (1999) Invasion of one insect species, *Adalia bipunctata*, by two different male-killing bacteria. *Insect molecular biology* 8: 133.

Hussein, A.S., Kichenin, K., Selkirk, M.E., (2002) Suppression of secreted acetylcholinesterase expression in *Nippostrongylus brasiliensis* by RNA interference. *Mol Biochem Parasitol* 122: 91.

Issa, Z., Grant, W.N., Stasiuk, S., Shoemaker, C.B., (2005) Development of methods for RNA interference in the sheep gastrointestinal parasite, *Trichostrongylus colubriformis*. *Int J Parasitol* 35: 935.

Jiggins, F.M., (2002a) The rate of recombination in *Wolbachia* bacteria. *Molecular biology and evolution* 19: 1640.

Jiggins, F.M., Hurst, G.D., Yang, Z., (2002b) Host-symbiont conflicts: positive selection on an outer membrane protein of parasitic but not mutualistic Rickettsiaceae. *Molecular biology and evolution* 19: 1341.

Johnson, N.M., Behm, C.A., Trowell, S.C., (2005) Heritable and inducible gene knockdown in *C. elegans* using Wormgate and the ORFeome. *Gene* 359: 26.

Kamath, R.S., Ahringer, J., (2003) Genome-wide RNAi screening in *Caenorhabditis elegans*. *Methods* 30: 313.

Kang, S., Hong, Y.S., (2008) RNA interference in infectious tropical diseases. *The Korean journal of parasitology* 46: 1.

Keiser, P.B., Reynolds, S.M., Awadzi, K., Ottesen, E.A., Taylor, M.J., Nutman, T.B., (2002) Bacterial endosymbionts of *Onchocerca volvulus* in the pathogenesis of posttreatment reactions. *The Journal of infectious diseases* 185: 805.

Klasson, L., Walker, T., Sebaihia, M., Sanders, M.J., Quail, M.A., Lord, A., Sanders, S., Earl, J., O'Neill, S.L., Thomson, N., Sinkins, S.P., Parkhill, J., (2008) Genome evolution of *Wolbachia* strain *w*Pip from the *Culex pipiens* group. *Molecular biology and evolution* 25: 1877.

Knox, D.P., Geldhof, P., Visser, A., Britton, C., (2007) RNA interference in parasitic nematodes of animals: a reality check? *Trends Parasitol* 23: 105.

Kopf, M., Brombacher, F., Hodgkin, P.D., Ramsay, A.J., Milbourne, E.A., Dai, W.J., Ovington, K.S., Behm, C.A., Kohler, G., Young, I.G., Matthaei, K.I., (1996) IL-5-deficient mice have a developmental defect in CD5+ B-1 cells and lack eosinophilia but have normal antibody and cytotoxic T cell responses. *Immunity* 4: 15.

Kozek, W.J., (2005) What is new in the *Wolbachia/Dirofilaria* interaction? *Vet Parasitol* 133: 127.

Kozek, W.J., Marroquin, H.F., (1977) Intracytoplasmic bacteria in *Onchocerca volvulus. Am J Trop Med Hyg* 26: 663.

Langworthy, N.G., Renz, A., Mackenstedt, U., Henkle-Duhrsen, K., de Bronsvoort, M.B., Tanya, V.N., Donnelly, M.J., Trees, A.J., (2000) Macrofilaricidal activity of tetracycline against the filarial nematode *Onchocerca ochengi*: elimination of *Wolbachia* precedes worm death and suggests a dependent relationship. *Proc R Soc Lond B Biol Sci* 267: 1063.

Le Goff, L., Lamb, T.J., Graham, A.L., Harcus, Y., Allen, J.E., (2002) IL-4 is required to prevent filarial nematode development in resistant but not susceptible strains of mice. *Int J Parasitol* 32: 1277.

Lendner, M., Doligalska, M., Lucius, R., Hartmann, S., (2008) Attempts to establish RNA interference in the parasitic nematode *Heligmosomoides polygyrus. Mol Biochem Parasitol* 161: 21.

Liang, P., Averboukh, L., Pardee, A.B., (1993) Distribution and cloning of eukaryotic mRNAs by means of differential display: refinements and optimization. *Nucleic Acids Res* 21: 3269.

Liang, P., Pardee, A.B., (1992) Differential display of eukaryotic messenger RNA by means of the polymerase chain reaction. *Science* 257: 967.

Liang, P., Zhu, W., Zhang, X., Guo, Z., O'Connell, R.P., Averboukh, L., Wang, F., Pardee, A.B., (1994) Differential display using one-base anchored oligo-dT primers. *Nucleic Acids Res* 22: 5763.

Liebau, E., Eschbach, M.L., Tawe, W., Sommer, A., Fischer, P., Walter, R.D., Henkle-Duhrsen, K., (2000) Identification of a stress-responsive *Onchocerca volvulus* glutathione S-transferase (*Ov-GST-3*) by RT-PCR differential display. *Mol Biochem Parasitol* 109: 101.

Little, M.P., Breitling, L.P., Basanez, M.G., Alley, E.S., Boatin, B.A., (2004) Association between microfilarial load and excess mortality in onchocerciasis: an epidemiological study. *Lancet* 363: 1514.

Liu, L.X., Blaxter, M.L., Shi, A., (1996) The 5S ribosomal RNA intergenic region of parasitic nematodes: variation in size and presence of SL1 RNA. *Mol Biochem Parasitol* 83: 235.

Liu, Q., Rand, T.A., Kalidas, S., Du, F., Kim, H.E., Smith, D.P., Wang, X., (2003) R2D2, a bridge between the initiation and effector steps of the *Drosophila* RNAi pathway. *Science* 301: 1921.

Lo, N., Casiraghi, M., Salati, E., Bazzocchi, C., Bandi, C., (2002) How many *Wolbachia* supergroups exist? *Molecular biology and evolution* 19: 341.

Lo, N., Paraskevopoulos, C., Bourtzis, K., O'Neill, S.L., Werren, J.H., Bordenstein, S.R., Bandi, C., (2007) Taxonomic status of the intracellular bacterium *Wolbachia pipientis. International journal of systematic and evolutionary microbiology* 57: 654.

Lucius, R., Textor, G., (1995) *Acanthocheilonema viteae*: rational design of the life cycle to increase production of parasite material using less experimental animals. *Appl Parasitol* 36: 22.

Lustigman, S., Zhang, J., Liu, J., Oksov, Y., Hashmi, S., (2004) RNA interference targeting cathepsin L and Z-like cysteine proteases of *Onchocerca volvulus* confirmed their essential function during L3 molting. *Mol Biochem Parasitol* 138: 165.

Maeda, I., Kohara, Y., Yamamoto, M., Sugimoto, A., (2001) Large-scale analysis of gene function in *Caenorhabditis elegans* by high-throughput RNAi. *Curr Biol* 11: 171.

Maine, E.M., (2000) A conserved mechanism for post-transcriptional gene silencing? *Genome Biol* 1: REVIEWS1018.

Marechal, P., Le Goff, L., Petit, G., Diagne, M., Taylor, D.W., Bain, O., (1996) The fate of the filaria *Litomosoides sigmodontis* in susceptible and naturally resistant mice. *Parasite* 3: 25.

Martin, C., Al-Qaoud, K.M., Ungeheuer, M.N., Paehle, K., Vuong, P.N., Bain, O., Fleischer, B., Hoerauf, A., (2000) IL-5 is essential for vaccine-induced protection and for resolution of primary infection in murine filariasis. *Med Microbiol Immunol (Berl)* 189: 67.

Martinez, J., Patkaniowska, A., Urlaub, H., Luhrmann, R., Tuschl, T., (2002) Single-stranded antisense siRNAs guide target RNA cleavage in RNAi. *Cell* 110: 563.

Masud, H., Qureshi, T.Q., Dukley, M., (2009) Effects of Ivermectin with and without Doxycycline on Clinical Symptoms of Onchocerciasis. *J Coll Physicians Surg Pak* 19: 34.

Masui, S., Sasaki, T., Ishikawa, H., (2000) Genes for the type IV secretion system in an intracellular symbiont, *Wolbachia*, a causative agent of various sexual alterations in arthropods. *Journal of bacteriology* 182: 6529.

McGarry, H.F., Egerton, G.L., Taylor, M.J., (2004) Population dynamics of *Wolbachia* bacterial endosymbionts in *Brugia malayi*. *Mol Biochem Parasitol* 135: 57.

McLaren, D.J., Worms, M.J., Laurence, B.R., Simpson, M.G., (1975) Micro-organisms in filarial larvae (Nematoda). *Trans R Soc Trop Med Hyg* 69: 509.

Meister, G., Tuschl, T., (2004) Mechanisms of gene silencing by double-stranded RNA. *Nature* 431: 343.

Mello, C.C., Conte, D., Jr., (2004) Revealing the world of RNA interference. *Nature* 431: 338.

Mello, C.C., Kramer, J.M., Stinchcomb, D., Ambros, V., (1991) Efficient gene transfer in *C.elegans*: extrachromosomal maintenance and integration of transforming sequences. *Embo J* 10: 3959.

Mohanty, B.P., (2001) *Wolbachia*: Potential targets for control of filariasis. *Current Science* 80.

Molyneux, D.H., Bradley, M., Hoerauf, A., Kyelem, D., Taylor, M.J., (2003) Mass drug treatment for lymphatic filariasis and onchocerciasis. *Trends Parasitol* 19: 516.

Molyneux, D.H., Zagaria, N., (2002) Lymphatic filariasis elimination: progress in global programme development. *Annals of tropical medicine and parasitology* 96 Suppl 2: S15.

Montgomery, M.K., Fire, A., (1998) Double-stranded RNA as a mediator in sequence-specific genetic silencing and co-suppression. *Trends Genet* 14: 255.

Nicholas, K.B., Nicholas, H.B.J., (1997) GeneDoc: a tool for editing and annotating multiple sequence alignments. In., pp.

Nilsen, T.W., (1993) Trans-splicing of nematode premessenger RNA. *Annual review of microbiology* 47: 413.

Nutman, T.B., Miller, K.D., Mulligan, M., Ottesen, E.A., (1986) *Loa loa* infection in temporary residents of endemic regions: recognition of a hyperresponsive syndrome with characteristic clinical manifestations. *The Journal of infectious diseases* 154: 10.

O'Neill, S.L., Giordano, R., Colbert, A.M., Karr, T.L., Robertson, H.M., (1992) 16S rRNA phylogenetic analysis of the bacterial endosymbionts associated with cytoplasmic incompatibility in insects. *Proc Natl Acad Sci U S A* 89: 2699.

Orihel, T.C., Ash, L.R., (1995) *Parasites in Human Tissues*. American Society for Clinical Pathology, Hongkong.

Ottesen, E.A., (1994) The human filariases: new understandings, new therapeutic strategies. *Current Opinion in Infectious Diseases* 7: 550 558.

Ottesen, E.A., (2002) Major progress toward eliminating lymphatic filariasis. *The New England journal of medicine* 347: 1885.

Page, A.P., Hamilton, A.J., Maizels, R.M., (1992) *Toxocara canis*: monoclonal antibodies to carbohydrate epitopes of secreted (TES) antigens localize to different secretion-related structures in infective larvae. *Exp Parasitol* 75: 56.

Parkinson, J., Whitton, C., Schmid, R., Thomson, M., Blaxter, M., (2004) NEMBASE: a resource for parasitic nematode ESTs. *Nucleic Acids Res* 32: D427.

Persengiev, S.P., Zhu, X., Green, M.R., (2004) Nonspecific, concentration-dependent stimulation and repression of mammalian gene expression by small interfering RNAs (siRNAs). In., pp. Vol 10: Issue 1: 12.

Petit, G., Diagne, M., Marechal, P., Owen, D., Taylor, D., Bain, O., (1992) Maturation of the filaria *Litomosoides sigmodontis* in BALB/c mice; comparative susceptibility of nine other inbred strains. *Annales de parasitologie humaine et comparee* 67: 144.

Pfarr, K., **Heider, U**., Hoerauf, A., (2006) RNAi mediated silencing of actin expression in adult *Litomosoides sigmodontis* is specific, persistent and results in a phenotype. *Int J Parasitol* 36: 661.

Pfarr, K., Hoerauf, A., (2005) The annotated genome of *Wolbachia* from the filarial nematode *Brugia malayi*: what it means for progress in antifilarial medicine. *PLoS Med* 2: e110.

Pfarr, K.M., **Heider, U**., Schmetz, C., Buttner, D.W., Hoerauf, A., (2008) The mitochondrial heat shock protein 60 (HSP60) is up-regulated in *Onchocerca volvulus* after the depletion of *Wolbachia*. *Parasitology* 135: 529.

Pfarr, K.M., Hoerauf, A.M., (2006) Antibiotics which target the *Wolbachia* endosymbionts of filarial parasites: a new strategy for control of filariasis and amelioration of pathology. *Mini reviews in medicinal chemistry* 6: 203.

Pion, S.D., Kamgno, J., Demanga, N., Boussinesq, M., (2002) Excess mortality associated with blindness in the onchocerciasis focus of the Mbam Valley, Cameroon. *Annals of tropical medicine and parasitology* 96: 181.

Poirier, G.M., Erlander, M.G., (1998) Postdifferential display: parallel processing of candidates using small amounts of RNA. *Methods* 16: 444.

Rances, E., Voronin, D., Tran-Van, V., Mavingui, P., (2008) Genetic and functional characterization of the type IV secretion system in *Wolbachia*. *Journal of bacteriology* 190: 5020.

Reichhart, J.M., Ligoxygakis, P., Naitza, S., Woerfel, G., Imler, J.L., Gubb, D., (2002) Splice-activated UAS hairpin vector gives complete RNAi knockout of single or double target transcripts in *Drosophila melanogaster*. *Genesis* 34: 160.

Richards, F.O., Jr., Boatin, B., Sauerbrey, M., Seketeli, A., (2001) Control of onchocerciasis today: status and challenges. *Trends Parasitol* 17: 558.

Ros, V.I., Fleming, V.M., Feil, E.J., Breeuwer, J.A., (2009) How diverse is the genus *Wolbachia*? Multiple-gene sequencing reveals a putatively new *Wolbachia* supergroup recovered from spider mites (Acari: Tetranychidae). *Applied and environmental microbiology* 75: 1036.

Rost, B., Fariselli, P., Casadio, R., (1996) Topology prediction for helical transmembrane proteins at 86% accuracy. *Protein Sci* 5: 1704.

Rowley, S.M., Raven, R.J., McGraw, E.A., (2004) *Wolbachia pipientis* in Australian spiders. *Current microbiology* 49: 208.

Sacchi, L., Corona, S., Casiraghi, M., Bandi, C., (2002) Does fertilization in the filarial nematode *Dirofilaria immitis* occur through endocytosis of spermatozoa? *Parasitology* 124: 87.

Scherer, L.J., Rossi, J.J., (2003) Approaches for the sequence-specific knockdown of mRNA. *Nat Biotechnol* 21: 1457.

Shambaugh, J.D., Hannon, G.E., Nilsen, T.W., (1994) The spliceosomal U small nuclear RNAs of *Ascaris lumbricoides*. *Mol Biochem Parasitol* 64: 349.

Shi, H., Djikeng, A., Mark, T., Wirtz, E., Tschudi, C., Ullu, E., (2000) Genetic interference in *Trypanosoma brucei* by heritable and inducible double-stranded RNA. *Rna* 6: 1069.

Simmer, F., Moorman, C., van der Linden, A.M., Kuijk, E., van den Berghe, P.V., Kamath, R.S., Fraser, A.G., Ahringer, J., Plasterk, R.H., (2003) Genome-wide RNAi of *C. elegans* using the hypersensitive rrf-3 strain reveals novel gene functions. *PLoS Biol* 1: E12.

Sonnichsen, B., Koski, L.B., Walsh, A., Marschall, P., Neumann, B., Brehm, M., Alleaume, A.M., Artelt, J., Bettencourt, P., Cassin, E., Hewitson, M., Holz, C., Khan, M., Lazik, S., Martin, C., Nitzsche, B., Ruer, M., Stamford, J., Winzi, M., Heinkel, R., Roder, M., Finell, J., Hantsch, H., Jones, S.J., Jones, M., Piano, F., Gunsalus, K.C., Oegema, K., Gonczy, P., Coulson, A., Hyman, A.A., Echeverri, C.J., (2005) Full-genome RNAi profiling of early embryogenesis in *Caenorhabditis elegans*. *Nature* 434: 462.

Stein, L.D., Bao, Z., Blasiar, D., Blumenthal, T., Brent, M.R., Chen, N., Chinwalla, A., Clarke, L., Clee, C., Coghlan, A., Coulson, A., D'Eustachio, P., Fitch, D.H., Fulton, L.A., Fulton, R.E., Griffiths-Jones, S., Harris, T.W., Hillier, L.W., Kamath, R., Kuwabara, P.E., Mardis, E.R., Marra, M.A., Miner, T.L., Minx, P., Mullikin, J.C., Plumb, R.W., Rogers, J., Schein, J.E., Sohrmann, M., Spieth, J., Stajich, J.E., Wei, C., Willey, D., Wilson, R.K., Durbin, R., Waterston, R.H., (2003) The genome sequence of Caenorhabditis briggsae: a platform for comparative genomics. *PLoS Biol* 1: E45.

Stolk, W.A., de Vlas, S.J., Habbema, J.D., (2006) Advances and challenges in predicting the impact of lymphatic filariasis elimination programmes by mathematical modelling. *Filaria J* 5: 5.

Stouthamer, R., Breeuwer, J.A., Hurst, G.D., (1999) *Wolbachia pipientis*: microbial manipulator of arthropod reproduction. *Annual review of microbiology* 53: 71.

Stouthamer, R., Breeuwert, J.A., Luck, R.F., Werren, J.H., (1993) Molecular identification of microorganisms associated with parthenogenesis. *Nature* 361: 66.

Sun, L.V., Foster, J.M., Tzertzinis, G., Ono, M., Bandi, C., Slatko, B.E., O'Neill, S.L., (2001) Determination of *Wolbachia* genome size by pulsed-field gel electrophoresis. *Journal of bacteriology* 183: 2219.

Supali, T., Djuardi, Y., Pfarr, K.M., Wibowo, H., Taylor, M.J., Hoerauf, A., Houwing-Duistermaat, J.J., Yazdanbakhsh, M., Sartono, E., (2008) Doxycycline treatment of *Brugia malayi*-infected persons reduces microfilaremia and adverse reactions after diethylcarbamazine and albendazole treatment. *Clin Infect Dis* 46: 1385.

Tabara, H., Grishok, A., Mello, C.C., (1998) RNAi in *C. elegans*: soaking in the genome sequence. *Science* 282: 430.

Tavernarakis, N., Wang, S.L., Dorovkov, M., Ryazanov, A., Driscoll, M., (2000) Heritable and inducible genetic interference by double-stranded RNA encoded by transgenes. *Nature genetics* 24: 180.

Taylor, M.J., Bandi, C., Hoerauf, A., (2005a) *Wolbachia* bacterial endosymbionts of filarial nematodes. *Advances in parasitology* 60: 245.

Taylor, M.J., Bandi, C., Hoerauf, A.M., Lazdins, J., (2000) *Wolbachia* bacteria of filarial nematodes: a target for control? *Parasitol Today* 16: 179.

Taylor, M.J., Hoerauf, A., (1999) *Wolbachia* bacteria of filarial nematodes. *Parasitol Today* 15: 437.

Taylor, M.J., Hoerauf, A., (2001) A new approach to the treatment of filariasis. *Curr Opin Infect Dis* 14: 727.

Taylor, M.J., Makunde, W.H., McGarry, H.F., Turner, J.D., Mand, S., Hoerauf, A., (2005b) Macrofilaricidal activity after doxycycline treatment of *Wuchereria bancrofti*: a double-blind, randomised placebo-controlled trial. *Lancet* 365: 2116.

The *C. elegans* Genome Sequencing Consortium, (1998) Genome sequence of the nematode *C. elegans*: a platform for investigating biology. *Science* 282: 2012.

Thompson, F.J., Cockroft, A.C., Wheatley, I., Britton, C., Devaney, E., (2001) Heat shock and developmental expression of *hsp83* in the filarial nematode *Brugia pahangi*. *Eur J Biochem* 268: 5808.

Timmons, L., Court, D.L., Fire, A., (2001) Ingestion of bacterially expressed dsRNAs can produce specific and potent genetic interference in *Caenorhabditis elegans*. *Gene* 263: 103.

Timmons, L., Fire, A., (1998) Specific interference by ingested dsRNA. *Nature* 395: 854.

Turner, J.D., Mand, S., Debrah, A.Y., Muehlfeld, J., Pfarr, K., McGarry, H.F., Adjei, O., Taylor, M.J., Hoerauf, A., (2006) A randomized, double-blind clinical trial of a 3-week course of doxycycline plus albendazole and ivermectin for the treatment of *Wuchereria bancrofti* infection. *Clin Infect Dis* 42: 1081.

Tusnady, G.E., Simon, I., (1998) Principles governing amino acid composition of integral membrane proteins: application to topology prediction. *Journal of molecular biology* 283: 489.

Ullu, E., Tschudi, C., Chakraborty, T., (2004) RNA interference in protozoan parasites. *Cell Microbiol* 6: 509.

Urwin, P.E., Lilley, C.J., Atkinson, H.J., (2002) Ingestion of double-stranded RNA by preparasitic juvenile cyst nematodes leads to RNA interference. *Mol Plant Microbe Interact* 15: 747.

Versaw, W.K., Metzenberg, R.L., (1995) Repressible cation-phosphate symporters in Neurospora crassa. *Proc Natl Acad Sci U S A* 92: 3884.

Viney, M.E., Thompson, F.J., (2008) Two hypotheses to explain why RNA interference does not work in animal parasitic nematodes. *Int J Parasitol* 38: 43.

Visser, A., Geldhof, P., de Maere, V., Knox, D.P., Vercruysse, J., Claerebout, E., (2006) Efficacy and specificity of RNA interference in larval life-stages of *Ostertagia ostertagi*. *Parasitology* 133: 777.

Volkmann, L., Bain, O., Saeftel, M., Specht, S., Fischer, K., Brombacher, F., Matthaei, K.I., Hoerauf, A., (2003a) Murine filariasis: interleukin 4 and interleukin 5 lead to containment of different worm developmental stages. *Med Microbiol Immunol (Berl)* 192: 23.

Volkmann, L., Fischer, K., Taylor, M., Hoerauf, A., (2003b) Antibiotic therapy in murine filariasis (*Litomosoides sigmodontis*): comparative effects of doxycycline and rifampicin on *Wolbachia* and filarial viability. *Trop Med Int Health* 8: 392.

Volkmann, L., Saeftel, M., Bain, O., Fischer, K., Fleischer, B., Hoerauf, A., (2001) Interleukin-4 is essential for the control of microfilariae in murine infection with the filaria *Litomosoides sigmodontis*. *Infect Immun* 69: 2950.

von Heijne, G., (1998) Life and death of a signal peptide. *Nature* 396: 111.

Warbrick, E.V., Barker, G.C., Rees, H.H., Howells, R.E., (1993) The effect of invertebrate hormones and potential hormone inhibitors on the third larval moult of the filarial nematode, *Dirofilaria immitis, in vitro*. *Parasitology* 107 (Pt 4): 459.

Weiner, A., (2003) Soaking up RNAi. *Mol Cell* 12: 535.

Werren, J.H., (1997) Biology of *Wolbachia*. *Annual review of entomology* 42: 587.

WHO, (1992) Lymphatic Filariasis: The Disease and its Control. *WHO Technical Report Series 821*.

WHO, (1995) Onchocerciasis and its Control. *WHO Technical Report Series 852*: 1.

WHO, (2000a) Lymphatic filariasis. *WHO Fact Sheet* 102.

WHO, (2000b) Onchocerciasis (River Blindness). *WHO Fact Sheet* 95.

WHO, (2008) Global programme to eliminate lymphatic filariasis. *WHO Weekly epidemiological record* 83 333.

Wu, M., Sun, L.V., Vamathevan, J., Riegler, M., Deboy, R., Brownlie, J.C., McGraw, E.A., Martin, W., Esser, C., Ahmadinejad, N., Wiegand, C., Madupu, R., Beanan, M.J., Brinkac, L.M., Daugherty, S.C., Durkin, A.S., Kolonay, J.F., Nelson, W.C., Mohamoud, Y., Lee, P., Berry, K., Young, M.B., Utterback, T., Weidman, J., Nierman, W.C., Paulsen, I.T., Nelson, K.E., Tettelin, H., O'Neill, S.L., Eisen, J.A., (2004) Phylogenomics of the reproductive parasite *Wolbachia pipientis w*Mel: a streamlined genome overrun by mobile genetic elements. *PLoS Biol* 2: E69.

Xie, H., Bain, O., Williams, S.A., (1994) Molecular phylogenetic studies on filarial parasites based on 5S ribosomal spacer sequences. *Parasite* 1: 141.

Yang, D., Lu, H., Erickson, J.W., (2000) Evidence that processed small dsRNAs may mediate sequence-specific mRNA degradation during RNAi in *Drosophila* embryos. *Curr Biol* 10: 1191.

Yoneda, T., Benedetti, C., Urano, F., Clark, S.G., Harding, H.P., Ron, D., (2004) Compartment-specific perturbation of protein handling activates genes encoding mitochondrial chaperones. *J Cell Sci* 117: 4055.

Zahner, H., Wegerhof, P.H., (1986) Immunity to *Litomosoides carinii* in *Mastomys natalensis*. II. Effects of chemotherapeutically abbreviated and postpatent primary infections on challenges with various stages of the parasite. *Z Parasitenkd*. 72: 789.

Zawadzki, J.L., Presidente, P.J., Meeusen, E.N., De Veer, M.J., (2006) RNAi in *Haemonchus contortus*: a potential method for target validation. *Trends Parasitol* 22: 495.

Zhao, Q., Wang, J., Levichkin, I.V., Stasinopoulos, S., Ryan, M.T., Hoogenraad, N.J., (2002) A mitochondrial specific stress response in mammalian cells. *Embo J* 21: 4411.

Zhou, H., Zhou, Y., (2003) Predicting the topology of transmembrane helical proteins using mean burial propensity and a hidden-Markov-model-based method. *Protein Sci* 12: 1547.

Appendix A

CLUSTAL W (1.74) multiple sequence alignment for the 3 *Ls-ppe-1* variants

```
                     spliced leader 1
Ls_phos_perm1    AAAGGTTTAATTACCCAAGTTTGAG--------------------------------------
Ls_phos_perm2    AAAGGTTTAATTACCCAAGTTTGAGAGTGTATAATTTCGGATGGTTCTTTTTTCAAACGG
Ls_phos_perm3    AAAGGTTTAATTACCCAAGTTTGAGAGTGTATAATTTCGGATGGTTCTTTTTTCAAACGG
                 ***********************

Ls_phos_perm1    -------------------------------------------GTTAACTGAGAAATAAA
Ls_phos_perm2    TTATGTGCGCATCACGTCCATCCTGTTATTTCATCACTATATTGTTAACTGAGAAATAAA
Ls_phos_perm3    TTATGTGCGCATCACGTCCATCCTGTTATTTCATCACTATATTGTTAACTGAGAAATAAA
                                                            ****************

Ls_phos_perm1    GGAAGATGTCAACATTGACAGTAACTACGCTAATGCCATCCTCTTCTACAATGTCAGAAG
Ls_phos_perm2    GGAAGATGTCAACATTGACAGTAACTACGCTAATGCCATCCTCTTCTACAATGTCAGAAG
Ls_phos_perm3    GGAAGATGTCAACATTGACAGTAACTACGCTAATGCCATCCTCTTCTACAATGTCAGAAG
                 ************************************************************

Ls_phos_perm1    CATTCATAGCCGCCTTTCGGAATGATGTATTATGGGCATTAATATGTGGTGTAATTTTGG
Ls_phos_perm2    CATTCATAGCCGCCTTTCGGAATGATGTATTATGGGCATTAATATGTGGTGTAATTTTGG
Ls_phos_perm3    CATTCATAGCCGCCTTTCGGAATGATGTATTATGGGCATTAATATGTGGTGTAATTTTGG
                 ************************************************************

Ls_phos_perm1    CTTTTGTGCTTGGTTTTGCGATGGGTGCAAATGACGTTGCAAATGCTTTTGGTACATCGG
Ls_phos_perm2    CTTTTGTGCTTGGTTTTGCGATGGGTGCAAATGACGTTGCAAATGCTTTTGGTACATCGG
Ls_phos_perm3    CTTTTGTGCTTGGTTTTGCGATGGGTGCAAATGACGTTGCAAATGCTTTTGGTACATCGG
                 ************************************************************

Ls_phos_perm1    TTGGTAGCAAAGTGCTGACATTACGGCAAGCTTATATACTTGCAGTAATTTTTGAAACAC
Ls_phos_perm2    TTGGTAGCAAAGTGCTGACATTACGGCAAGCTTATATACTTGCAGTAATTTTTGAAGCAC
Ls_phos_perm3    TTGGTAGCAAAGTGCTGACATTACGGCAAGCTTATATACTTGCAGTAATTTTTGAAGCAC
                 ********************************************************** ***

Ls_phos_perm1    TTGGAGCACTGCTTATCGGTTACAACGTAACGGATACGGTACGTAAAGGTGTCATCGATC
Ls_phos_perm2    TTGGAGCACTGCTTATCGGTTACAACGTAACGGATACGGTACGTAAAGGTGTCATCGATC
Ls_phos_perm3    TTGGAGCACTGCTTATCGGTTACAACGTAACGGATACGGTACGTAAAGGTGTCATCGATC
                 ************************************************************

Ls_phos_perm1    TGACGTTATATGAAGATAAACCAAAAGAGATTTTCATTGGGCAAATCGCCATTCTTGGAG
Ls_phos_perm2    TGACGTTATATGAAGATAAACCAAAAGAGATTTTCATTGGGCAAATCGCCATTCTTGGAG
Ls_phos_perm3    TGACGTTATATGAAGATAAACCAAAAGAGATTTTCATTGGGCAAATCGCCATTCTTGGAG
                 ************************************************************

Ls_phos_perm1    GTTGCTCATTATGGTTATTAATTGCTACACTTGCGCGTCTACCTGTATCATCAACTCATA
Ls_phos_perm2    GTTGCTCATTATGGTTATTAATTGCTACACTTGCGCGTCTACCTGTATCATCAACTCATA
Ls_phos_perm3    GTTGCTCATTATGGTTATTAATTGCTACACTTGCGCGTCTACCTGTATCATCAACTCATA
                 ************************************************************

Ls_phos_perm1    GTGTCACTGGAGCTACTGTAGGATTTGGCTTGATGACACGAGGTGTTGCTGGAATACAAT
Ls_phos_perm2    GTGTCACTGGAGCTACTGTAGGATTTGGCTTGATGACACGAGGTGTTGCTGGAATACAAT
Ls_phos_perm3    GTGTCACTGGAGCTACTGTAGGATTTGGCTTGATGACACGAGGTGTTGCTGGAATACAAT
                 ************************************************************

Ls_phos_perm1    GGAAAAAAATTGCTCATATTGTTGCTTCATGGTTTTTATCACCGATATTGTCTGGCGTCG
Ls_phos_perm2    GGAAAAAAATTGCTCATATTGTTGCTTCATGGTTTTTATCACCGATATTGTCTGGCGTCG
Ls_phos_perm3    GGAAAAAAATTGCTCATATTGTTGCTTCATGGTTTTTATCACCGATATTGTCTGGCGTCG
                 ************************************************************

Ls_phos_perm1    TGTCAGCCGTTCTGTACATTATTGTTGACCATTCAGTTCTCAGACGGAAGGATCCATTTC
Ls_phos_perm2    TGTCAGCCGTTCTGTACATTATTGTTGACCATTCAGTTCTCAGACGGAAGGATCCATTTC
Ls_phos_perm3    TGTCAGCCGTTCTGTACATTATTGTTGACCATTCAGTTCTCAGACGGAAGGATCCATTTC
                 ************************************************************

Ls_phos_perm1    GTTGTGGTTTGAGAGCTTTGCCAATATTTTACTGGTTTTGTATCGCATTTAATATTTTCA
Ls_phos_perm2    GTTGTGGTTTGAGAGCTTTGCCAATATTTTACTGGTTTTGTATCGCATTTAATATTTTCA
Ls_phos_perm3    GTTGTGGTTTGAGAGCTTTGCCAATATTTTACTGGTTTTGTATCGCATTTAATATTTTCA
                 ************************************************************

Ls_phos_perm1    CCGCTAGCTATCAAGGATTGAAATTACTTCGCCTGTCAAAGTTGCCGTTGTGGTTGAGCT
Ls_phos_perm2    CCGCTAGCTATCAAGGATTGAAATTACTTCGCCTGTCAAAGTTGCCGTTGTGGTTGAGCT
Ls_phos_perm3    CCGCTAGCTATCAAGGATTGAAATTACTTCGCCTGTCAAAGTTGCCGTTGTGGTTGAGCT
                 ************************************************************
```

```
Ls_phos_perm1    CATTAGTGAGTATTGGATGTGCAACAGTTGGCTCCATCGCTATTTACTTTTTGCTCTTGC
Ls_phos_perm2    CATTAGTGAGTATTGGATGTGCAACAGTTGGCTCCATCGCTATTTACTTTTTGCTCTTGC
Ls_phos_perm3    CATTAGTGAGTATTGGATGTGCAACAGTTGGCTCCATCGCTATTTACTTTTTGCTCTTGC
                 ************************************************************


Ls_phos_perm1    CGAGGCTGAAAATCTGGATAAACAATTCACTTGGCAGTAATACAGCTAGAGACGATTCGT
Ls_phos_perm2    CGAGGCTGAAAATCTGGATAAACAATTCACTTGGCAGTAATACAGCTAGAGACGATTCGT
Ls_phos_perm3    CGAGGCTGAAAATCTGGATAAACAATTCACTTGGCAGTAATACAGCTAGAGACGATTCGT
                 ************************************************************


Ls_phos_perm1    TTGAAGTGCAGACTATAAGTAATGCGGTTCAATTGGAGGGAAATGTGATAAATCAAAAAT
Ls_phos_perm2    TTGAAGTGCAGACTATAAGTAATGCGGTTCAATTGGAGGGAAATGTGATAAATCAAAAAT
Ls_phos_perm3    TTGAAGTGCAGACTATAAGTAATGCGGTTCAATTGGAGGGAAATGTGATAAATCAAAAAT
                 ************************************************************


Ls_phos_perm1    GTCAAGCATCGAAGACAGAAAATGTTGAGAGTTCAACTGTTATCAAAAGCGATAGCAAAA
Ls_phos_perm2    GTCAAGCATCGAAGACAGAAAATGTTGAGAGTTCAACTGTTATCAAAAGCGATAGCAAAA
Ls_phos_perm3    GTCAAGCATCGAAGACAGAAAATGTTGAGAGTTCAACTGTTATCAAAAGCGATAGCAAAA
                 ************************************************************


Ls_phos_perm1    TCATCGAGAGTATGGCGAAAAAGGGTGAAGAAAAGAAACTAACCGATAATACAGTAATGA
Ls_phos_perm2    TCATCGAGAGTATGGCGAAAAAGGGTGAAGAAAAGAAACTAACCGATAATACAGTAATGA
Ls_phos_perm3    TCATCGAGAGTATGGCGAAAAAGGGTGAAGAAAAGAAACTAACCGATAATACAGTAATGA
                 ************************************************************


Ls_phos_perm1    AGTTCATTCGTTGGATATTGCCGACTGATAATAGAGCAACGGACAATAGAACAATGAAAA
Ls_phos_perm2    AGTTCATTCGTTGGATATTGCCGACTGATAATAGAGCAACGGACAATAGAACAATGAAAA
Ls_phos_perm3    AGTTCATTCGTTGGATATTGCCGACTGATAATAGAGCAACGGACAATAGAACAATGAAAA
                 ************************************************************


Ls_phos_perm1    TATTTAGTTCGATACAAGCTTTTACCGCGTGCTTTGCTGGATTTGCGCATGGCGCTAATG
Ls_phos_perm2    TATTTAGTTCGATACAAGCTTTTACCGCGTGCTTTGCTGGATTTGCGCATGGCGCTAATG
Ls_phos_perm3    TATTTAGTTCGATACAAGCTTTTACCGCGTGCTTTGCTGGATTTGCGCATGGCGCTAATG
                 ************************************************************


Ls_phos_perm1    ACGTCGGGAATGCAATAGCTCCGCTGACAGCATTGATATCGATTTACAGTAATCTGGATG
Ls_phos_perm2    ACGTCGGGAATGCAATAGCTCCGCTGACAGCATTGATATCGATTTACAGTAATCTGGATG
Ls_phos_perm3    ACGTCGGGAATGCAATAGCTCCGCTGACAGCATTGATATCGATTTACAGTAATCTGGATG
                 ************************************************************


Ls_phos_perm1    TTCGACAACGAAGTGAAACACCGATCTATGTGTTACTGTACGGCGTACTTGCAATATGTG
Ls_phos_perm2    TTCGACAACGAAGTGAAACACCGATCTATGTGTTACTGTACGGCGTACTTGCAATATGTG
Ls_phos_perm3    TTCGACAACGAAGTGAAACACCGATCTATGTGTTACTGTACGGCGTACTTGCAATATGTG
                 ************************************************************


Ls_phos_perm1    TTGGACTTGTGGTACTTGGACATCACGTAATACAAACTATTGGTACTGATATGTCTACGA
Ls_phos_perm2    TTGGACTTGTGGTACTTGGACATCACGTAATACAAACTATTGGTACTGATATGTCTACGA
Ls_phos_perm3    TTGGACTTGTGGTACTTGGACATCACGTAATACAAACTATTGGTACTGATATGTCTACGA
                 ************************************************************


Ls_phos_perm1    TCAATGCTGCTAGCGGTTTTACAATCGAATTCGGTGCAGCGGTAACTTCACTAACAGCCA
Ls_phos_perm2    TCAATGCTGCTAGCGGTTTTACAATCGAATTCGGTGCAGCGGTAACTTCACTAACAGCCA
Ls_phos_perm3    TCAATGCTGCTAGCGGTTTTACAATCGAATTCGGTGCAGCGGTAACTTCACTAACAGCCA
                 ************************************************************


Ls_phos_perm1    GTAAACTTGGCCTACCAATTAGTACAACCCATTCATTGGTGGGAAGCGTGGTATTCGTTG
Ls_phos_perm2    GTAAACTTGGCCTACCAATTAGTACAACCCATTCATTGGTGGGAAGCGTGGTATTCGTTG
Ls_phos_perm3    GTAAACTTGGCCTACCAATTAGTACAACCCATTCATTGGTGGGAAGCGTGGTATTCGTTG
                 ************************************************************


Ls_phos_perm1    GAATGGTGCGTGCCAAGAAAGGTGTCCAGTGGTTAATATTCCGAAACATTGCCTTATCGT
Ls_phos_perm2    GAATGGTGCGTGCCAAGAAAGGTGTCCAGTGGTTAATATTCCGAAACATTGCCTTATCGT
Ls_phos_perm3    GAATGGTGCGTGCCAAGAAAGGTGTCCAGTGGTTAATATTCCGAAACATTGCCTTATCGT
                 ************************************************************


Ls_phos_perm1    GGATTTTAACGTTGCCTATTTCAGGTCTTTTGGCAATGGGTTTGACGTTAATCCTCAAGT
Ls_phos_perm2    GGATTTTAACGTTGCCTATTTCAGGTCTTTTGGCAATGGGTTTGACGTTAATCCTCAAGT
Ls_phos_perm3    GGATTTTAACGTTGCCTATTTCAGGTCTTTTGGCAATGGGTTTGACGTTAATCCTCAAGT
                 ************************************************************


Ls_phos_perm1    TTTCACTTTGAGAGTGTAGTTGGACATTTATTTTTTCTTGTACATTTGTTACTTTGTTGT
Ls_phos_perm2    TTTCACTTTGAGAGTGTAGTTGGACATTTATTTTTTCTTGTACACTTGTTACTTTGTTGT
Ls_phos_perm3    TTTCACTTTGAGAGTGTAGTTGGACATTTATTTTTTCTTGTACACTTGTTACTTTGTTGT
                 ********************************************* **************
                                                                    polyA signal
Ls_phos_perm1    ATATTTTCATCAGTTCACCCATTCTCATCTTTGTTTACTTTAATTTTTTT-GACTAAAAA
Ls_phos_perm2    ATATTTTCATCAGTTCACTCATTCTCATCTTTGTTTACTTTAATTTTTTTTGACTAAAAA
Ls_phos_perm3    ATATTTTCATCAGTTCACTCATTCTCATCTTTGTTTACTTTAATTTTTTTTGACTAAAAA
                 ******************* *************************** *********
```

```
Ls_phos_perm1    AAAAAAAA
Ls_phos_perm2    AAAGAATTTCACTATCATCAATTTTTCGTTAATTTTTATTTGTGTCCTTGAAAAAGCAAC
Ls_phos_perm3    AAAGAATTTCACTATCATCAATTTTTCATTAATTTTTATTTGTGTCCTTGAAAAAGCAAC
                 *** **


Ls_phos_perm1
Ls_phos_perm2    TACTTCCTTAAAAAAAAAGAAAAAAAAAAGAAAAAAAAAAA
Ls_phos_perm3    TACTTCCTTATATTGCAGCTCCACGATATAAATTGAAAGATCTTTGCTCAAATTAATTTC


Ls_phos_perm1
Ls_phos_perm2
Ls_phos_perm3    CATATTAGTTGATAGAAGGTAGGGTAATATTCTTCTGATTTCAATAATTCATCAATTACT


Ls_phos_perm1
Ls_phos_perm2
Ls_phos_perm3    TATTTAACTGCAATCAATGGCAAATCGTATTTGATGAGGGAAATGTTAGATTAAATTAAT


Ls_phos_perm1
Ls_phos_perm2
Ls_phos_perm3    CAATGTTTGAGAAAGAAGATTGACTTAATTTTATTAAAATTTTAATTGAAAAAAAAAAAA
```

Appendix B

Alignment of the available nematode homologues of *Ls-ppe-1*.

The *C. elegans* (Ce) and *C. briggsae* (Cb) genes are designated by their WormPep (Ce) (The *C. elegans* Genome Sequencing Consortium, 1998) and BriggPep (Cb) (Stein, 2003) names respectively. The sequences derived from ESTs are named using the NemBase cluster identifiers (Parkinson, 2004). The sequences derived from the *B. malayi* whole genome sequence assembly (Ghedin, 2004) are designated by their TIGR gene model names, suffixed with "MB" to indicate that these differ slightly from the current TIGR database versions because of re-prediction during this work. N- and C-terminal missing data is indicated by blank cells, while '-' indicates an introduced gap residue. One amino acid in OVC00569 was not predictable because of ambiguity in EST sequence (residue X). Residues with >80% conservation in aligned residues are shaded. Analysis by Mark Blaxter (Heider, 2006).

Block 1 (sequence names and end positions):

Sequence	Position
Ls_ppe_1	348
Bm_14967_n01567_MB	365
Ce_C48A7_2	369
Cb_CBP01602	377
Ce_F09G2_3	333
Cb_CBP04437	328
Ce_B0222_3	320
Cb_CBP19553	320
Ce_B0222_2	303
Ce_W05H5_3	336
Cb_CBP04968	333
Ce_B0331_2	361
Cb_CBP04505	408
Xl_XIC02915	408

Block 2:

Sequence	Position
Ls_ppe_1	446
Bm_14967_n01567_MB	458
Ce_C48A7_2	462
Cb_CBP01602	470
Ce_F09G2_3	431
Cb_CBP04437	426
Ce_B0222_3	418
Cb_CBP19553	418
Ce_B0222_2	401
Ce_W05H5_3	434
Cb_CBP04968	432
Ce_B0331_2	459
Cb_CBP04505	507
Gr_GRC01656	506

Block 3:

Sequence	Position
Ls_ppe_1	547
Bm_14967_n01567_MB	559
Ce_C48A7_2	563
Cb_CBP01602	570
Ce_F09G2_3	532
Cb_CBP04437	527
Ce_B0222_3	519
Cb_CBP19553	519
Ce_B0222_2	502
Ce_W05H5_3	535
Cb_CBP04968	533
Ce_B0331_2	561
Cb_CBP04505	561
Xl_XIC02915	609
Gr_GRC01656	607

127

Acknowledgment

First, I would like to thank Prof. Dr. Achim Hörauf who gave me the opportunity to join his group at the Bernhard-Nocht-Institute for Tropical Medicine in Hamburg and who took me over in 2004 to his new affiliation, the Institute for Medical Microbiology, Immunology and Parasitology (IMMIP) at the University Clinic Bonn.

I also want to thank Prof. Dr. Hans-Georg Sahl for accepting the co-supervision of this work as well as PD Dr. Gerhild van Echten-Deckert and Prof. Dr. Gerhard von der Emde for their participation and expertise in my thesis committee.

Additionally, I wish to thank my supervisor and friend Dr. Kenneth M. Pfarr for his consistently support and helpful guidance through all the good and bad times I had.

I also thank my lab mates for a really good working relationship and a lot of fun also outside of the lab, especially Sabine Specht, Anna Albers, Sandra Arriens Maria Brehm, Daniel Fernandez-Ruiz, Alex Debrah, Sabine Mand, Sridhar Arumugam, and others for their support and cooperation.

Thanks go also to all my friends and acquaintances that were interested in my work, especially to my old friend Dr. Kai Lamottke who found always the right words that let me focus again to find back on my path.

Furthermore I would like to thank my parents Christa and Wolfgang Heider who made my "way of life" in the first place possible, and of course for their unconditional support and encouragement all the time. My success will always be also yours.

Last but not least I will not forget to say thank you to my husband Frederic and our daughter Lina for their love that made me smiling also in tough times.

Declaration/Erklärung

Die vorliegende Arbeit wurde in der Zeit von Januar 2002 bis Dezember 2003 am Bernhard-Nocht-Institut für Tropenmedizin in Hamburg in der Arbeitsgruppe Helminthologie und ab Januar 2004 bis einschließlich März 2006 an der Uniklinik Bonn, Institut für Medizinische Mikrobiologie, Immunologie und Parasitologie, unter der Leitung von Prof. Dr. Achim Hörauf angefertigt.

Hiermit versichere ich, dass ich die vorliegende Arbeit selbst und ohne fremde Hilfe verfasst, andere als die angegebenen Quellen und Hilfsmittel nicht benutzt und die den benutzten Werken wörtlich oder inhaltlich entnommenen Stellen als solche kenntlich gemacht habe. Desweiteren versichere ich, dass ich diese oder eine ähnliche Arbeit noch keiner anderen Stelle als Dissertation vorgelegt habe, um ein Promotionsverfahren zu eröffnen.

This thesis has been written independently and with no other sources and aids than stated.

Bonn, June 2009   Ulrike Klemm

CURRICULUM VITAE
CLAUDIA ULRIKE KLEMM (NEE HEIDER)

COURSE OF EDUCATION

1978–1988	PRIMARY AND SECONDARY SCHOOL, Niesky
1988–1991	GYMNASIUM „HOHE LANDESSCHULE", Hanau (Abitur)
1991–1994	HOECHST AG Frankfurt/Main, Biology laboratory technician

RESEARCH EXPERIENCE

10/1994–12/1999	JOHANN WOLFGANG GOETHE UNIVERSITÄT Frankfurt/Main Department of Biology
01/2000–09/2000	AVENTIS PHARMA Germany, Frankfurt/Main; Diabetes Research group Practical diploma exam: Insulineffekt am isolierten Skelettmuskel der Ratte (Glukoseaufnahme, Expression und zelluläre Verteilung des Glukosetransporters 4 (GLUT-4) und seine Translokation in der Muskelzelle)
09/2000–11/2001	TEXAS A&M UNIVERSITY, Houston, TX (USA) Institute of Biosciences and Technology, Center of Structural Biology Research assistant/scientist
01/2002–12/2004	BERNHARD NOCHT INSTITUTE FOR TROPICAL MEDICINE, Hamburg Department: Helminthology Ph.D. thesis supervised by Prof. A. Hoerauf: Identification of a putative *Litomosoides sigmodontis* phosphate permease, *Ls-ppe-1*, and its role in the interaction between filarial nematodes and their *Wolbachia* endosymbionts and Establishment of RNA interference in the rodent filaria *Litomosoides sigmodontis*, a model of human filariasis.
01/2004–04/2006	UNIVERSITY CLINIC BONN Institute for Medical Microbiology, Immunology and Parasitology Ph.D. thesis continued under supervision of Prof. A. Hoerauf
04/2006–09/2007	Birth of my daughter – maternity leave
since 10/2007	BERNHARD NOCHT INSTITUTE FOR TROPICAL MEDICINE, Hamburg Postdoc position, Department: Helminth Immunology

Heider, U., Blaxter, M., Hoerauf, A., Pfarr, K.M.: Differential display of genes expressed in the filarial nematode *Litomosoides sigmodontis* reveals a putative phosphate permease up-regulated after depletion of *Wolbachia* endobacteria. (2006) Int J Med Microbiol 296: 287.

Heider, U. and Pfarr, K.M., Hoerauf, A.: RNAi mediated silencing of actin expression in adult *Litomosoides sigmodontis* is specific, persistent and results in a phenotype. (2006) Int J Parasitol 36: 661.

Pfarr, K.M., **Heider, U.**, Schmetz, C., Büttner, D.W., Hoerauf, A.: The mitochondrial heat shock protein 60 (HSP60) is up-regulated in *Onchocerca volvulus* after the depletion of *Wolbachia*. (2008) Parasitology 135: 529.

Eschbach, M.L., **Klemm, U**., Blankenhaus, B., Kolbaum, J., Brattig, N., Breloer, M.: The immune response to *Strongyloides* infection in mice. (2009) <submitted>